CHAPTER 3

Polar Ozone

Lead Author:
D.W. Fahey

Co-authors:
G. Braathen
D. Cariolle
Y. Kondo
W.A. Matthews
M.J. Molina
J.A. Pyle
R.B. Rood
J.M. Russell III
U. Schmidt
D.W. Toohey
J.W. Waters
C.R. Webster
S.C. Wofsy

Contributors:
T. Deshler
J.E. Dye
T.D.A. Fairlie
W.L. Grose
G.L. Manney
P.A. Newman
A. O'Neill
R.B. Pierce
W. Randel
A.E. Roche
C.R. Trepte

CHAPTER 3

POLAR OZONE

Contents

SCIENTIFIC SUMMARY

Substantial new results have been obtained since the last assessment in the areas of observations, laboratory measurements, and modeling. These new results reaffirm the key role of anthropogenic halocarbons as the cause of ozone loss in polar regions and increase confidence in the processes associated with this loss: the formation of a polar vortex in high-latitude winter, the growth of aerosol surfaces at low temperatures characteristic of the vortex, the conversion of inactive chlorine to active forms on these surfaces, the subsequent chlorine-catalyzed loss of ozone, the return of chlorine to inactive forms in the polar regions in spring, and the breakup of the vortex and its dispersal to lower latitudes.

Ozone

- Results of observational and modeling studies since the last assessment reaffirm the role of anthropogenic halocarbon species in Antarctic ozone depletion. Satellite observations show a strong spatial and temporal correlation of chlorine monoxide (ClO) abundances with ozone depletion in the Antarctic vortex. Photochemical model calculations of ozone depletion are consistent with observed losses in the Antarctic.

- Chlorine- and bromine-catalyzed ozone loss has been confirmed in the Arctic winter. Consistent with expectations, these losses are smaller than those observed over Antarctica. Photochemical model calculations constrained with *in situ* and satellite observations yield results consistent with the observed ozone loss.

- Interannual variability in the photochemical and dynamical conditions of the vortices continues to limit reliable predictions of future ozone changes in polar regions, particularly in the Northern Hemisphere.

Chlorine species

- Satellite measurements show that elevated ClO concentrations cover most of both polar vortex regions during much of the winter. This is consistent with the picture that virtually all available chlorine becomes fully activated in both winter vortices through heterogeneous reactions that occur on aerosol particles formed at low temperatures.

- *In situ* and remote measurements show that hydrochloric acid (HCl) and chlorine nitrate ($ClONO_2$) concentrations are markedly reduced in the vicinity of the elevated ClO concentrations. This anticorrelation is quantitatively consistent with the picture that HCl and $ClONO_2$ are converted to reactive chlorine. Chlorine in the stratosphere originates largely from anthropogenic halocarbons.

Aerosols

- Laboratory studies reaffirm that surface reactions on aerosol particles efficiently produce active chlorine from inactive forms. The rate of the principal reaction of HCl with $ClONO_2$ is a strong function of temperature and relative humidity, and depends to a lesser extent on bulk aerosol composition.

- Sulfate aerosol from the Mt. Pinatubo eruption reached high latitudes in the stratosphere, enhancing reactions involving aerosol particles in and near the polar vortices. This led to chlorine activation over larger regions in the high latitude stratosphere, especially near the vortex boundaries, and extended the spatial extent of halogen-related ozone loss.

- The formation and reactivity of aerosol particles within the vortex can be simulated, in part, by microphysical models. Two- and three-dimensional photochemical transport models confirm observations that chlorine can be activated efficiently throughout the entire vortex within days.

POLAR PROCESSES

- Aerosol particles in the polar stratosphere are known ternary condensates of nitric acid (HNO_3), sulfuric acid (H_2SO_4), and water (H_2O). Important progress has been made in the characterization of these condensates in theoretical and laboratory studies.

- Satellite measurements confirm that the sequestering and removal of HNO_3 by aerosol particles is a predominant feature of the Antarctic vortex for much of the winter, whereas removal in the Arctic is generally less intense and more localized.

- Despite extensive observational evidence for dehydration and denitrification, the underlying microphysical mechanisms and necessary atmospheric conditions that control particle formation and sedimentation have not been adequately described. This is an important limitation for reliably predicting ozone loss in polar regions, particularly in the Northern Hemisphere.

Vortex

- New satellite observations of long-lived tracers and modeling studies confirm that air within the center of the polar winter vortices is substantially isolated from extravortical air, especially in the Antarctic.

- Nearly all observational and modeling studies are consistent with a time scale of three to four months to replace a substantial fraction of inner Antarctic vortex air.

- Models show that most mass transport out of the vortex in the lower stratosphere occurs below about 16 km altitude.

- Erosion by planetary and synoptic wave activity transports air from the vortex edge region to lower latitudes. Data and model studies provide conflicting interpretations of the magnitude of this transport and its effect on lower latitudes. There is little evidence of significant lateral mixing into the vortex except during strong wave events in the Arctic.

- Observed correlations of nitrous oxide abundances with those of inactive chlorine species, reactive nitrogen, and ozone over broad regions at high latitudes in the lower stratosphere have proved useful for diagnosing ozone destruction throughout the vortex.

3.1 INTRODUCTION

Depletion of polar ozone in the winter seasons continues to be an important scientific issue for both hemispheres. While the "ozone hole" has become an annual feature in the Southern Hemisphere, increased losses have been noted in the Northern Hemisphere in recent years. Increased losses at midlatitudes may be connected to the more intense loss processes occurring in polar regions. The World Meteorological Organization (WMO) *Scientific Assessment of Ozone Depletion: 1991* reaffirmed halogen chemistry as the cause of severe ozone depletion in the Antarctic as well as of smaller losses in the Arctic (WMO, 1992). The causes for the observed year-to-year variability of such losses and effects at midlatitudes were left as uncertain. For this assessment, a wide variety of new evidence is available to confirm the basic paradigm of ozone loss in polar regions. This new evidence, which follows from a high level of activity involving observational, laboratory, and modeling studies that took place in the period 1991-1994, has better defined a number of the photochemical and dynamical aspects of polar ozone depletion.

The principal cause of ozone loss in the polar regions is photochemistry involving the halogen species, chlorine and bromine. Long-lived halogens species, primarily chlorofluorocarbons, are released in the troposphere from human activities. The photochemical degradation of these organic source molecules in the stratosphere leads to the formation of inorganic halogen species, of which chlorine monoxide (ClO), chlorine nitrate ($ClONO_2$), hydrochloric acid (HCl), bromine monoxide (BrO), and bromine nitrate ($BrONO_2$) are most important. The release of chlorine from the more stable reservoirs occurs in high-latitude winter in reactions on surfaces of stratospheric aerosol particles. The formation and reactivity of these particles are enhanced at the low temperatures characteristic of the interior of the polar vortices. This reactive processing maintains high levels of active chlorine species that, along with BrO, catalytically destroy ozone as this air encounters sunlight. With sufficient insolation and warmer temperatures, chlorine is returned to its reservoir forms during a photochemical recovery period and ozone destruction slows. The removal of reactive nitrogen by aerosol particle sedimentation in the vortex, a process defined as denitrification, strongly regulates the rate of recovery by controlling the availability of active chlorine. This paradigm, illustrated in Figure 3-1, has been broadly supported by a wide variety of data and interpretation in previous WMO assessments and has been strengthened substantially in this assessment period.

This assessment period was marked by the launch of the National Aeronautics and Space Administration (NASA) Upper Atmosphere Research Satellite (UARS) in late 1991, after more than a decade of preparation (Reber, 1990; Reber *et al.*, 1993). The satellite contains four instruments for the measurement of trace species in the stratosphere (Barath *et al.*, 1993; Russell *et al.*, 1993a; Roche *et al.*, 1993a; Taylor *et al.*, 1993) and other instruments for wind, solar radiation, and energetic particles. From an orbit of 600 km inclined 57° to the equator, UARS provides broad coverage in both hemispheres with a maximum latitude of 80°. The precession of the orbit with respect to the Sun provides measurements during all local solar times over a month-long period. Of particular importance for this assessment are the UARS observations at high latitudes of the chlorine reservoir species $ClONO_2$ and HCl, active chlorine in the form of ClO, the reactive nitrogen species nitric acid (HNO_3), water vapor, aerosol extinction, and the long-lived tracers nitrous oxide (N_2O), methane (CH_4), and hydrofluoric acid (HF). In addition, ozone measurements show the distribution and evolution of ozone loss in the polar regions. New aspects of the transport of air in and near the vortex are evident from the observations of long-lived tracers. The interpretation of UARS data will remain an active research area as the data set continues to grow.

The body of *in situ* observations in the stratosphere was greatly increased with aircraft and balloon measurements made during the European Arctic Stratospheric Ozone Experiment (EASOE) (Pyle *et al.*, 1994) and the NASA Airborne Arctic Stratospheric Expedition II (AASE II) (Anderson and Toon, 1993), which were both held during the Northern Hemisphere winter of 1991/92. Each included measurements of reactive nitrogen and chlorine species, long-lived tracers and reservoir species, and aerosols, combined with modeling studies of observed photochemical and dynamical changes. The observation period extended from pre-vortex conditions in fall, through the lowest temperature conditions marked by chlorine activation, and into the photochemical recovery period in early spring. The breadth of

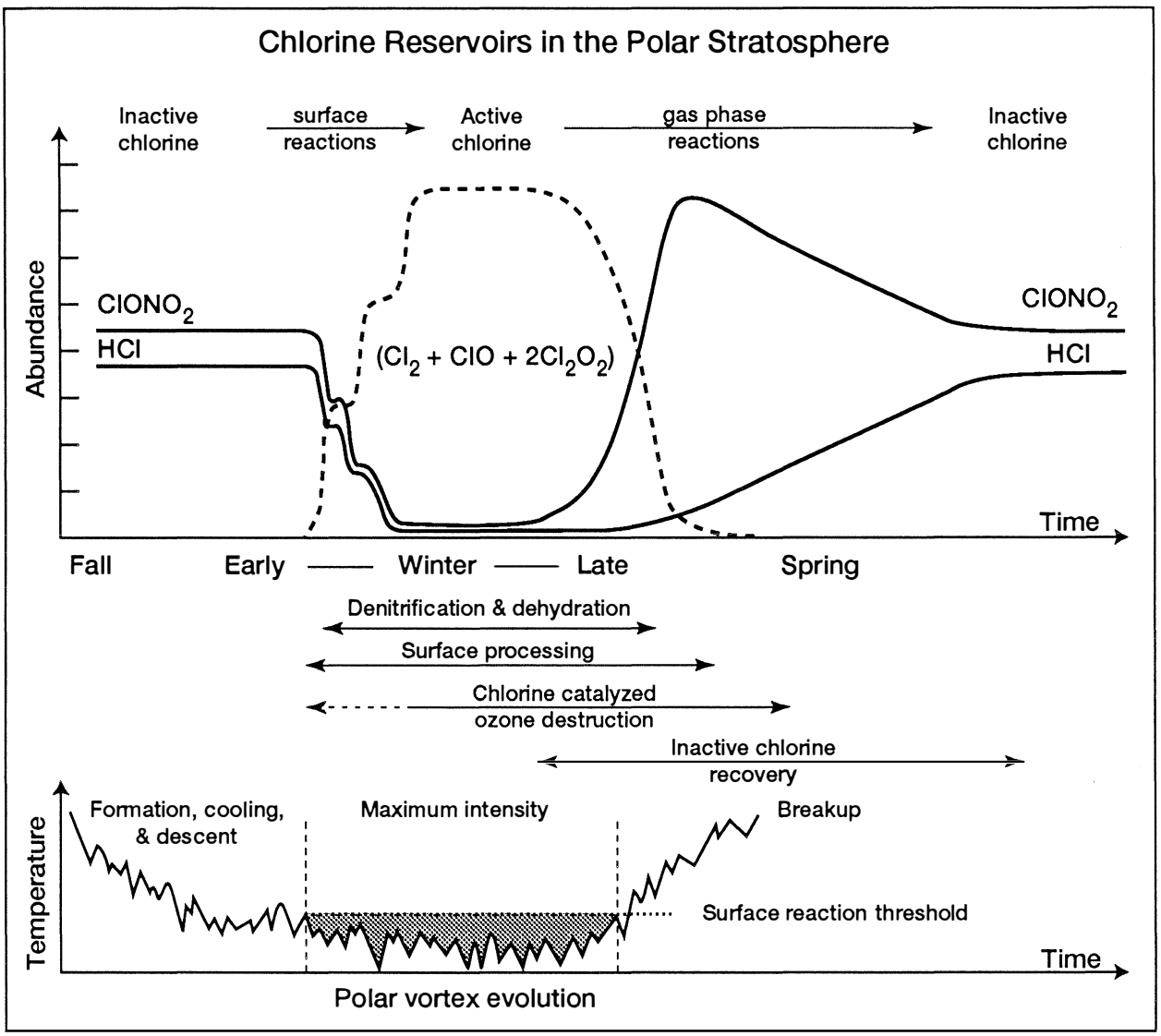

Figure 3-1. Schematic of the photochemical and dynamical features of the polar regions related to ozone depletion. The upper panel represents the conversion of chlorine from inactive to active forms in winter in the lower stratosphere and the reformation of inactive forms in spring. The partitioning between the active chlorine species Cl_2, ClO, and Cl_2O_2 depends on exposure to sunlight after polar stratospheric cloud (PSC) processing. The corresponding stages of the polar vortex are indicated in the lower panel, where the temperature scale represents changes in the minimum polar temperatures in the lower stratosphere (see Figure 3-3) (adapted from Webster *et al.*, 1993a).

instrumentation and period of measurements have resulted in a unique data set for the examination of the paradigm in Figure 3-1. In addition, ground-based observations during EASOE and separate efforts in Antarctica have also yielded important insights into the evolution of reactive chlorine and nitrogen during the winter season.

Modeling studies continue to advance with improvements in computational facilities and algorithms and with new atmospheric data. Specifically, photochemical models that incorporate observations of long-lived tracers, reservoir species, new kinetic data, and meteorological conditions are now able to make more representative calculations of ozone loss in the polar vortex. Studies of the fluid dynamics near the vortex now provide more detailed descriptions of air parcel motion in regions of high potential vorticity (PV) gradients, improving estimates of the transport into and out of the vortex interior. The continued refinement of such models is an essential component for future predictions of ozone loss and its variability.

New laboratory studies have examined aspects of the homogeneous and heterogeneous chemistry underlying the kinetics of ozone loss. Specifically, new photolysis cross section measurements have been made for HNO_3 and $ClONO_2$ under stratospheric conditions. Photolysis of HNO_3 is a limiting step for photochemical recovery in early spring in the vortex. Significant advances have been made in the understanding of the formation and growth of aerosols and the reactivity of aerosol surfaces in polar regions. These advances build on the extensive effort expended in recent years to develop new laboratory techniques to characterize multiphase surface growth under stratospheric conditions. At the same time, the understanding of the thermodynamics of aerosol growth has progressed to explain laboratory and atmospheric observations.

Finally, the assessment period was marked by the eruption of Mt. Pinatubo in the Philippines in June 1991, months before the launch of the UARS satellite and the start of the EASOE and AASE II campaigns. The increased loading of stratospheric aerosol was predicted to cause significant changes in ozone at midlatitudes as a result of increased heterogeneous reactivity (Brasseur and Granier, 1992; Prather, 1992; Hofmann and Solomon, 1989) (see Chapter 4). The aerosol did not reach polar regions in abundance until the southern winter of 1992 and the northern winter of 1992-93. Observational and modeling evidence suggests the enhancement of volcanic aerosol near the vortex will increase ozone loss associated with heterogeneous processes in that region. Studies have continued as the volcanic aerosol in the stratosphere gradually diminished over a period of several years following the eruption.

3.2 VORTEX FORMATION AND TRACER RELATIONS

The vortex that forms in each winter hemisphere in the polar region sets the context of ozone depletion (see Figures 3-1 and 3-2). The temporal as well as the

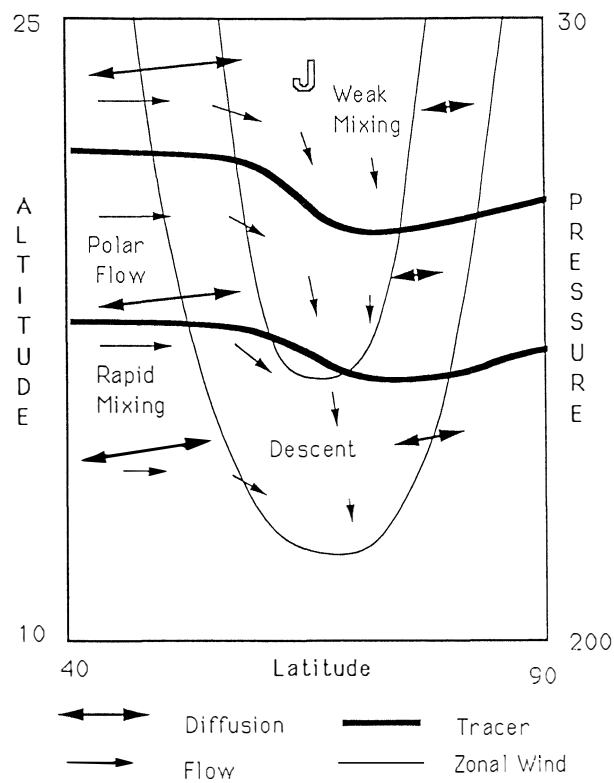

Figure 3-2. Schematic of the circulation and mixing associated with the polar vortex in the Arctic midwinter or Antarctic early spring periods. The vertical scale is shown in altitude (km) and pressure (mb) units. The horizontal scale is latitude in degrees. Arrows indicate mixing (double) and flow (single), with longer arrows representing larger rates. Other features are zonal wind contours (thin lines), jet core (J), and long-lived tracer isopleths (thick lines) (Schoeberl *et al.*, 1992).

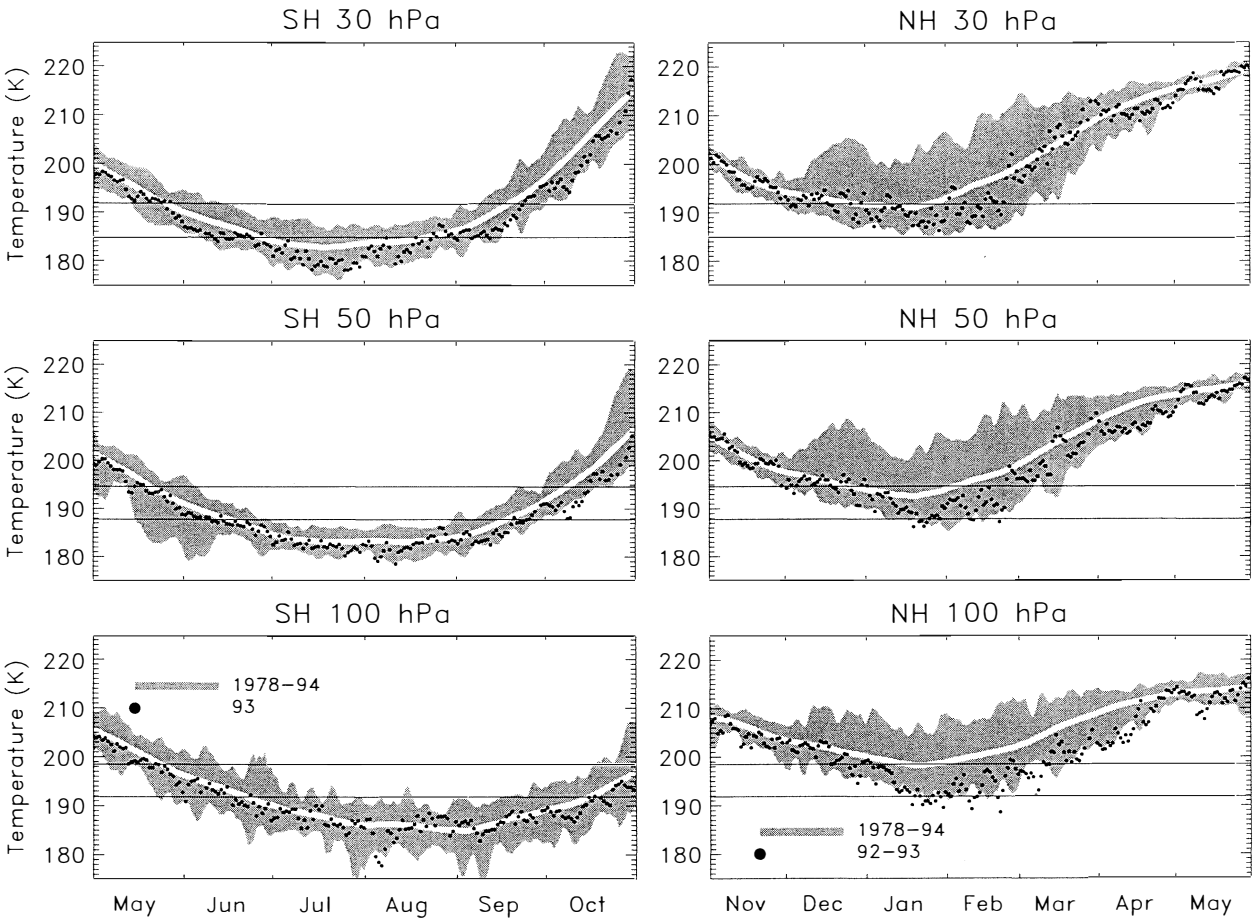

Figure 3-3. A summary of the minimum polar vortex temperatures in the period 1978 to 1994 at 30 hPa, 50 hPa, and 100 hPa (1 hPa = 1 mb) in the lower stratosphere in the Northern (NH) and Southern (SH) hemispheres (National Meteorological Center analysis). The range of observations between 1978 and 1992 is given by the shaded region. The narrow white band is the average of the data set. The black dots represent data for 1993 in the Antarctic and 1992-93 in the Arctic winter. Lines indicate approximate temperature thresholds for Type I (upper) and Type II (lower) PSC formation (adapted from Nagatani *et al.*, 1990).

spatial scale of the activation of chlorine that catalytically destroys ozone is associated with the extent of low temperatures inside the vortex. In addition, the dynamical features of the vortex determine the distribution of air from the vortex to lower latitudes and the incorporation of lower latitude air into the vortex. Many features of vortex formation are understood from observational and modeling studies (Schoeberl and Hartmann, 1991; Schoeberl *et al.*, 1992; Dritschel and Legras, 1993; Manney and Zurek, 1993; Strahan and Mahlman, 1994a, b). After autumn equinox, increasing polar darkness and radiative cooling of polar air lead to the formation of a circumpolar wind belt. This westerly wind belt, or polar night jet, defines the polar vortex in each hemisphere (see Figure 3-2). The vortex edge region is characterized by large gradients in PV and mixing and transport properties. Large differences in the wind and temperature fields of the vortex exist between hemispheres (see Figure 3-3) (Manney and Zurek, 1993). The vortex in the Southern Hemisphere is stronger, develops lower temperatures, and persists longer than the northern vortex. The cause is related to differences in planetary wave activity that modifies the temperature and dynamical structure of the vortex. Wave activity is more frequent and of larger amplitude in the north, owing to more dominant orographic features and the greater land/sea

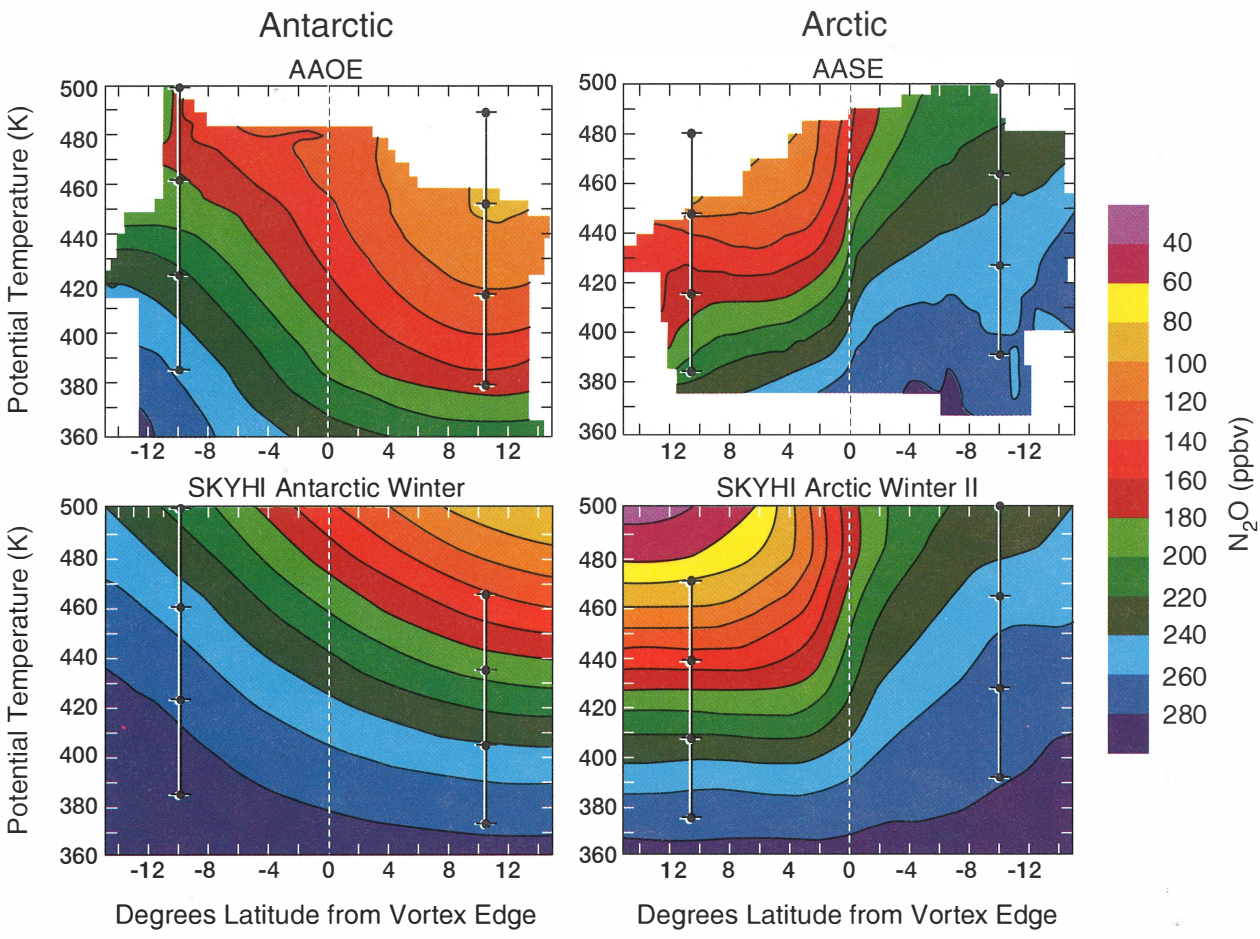

Figure 3-4. Top panels: Mean N_2O mixing ratios on potential temperature surfaces calculated from aircraft flight data in high-latitude winter. Bottom panels: Same, except using the Geophysical Fluid Dynamics Laboratory SKYHI model results from 24 days covering the same spatial and temporal region. Positive values on the abscissa represent degrees of latitude poleward of the vortex edge. The internal four-point vertical scales in each panel represent approximate pressure altitudes inside and outside the vortex. From top to bottom, the points correspond to altitudes of 20, 18, 16, and 14 km, respectively (adapted from Strahan and Mahlman, 1994a). (See Garcia *et al.* [1992] for two-dimensional model results.)

contrast. Because ozone depletion depends on the interaction of the vortex wind field with local regions of low temperatures and the resultant chemical processing, the temperature differences represented in Figure 3-3 underlie the large differences in ozone depletion observed between the hemispheres (see Section 3.4). Thus, predictions of future ozone losses and the role of climate change in polar processes depend directly on factors that change the temperature and wind fields during the winter seasons.

An important diagnostic for the formation of the polar vortices and subsequent ozone loss is the high-latitude distribution of long-lived trace species such as N_2O, CH_4, and the chlorofluorocarbons CFC-11 and CFC-113. All have large gradients in the stratosphere (decreasing with altitude) resulting from photochemical loss and transport. Air descending into the center of the vortex reduces values of these traces species, thereby creating horizontal gradients inside the vortex (see Figure 3-4). Balloon and aircraft measurements of N_2O beginning before vortex formation serve as a baseline for documenting the temporal variation of the vertical structure within the vortex (Bauer *et al.*, 1994; Podolske *et al.*, 1993). A comparison of the location of high PV from

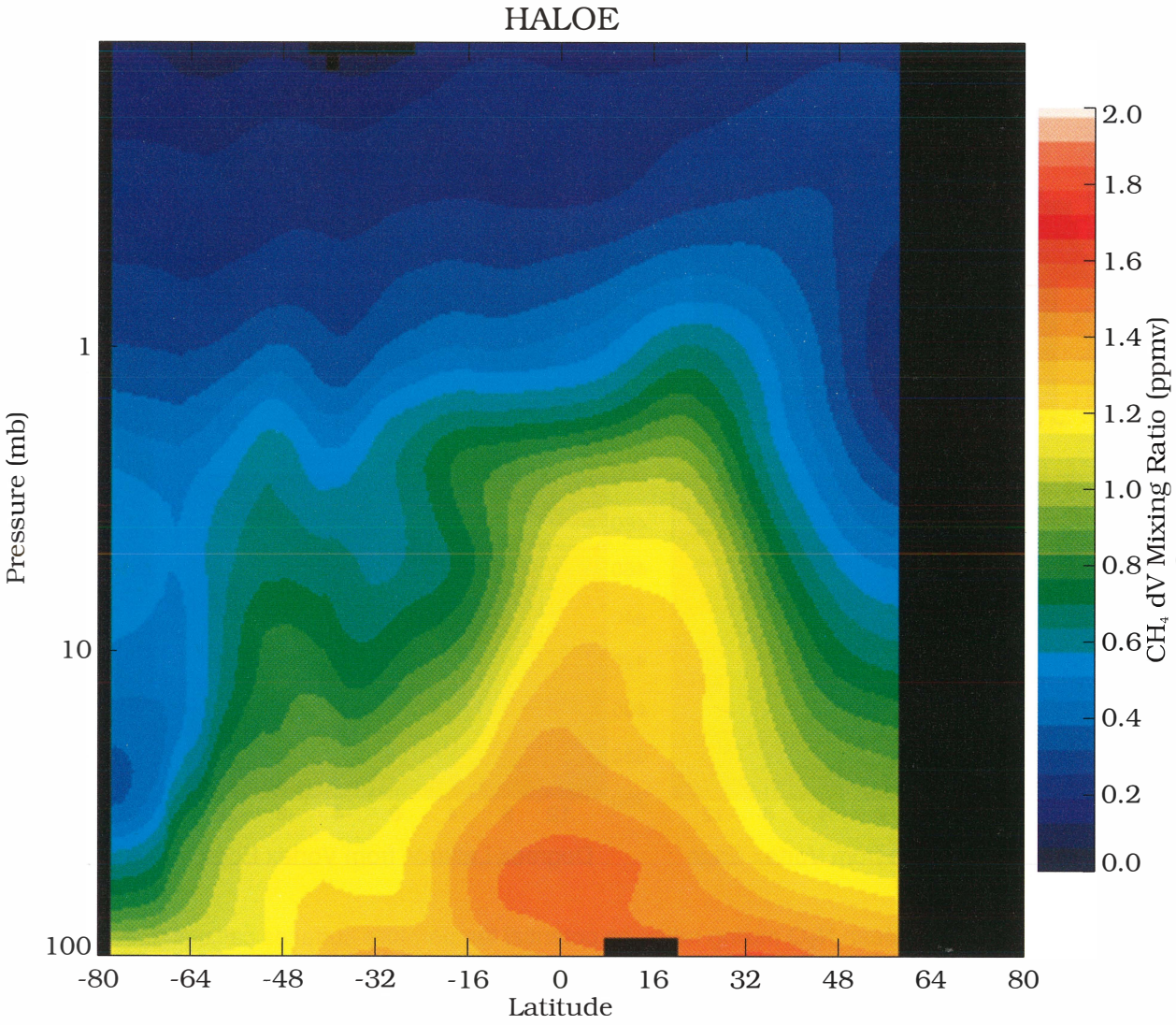

Figure 3-5. Pressure versus latitude cross section of CH_4 from the UARS Halogen Occultation Experiment (HALOE) satellite instrument. Data are from sunset scans over the period 21 September to 15 October 1992 analyzed with the version-17 algorithm. The pressure range corresponds to altitudes between about 16 and 65 km. Latitude is expressed in degrees, with negative latitude values corresponding to the Southern Hemisphere (adapted from Russell *et al.*, 1993b).

meteorological analyses and low N_2O from satellite fields shows excellent correspondence in the Arctic, thereby increasing confidence in the analysis of vortex structure (Manney *et al.*, 1994a). Simulations using a general circulation model and an improved two-dimensional model successfully reproduce important features of the observed N_2O distributions in and near the northern vortex (see Figure 3-4 and Section 3.5.5) (Strahan and Mahlman, 1994a; Garcia *et al.*, 1992).

Satellite observations of CH_4 and HF reveal unmixed vertical descent taking place at the center of the vortex in the Antarctic (see Figure 3-5) (Russell *et al.*, 1993b). The lack of vertical gradient indicates that air at lower altitudes containing larger CH_4 values has not been mixed with the descending air. Although not observed before, the strong descent implied by the observations matches earlier predictions (Danielsen and Houben, 1988). The observations are qualitatively simu-

lated with a mechanistic three-dimensional (3-D) model (see Section 3.5.5), following many atmospheric air parcels as they undergo transport from the mesosphere as a result of radiative cooling in winter and early spring (Fisher *et al.*, 1993). These results augment the depiction of the vortex in Figure 3-2, further clarifying its dynamical evolution.

Observations have established that simple, compact relationships exist in the lower stratosphere between N_2O and other long-lived species that also are photochemically destroyed in the stratosphere. These relationships result when photochemical lifetimes are long compared to transport and mixing times between low- and high-latitude regions (Plumb and Ko, 1992; Mahlman *et al.*, 1980). The compactness of the relationship allows one of the species to be predicted confidently from a measurement of the other. The distribution of N_2O in and near the vortex is often related to the distribution of PV and potential temperature (Strahan and Mahlman, 1994a, b). Thus, these relationships are useful in predicting conditions throughout the vortex relevant to the specific reactive processes that control ozone. However, since the knowledge of these relationships is based on limited data sets, assimilation of further data must continue in order to establish the range of applicability.

The first of three important examples of these relationships is that of N_2O to organic and inorganic chlorine reservoirs (see Figure 3-6) (Woodbridge *et al.*, 1994; Schmidt *et al.*, 1991, 1994; Schauffler *et al.*, 1993; Kawa *et al.*, 1992a). The principal species in the organic chlorine reservoir, CCl_y,

$$\begin{aligned} CCl_y = {} & CCl_2F_2 \text{ (CFC-12)} + CCl_3F \text{ (CFC-11)} + \\ & CCl_2FCClF_2 \text{ (CFC-113)} + \\ & CCl_4 \text{ (carbon tetrachloride)} + \\ & CH_3CCl_3 \text{ (CFC-140a)} + \\ & CHClF_2 \text{ (CFC-22)} + CH_3Cl \text{ (methyl chloride)} \end{aligned} \tag{3-1a}$$

include those species that comprise over 95 percent of the available organic chlorine in the stratosphere. Each species displays a compact correlation with N_2O, where the slope is related to the ratio of lifetimes in the stratosphere (see Chapter 2). As a consequence, CCl_y, as the sum over organic species, also shows a compact relation with N_2O. The inorganic chlorine reservoir, Cl_y,

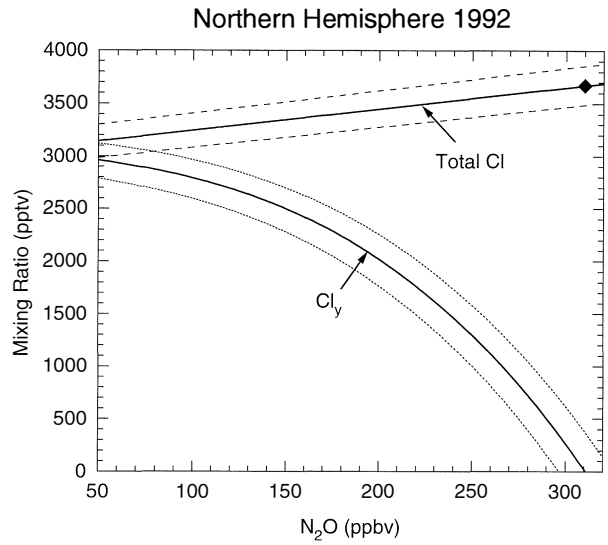

Figure 3-6. Total available chlorine (upper line) and total inorganic chlorine (Cl_y) (lower line) plotted versus N_2O from aircraft observations in the Arctic winter of 1991/92. The vertical scale is in parts per trillion by volume (pptv). Total organic chlorine (CCl_y) is the difference between total available chlorine and Cl_y. As the residence time of air increases in the stratosphere, photochemical reactions decrease N_2O values in an air parcel and convert CCl_y species to Cl_y species. The diamond symbol represents the reference point for tropospheric chlorine in 1991/92 of 3.67 ppbv. The dashed lines represent estimated uncertainties (Woodbridge *et al.*, 1994).

$$\begin{aligned} Cl_y = {} & Cl + 2Cl_2 + ClO + OClO + 2Cl_2O_2 + HOCl + \\ & HCl + BrCl + ClONO_2 \end{aligned} \tag{3-1b}$$

is produced as CCl_y and N_2O are destroyed in the stratosphere. Since Cl_y contains ClO, an effective reactant in ozone destruction, the distribution of Cl_y in polar regions is of great interest. The combination of the distribution of N_2O at high latitudes in Figure 3-4 and the compact relations in Figure 3-6 indicates how CCl_y and Cl_y are distributed throughout both vortices. Modeling of ozone loss throughout the vortex can be usefully constrained by knowledge of these distributions (Salawitch *et al.*, 1993).

The second example is the linear relationship between N_2O and the reactive nitrogen reservoir, NO_y (Fahey *et al.*, 1990a; Loewenstein *et al.*, 1993; Kondo *et al.*, 1994a). The primary source of NO_y,

$$NO_y = NO + NO_2 + NO_3 + 2N_2O_5 + HONO + HO_2NO_2 + HNO_3 + CH_3C(O)OONO_2 + ClONO_2 + BrONO_2 + \text{aerosol nitrate} + ..., \quad (3\text{-}2)$$

is the photochemical destruction of N_2O in the middle stratosphere. In the polar lower stratosphere in winter, the sequestering of active chlorine in the form of $ClONO_2$ moderates ozone destruction. The NO_y/N_2O correlation has been observed to be linear before vortex formation in the Northern Hemisphere and outside the vortex boundary in both hemispheres. Departures from linearity at low N_2O values have been observed as expected from the photochemical destruction of NO_y in the upper stratosphere. Departures from linearity at higher N_2O values demonstrate the irreversible removal of NO_y as a result of the sedimentation of aerosol particles containing NO_y species. This removal of NO_y greatly enhances the potential for ozone destruction in an air parcel located in the polar vortex in spring (Brune *et al.*, 1991; Salawitch *et al.*, 1993).

The third example is the correlation of ozone with N_2O that primarily follows from the production of ozone in regions where N_2O is photochemically destroyed. *In situ* aircraft measurements, satellite observations, and photochemical model simulations show linear correlations during winter months at mid- and high latitudes in the absence of significant polar ozone loss (Proffitt *et al.*, 1990, 1992, 1993; Weaver *et al.*, 1993). Since ozone also has loss processes in the stratosphere at other latitudes and during other seasons, deviations from a constant linear correlation cannot be attributed solely to vortex chemistry, particularly during summer and early fall at high latitudes (Perliski *et al.*, 1989; Proffitt *et al.*, 1992). However, during the vortex lifetime, changes in the correlation may be used to bound photochemical ozone loss in air parcels inside or near the vortex boundary (see Figure 3-7). This is especially useful inside and outside the Arctic vortex or outside the Antarctic vortex, where ozone changes are generally small in comparison to the natural variability.

3.3 PROCESSING ON AEROSOL SURFACES

3.3.1 Polar Stratospheric Cloud Formation and Reactivity

As shown in Figure 3-1, reservoir chlorine species are converted beginning in early winter to form the active chlorine species such as molecular chlorine (Cl_2) and, ultimately, ClO and its dimer Cl_2O_2. The conversion is attributed to processing of polar air by surface reactions involving both HCl and $ClONO_2$. The reactions occur on sulfate aerosol particles and polar stratospheric cloud (PSC) particles that form at the low temperatures and constituent concentrations characteristic of the interior of the winter vortices. The body of laboratory data on the formation thermodynamics and reactivities of these surfaces and the body of atmospheric observations of stratospheric aerosols and their constituents have continued to grow in this assessment period.

The basic features of the ternary condensation of nitric acid (HNO_3), sulfuric acid (H_2SO_4), and water (H_2O) in the stratosphere are illustrated in Figure 3-8. With an abundance ratio in the high-latitude lower stratosphere of these species of approximately 10 ppbv/1 ppbm/4 ppmv, respectively, H_2O is always the predominant constituent (ppbv = parts per billion by volume, ppbm = parts per billion by mass, ppmv = parts per million by volume). For volcanically perturbed conditions, the range of H_2SO_4 abundance can reach 100 ppbm. Volcanic activity over the past 25 years has increased the average H_2SO_4 abundance in the stratosphere to near 5 ppbm. Confidence in the features of the ternary system has been established in a wide variety of laboratory experiments and with the use of thermodynamical constraints (Molina *et al.*, 1993; Kolb *et al.*, 1994). At the highest temperatures, liquid aerosol particles composed primarily of H_2SO_4 and H_2O are present in the lower stratosphere at all latitudes. At lower temperatures (< 200 K), the H_2SO_4/H_2O liquid increasingly takes up HNO_3. If the particles undergo freezing, HNO_3 hydrates become stable: nitric acid dihydrate ($HNO_3{\cdot}2H_2O$ = NAD) and nitric acid trihydrate ($HNO_3{\cdot}3H_2O$ = NAT). Liquid or frozen particles that contain appreciable HNO_3 at temperatures above the frost point are termed Type I PSC particles. In the absence of HNO_3, the H_2SO_4/H_2O liquid aerosol can freeze to form sulfuric acid tetrahydrate (SAT) or other sulfate hydrates. Below

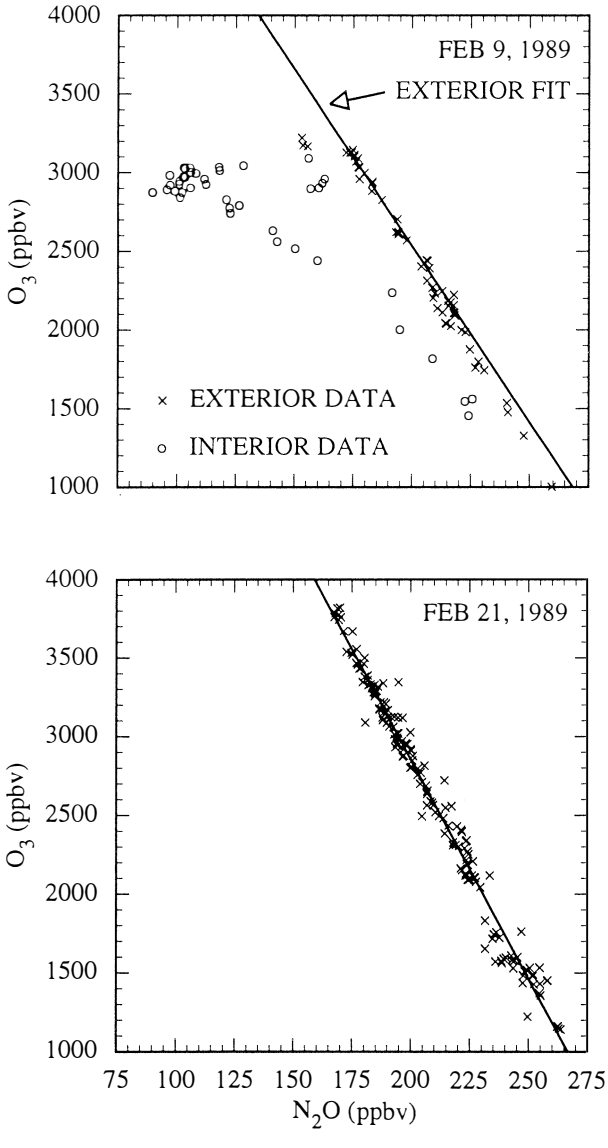

Figure 3-7. Average ozone and N_2O values from aircraft observations. Top: Data from the Arctic polar vortex (60°N to 80°N) on 9 February 1989. Bottom: Data from the continental United States (37°N to 39°N) on 21 February 1989. Data taken inside and outside the vortex are denoted as interior and exterior data, respectively (adapted from Proffitt *et al.*, 1992).

the frost point, Type II PSCs are formed as the condensation of H_2O predominates in the continued growth of the particles, with condensation of HNO_3 playing a lesser role. Recent laboratory results that underlie the PSC formation features in Figure 3-8 are the following:

- HNO_3 is soluble in liquid H_2SO_4/H_2O aerosols as temperatures approach the frost point where the aerosol composition becomes 8 to 12 weight percent (wt%) HNO_3 and 35 to 40 wt% H_2SO_4 (Molina *et al.*, 1993; Reihs *et al.*, 1990; Zhang *et al.*, 1993a, b). Thermodynamic models suggest that dramatic changes take place when the frost point is approached, rendering the aerosol into a binary HNO_3/H_2O solution (Carslaw *et al.*, 1994; Tabazadeh *et al.*, 1994).
- As temperatures are reduced in $HNO_3/H_2SO_4/H_2O$ mixtures, NAD nucleates from the vapor phase before NAT under some conditions (Middlebrook *et al.*, 1992; Worsnop *et al.*, 1993).
- $HNO_3/H_2SO_4/H_2O$ solutions with compositions similar to those estimated for the high-latitude stratospheric aerosols yield NAT, SAT, and possibly other hydrates upon freezing (Molina *et al.*, 1993).
- Solutions containing only H_2SO_4 and H_2O crystallize with difficulty for compositions corresponding to stratospheric abundances and temperatures greater than but near the frost point (Molina *et al.*, 1993; Ohtake, 1993; Luo *et al.*, 1994a).
- NAT crystallizes readily from $HNO_3/H_2SO_4/H_2O$ solutions at temperatures for which HNO_3 is supersaturated (> 10) with respect to NAT formation. Typically, this occurs several degrees above the frost point in the lower stratosphere (Molina *et al.*, 1993). The relationship of bulk solution properties to those of stratospheric aerosols has not been determined (Carslaw *et al.*, 1994).
- SAT melts at 220 to 230 K when exposed to partial pressures of H_2O that are typical of the lower stratosphere (Middlebrook *et al.*, 1994; Zhang *et al.*, 1993a).

Both NAT and NAD may play a role in Type I PSC formation when saturation ratios for HNO_3 are greater than unity. However, the phase of Type I PSCs is not certain in this temperature range, as illustrated in Figure 3-8 (Dye *et al.*, 1992). Once frozen, SAT within the particles may remain a solid well above the initial freezing tempera-

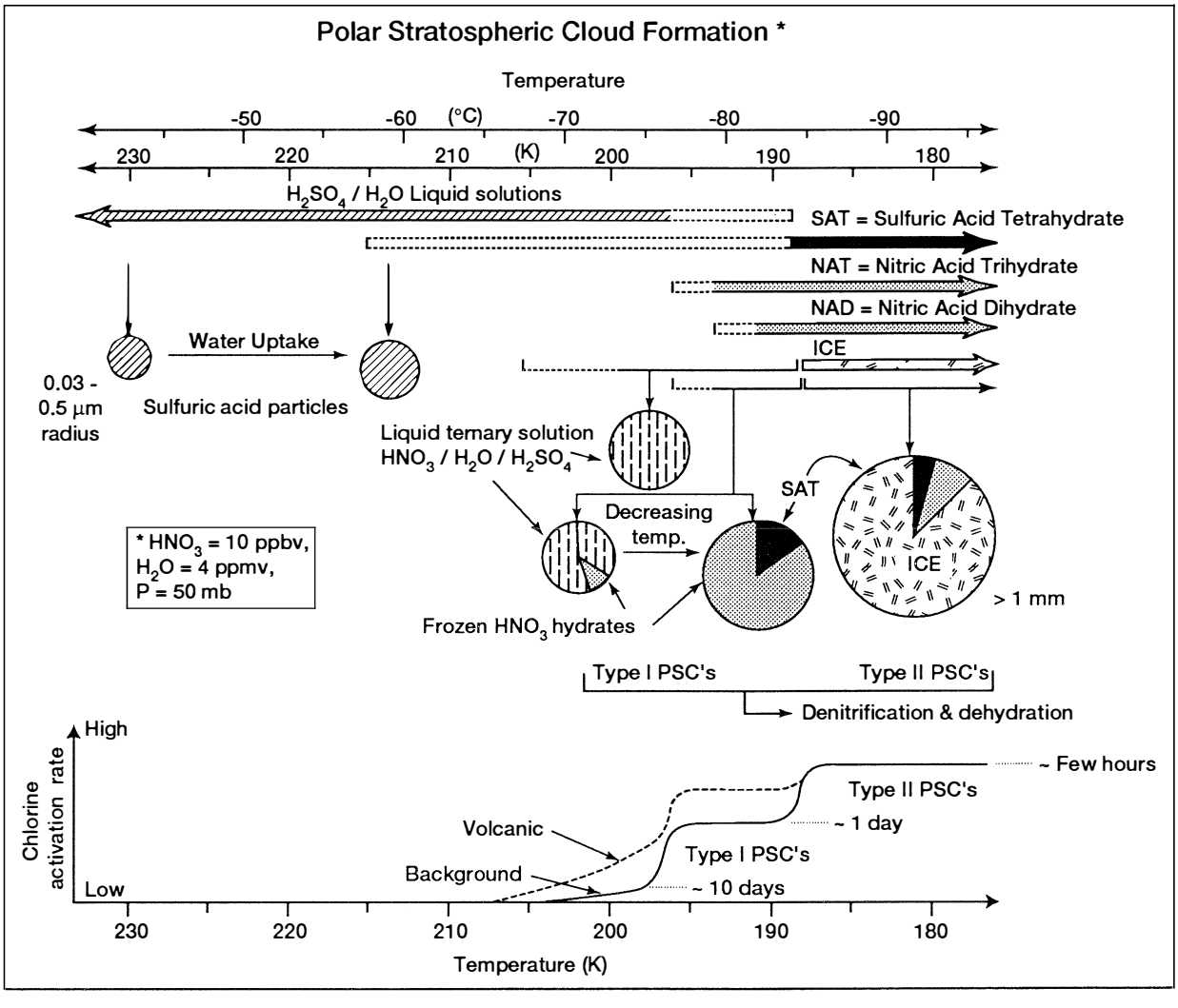

Figure 3-8. Schematic representation of the ternary condensation system for nitric acid (HNO_3), sulfuric acid (H_2SO_4), and water (H_2O) over a range of temperatures where growth of aerosols occurs to form Type I and II PSC particles in the stratosphere. The changes are represented for nominal abundances of condensing species in the lower polar stratosphere as indicated. The shading in the horizontal arrows and circular particle diagrams represents various binary and ternary compositions as indicated. In the lower part, the chlorine activation rate on PSCs is represented as a function of temperature (adapted from J. E. Dye, private communication, 1994).

ture. The phase of the particles above the frost point affects the rate of surface conversion for reactive nitrogen and chlorine species (see Table 3-1).

The principal heterogeneous reactions of H_2SO_4/HNO_3/H_2O aerosols in Figure 3-8 are listed in Table 3-1. Reaction rates are considered fast if reaction probabilities are in the range 0.01-0.1 for temperatures and reactant abundances characteristic of the stratosphere. Reactions involving H_2O are influenced by its ubiquitous presence in aerosol particles throughout the stratospheric temperature range. Reactions with HCl depend on the solubility of HCl in an aerosol particle. Laboratory studies of Reaction (3-3) reveal that the reaction probability depends strongly on relative humidity and, to a lesser extent, on aerosol composition. Specifically, the reaction probabilities for Reaction (3-3) are similar on Type I PSCs, SAT, and liquid sulfuric acid over a wide temperature range at stratospheric relative humidity (see Figure 3-9) (Molina *et al.*, 1993; Hanson and Ravishankara, 1994). The probability for Reaction (3-5) increases exponentially as the sulfate aerosol dilutes with H_2O near 200 K and below (Cox *et al.*, 1994), as does the probability of Reaction (3-4) due to enhanced uptake of HCl (Hanson and Ravishankara, 1993; Luo *et al.*, 1994b). The increase suggests that Reactions (3-4) and (3-5) may play a significant role in chlorine processing when temperatures are low but do not reach Type I or Type II temperatures (Solomon *et al.*, 1993; Hanson *et al.*, 1994).

The growth of the ternary aerosol system from sulfate aerosols to Type I and II PSCs and the surface reactions in Table 3-1 combine effectively to release active chlorine in the polar regions. In Figure 3-8, the rate of chlorine activation is qualitatively noted as a function of temperature. Some activation occurs on background aerosol particles prior to temperatures decreasing to Type I formation temperatures. The rate increases significantly as more surface area containing HNO_3 hydrates and ice forms. Inside the polar vortices, full activation within an air parcel is estimated to occur within a day or perhaps a few hours. Thus, the initial activation of the entire vortex can occur in a matter of days (Newman *et al.*, 1993). When aerosol particle size and surface area are increased by volcanic eruptions, the rate of activation can be significantly enhanced at temperatures above Type I formation.

Table 3-1. Rates of heterogeneous reactions on polar stratospheric cloud particles and sulfate aerosol particles.

	PSCs		Sulfate Aerosols		
	Ice (Type II)	HNO_3 hydrates[a] (Type I)	Supercooled	Frozen	
$ClONO_2 + HCl \rightarrow Cl_2 + HNO_3$	Fast f(RH)[b]	Fast f(RH)[b]	f(wt% H_2SO_4)[b]	Fast f(RH)[b]	(3-3)
$HOCl + HCl \rightarrow Cl_2 + H_2O$	Fast f(RH)[b]	Fast f(RH)[b]	f(wt% H_2SO_4)[b]	Fast f(RH)[b]	(3-4)
$ClONO_2 + H_2O \rightarrow HOCl + HNO_3$	Fast	Slow	f(wt% H_2SO_4)[b]	Slow	(3-5)
$N_2O_5 + H_2O \rightarrow 2HNO_3$	Fast	Slow	Fast	Slow	(3-6)
$N_2O_5 + HCl \rightarrow ClNO_2 + HNO_3$	c	c	c	c	(3-7)

[a] Nitric acid trihydrate (NAT), nitric acid dihydrate (NAD)

[b] Rate is function of aerosol wt% H_2SO_4 or relative humidity (RH).

[c] Unlikely to be fast, but not well studied

References: Abbatt and Molina, 1992a, b; Chu *et al.*, 1994; Fried *et al.*, 1994; Hanson and Ravishankara, 1991, 1992, 1994; Kolb *et al.*, 1994; Middlebrook *et al.*, 1992, 1994; Molina *et al.*, 1993; Van Doren *et al.*, 1991; Zhang *et al.*, 1994

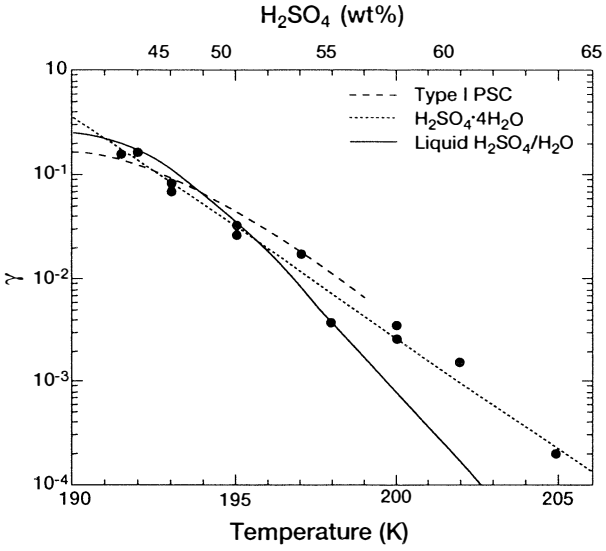

Figure 3-9. Temperature dependence of the reaction probability γ for Reaction (3-3), $ClONO_2$ + HCl, occurring on surfaces of sulfuric acid tetrahydrate ($H_2SO_4 \cdot 4H_2O$ = SAT), nitric acid trihydrate (NAT) or Type I PSCs, and liquid sulfuric acid and water solutions, H_2SO_4/H_2O. The measurements are made at a constant partial pressure of water vapor of 0.2 mTorr. Thus, relative humidity increases as temperature decreases. The weight percent (wt%) of the corresponding sulfuric acid/water solution is indicated on the top axis (adapted from Hanson and Ravishankara, 1994).

3.3.2 Atmospheric Observations

3.3.2.1 Aerosol Measurements

The threshold formation and growth of PSC aerosol particles have been observed *in situ* over a wide range of conditions in both polar regions (Hofmann *et al.*, 1989, 1990; Hofmann and Deshler, 1989). Satellites have made global aerosol observations using the extinction of solar illumination (Osborn *et al.*, 1990). The data show a persistent increase in aerosol extinction in polar regions when temperatures fall to the range below where Type I PSCs are expected (see Figure 3-10) (Poole and Pitts, 1994). The observations do not allow the phase of the aerosol to be determined. Lidar measurements in both polar regions also detect aerosol layers where temperatures reach estimated PSC thresholds (Gobbi and Adriani, 1993; Browell *et al.*, 1990). Lidar polarization measurements indicate that both spherical and nonspherical particles are present in cloud events (Kent *et al.*, 1990; Adriani *et al.*, 1994; Toon *et al.*, 1990a). *In situ* measurements with balloons show enhancements in the size distribution for larger particles (Deshler *et al.*, 1994). Distinct growth begins on some particles near the threshold for HNO_3 hydrates (Dye *et al.*, 1992) and involves all pre-existing particles before decreasing temperatures reach the frost point (Hofmann *et al.*, 1990). Other measurements near the edges of PSCs have been made with simultaneous constituent measurements of reactive nitrogen and water (Kawa *et al.*, 1992b). These measurements show definitively that the condensed phase includes reactive nitrogen species in the form of HNO_3, but that significant aerosol growth above background values often requires a large supersaturation of HNO_3 over the stable hydrate phases.

The systematic formation of aerosol containing HNO_3 is well documented. However, aerosol measurements of concentration, size, phase, and composition correlated with the gas phase abundance of the principal condensing species H_2SO_4, HNO_3, and H_2O are critically absent in observational studies. In addition, observations are not available to constrain important features of the nucleation and early growth stages in an aerosol. Without such measurements, the ability to predict the distribution of aerosol particles and their chemical reactivity remains limited.

3.3.2.2 Release of Active Chlorine

Active chlorine is produced as a result of the heterogeneous reactions in Table 3-1. The photolysis of the Cl_2 and hypochlorous acid (HOCl) reaction products forms Cl, which in turn reacts with ozone to produce ClO. ClO participates in catalytic reaction cycles that destroy ozone (see Section 3.4.1). The activation of chlorine over the winter poles has been clearly demonstrated by *in situ* and remote measurements of ClO (Anderson *et al.*, 1991; WMO, 1992; Toohey *et al.*, 1993; deZafra *et al.*, 1987). The spatial and temporal scale of ClO observations has been significantly extended by the UARS satellite (Waters *et al.*, 1993a, b; Manney *et al.*, 1994b). Observations are available in both polar regions from vortex formation to photochemical recovery in the 1991/92 northern winter and the 1992 southern winter (see Figure 3-11). In early northern winter (14 December), infrequent PSCs keep ClO values low inside the vortex

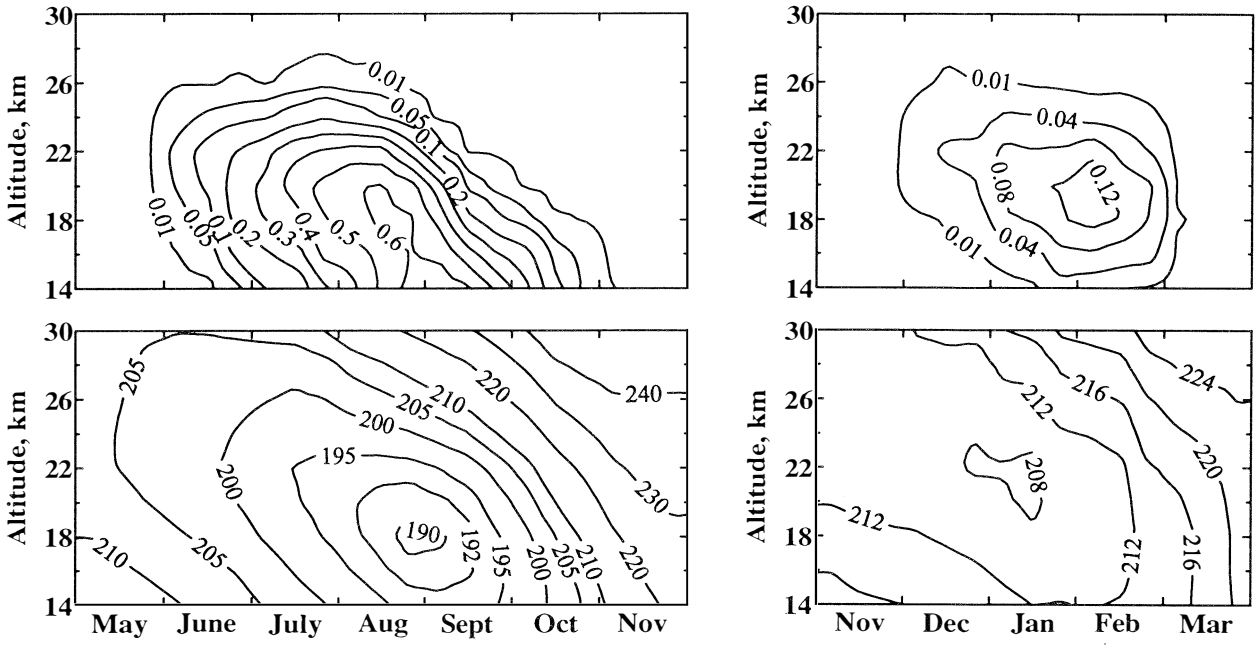

Figure 3-10. PSC sighting probabilities (top panels) as a function of altitude in the lower stratosphere during the winter months in the Antarctic (left) and in the Arctic (right). Data are zonal averages of the Stratospheric Aerosol Measurement II (SAM II) satellite data set for the years 1978 to 1989. The bottom panels represent the analyzed temperatures in Kelvin from the National Oceanic and Atmospheric Administration coinciding with the PSC observations in the upper panels. A PSC is identified as an extinction ratio significantly larger than that of the local background aerosol. The analysis is confined to the inside of the respective vortex defined by a maximum in the geopotential height gradient (Poole and Pitts, 1994).

near 18 km (465 K). In early southern winter (1 June), lower temperatures activate sulfate aerosol and begin the formation of PSCs, increasing ClO accordingly. In areas of darkness inside the vortex, active chlorine is in the form of Cl_2, Cl_2O_2, or HOCl. When air parcels make excursions to sunlit lower latitudes within the vortex flow, ClO values increase directly from the photolysis of Cl_2O_2 or indirectly from the photolysis of Cl_2. As the geographic area and frequency of PSCs continue to increase due to lower temperatures (2 January/11 July), ClO values and their extent increase substantially in both vortices. In some areas over both poles, ClO values indicate that essentially all available chlorine is in the active form. Outside the vortex, little ClO is formed. When PSCs cease to exist (17 February), ClO values fall as reservoir chlorine is photochemically reformed. In the southern vortex, high ClO values persist in September because gas phase HNO_3 is suppressed either due to temperatures below the PSC threshold, which sequester HNO_3 in aerosols, or to the removal of HNO_3 in denitrification (see Section 3.3.2.5). This sequence for the distribution of ClO is qualitatively and quantitatively consistent with other *in situ* and remote measurements (Toohey *et al.*, 1993; Crewell *et al.*, 1994; Gerber and Kämpfer, 1994).

Features of the ClO temporal and spatial distribution are consistent with the theoretical determination of PSC activity associated with low temperatures (Waters *et al.*, 1993a). The dependence of ClO on PSC activity and, hence, temperatures within the vortex, is demonstrated by contrasting ClO observations on 15 February in late northern winter for two consecutive years (see Figure 3-12). In 1993, the vortex contained temperatures below 195 K, significantly lower than found in 1992. Changes in available chlorine (Cl_y) cannot explain increased active chlorine found in 1993. Instead, the changes are attributed to increased formation and reactivity of aerosols at the lower stratospheric temperatures

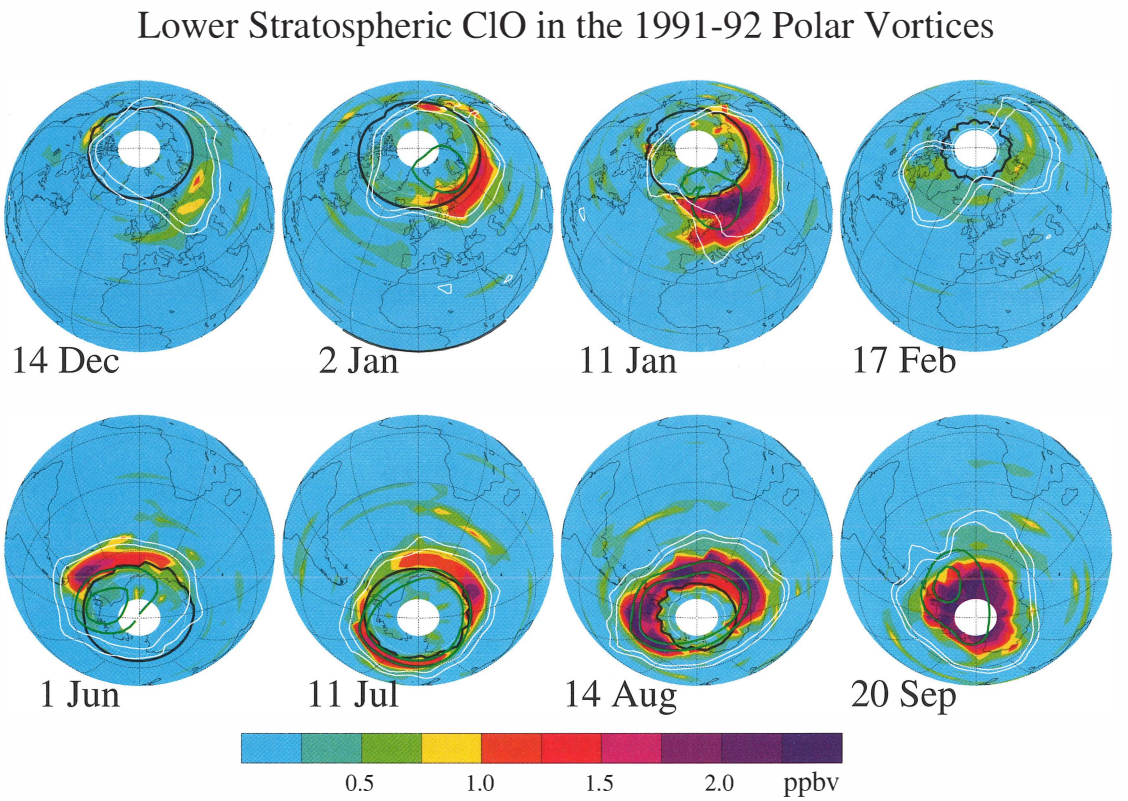

Figure 3-11. (a) Observations of lower stratospheric ClO in the 1991/92 northern winter (top row) and 1992 southern winter (bottom row) from the Microwave Limb Sounder (MLS) on UARS. The color bar gives ClO abundances in parts per billion by volume (ppbv) interpolated to the 465 K isentropic surface in the lower stratosphere (see Figure 3-4 for altitude reference). The irregular white lines are contours of potential vorticity (2.5 and 3.0 x 10^{-5} K $m^2kg^{-1}s^{-1}$) indicating the polar vortex boundary. Measurements poleward of the black contour were made for solar zenith angles greater than 91° (in darkness or edge of daylight). The edge of polar night is shown by the thin white circle concentric with the pole. No measurements are available in the white area poleward of 80° latitude. The green contours indicate temperatures of 190 K (inner) and 195 K (outer) (Waters *et al.*, 1993a, b).

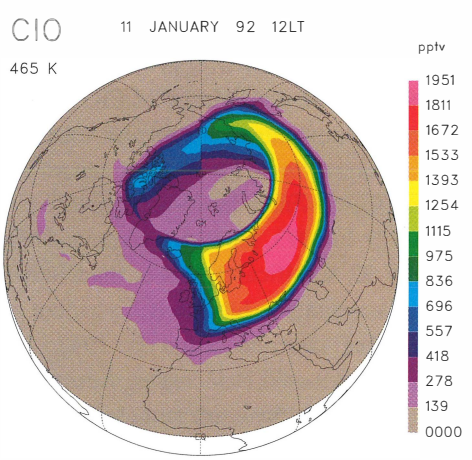

Figure 3-11. (b) ClO distribution calculated with a three-dimensional chemistry and transport model of the stratosphere. The ClO field for 11 January 1992 on the 465 K potential temperature surface was mapped at all locations for local noon to achieve better temporal coincidence with UARS satellite measurements in (a) (note discontinuity on both sides of date line) (Lefèvre *et al.*, 1994).

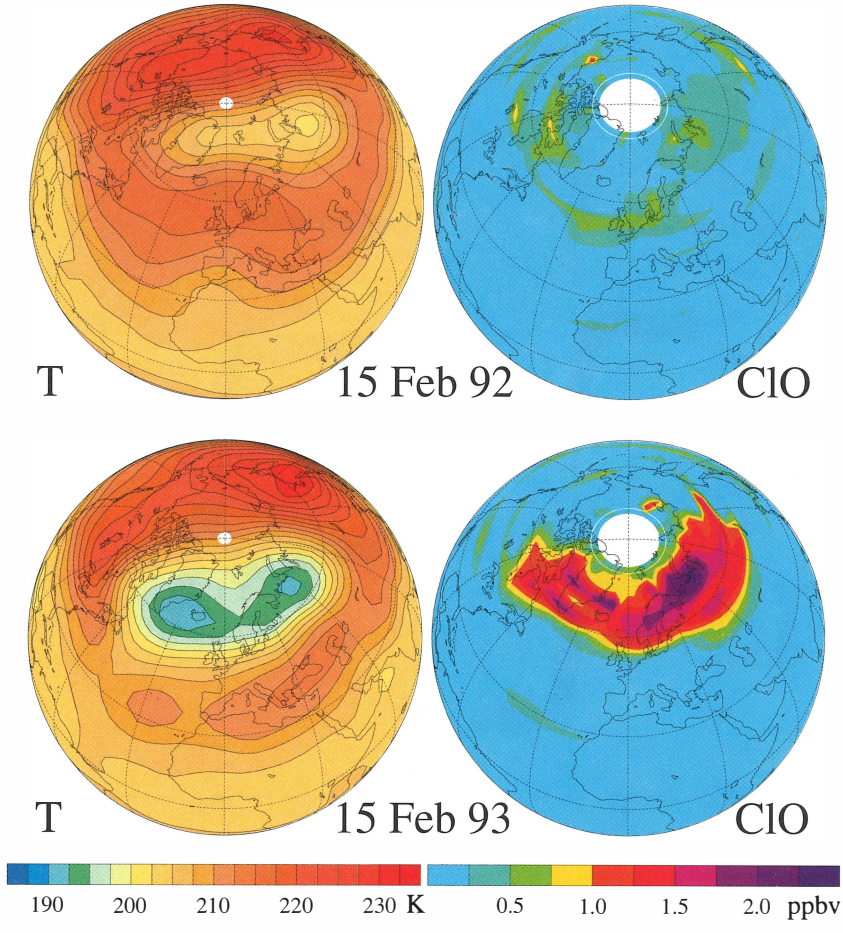

Figure 3-12. Observations of ClO from the UARS MLS satellite instrument and NMC temperatures in the lower stratosphere at 465 K potential temperature in the Northern Hemisphere on 15 February 1992 and 1993 (see Figure 3-4 for altitude reference). No measurements are available in the white area poleward of 80° latitude (Waters *et al.*, 1993a).

in 1993 as demonstrated in a 3-D model simulation (Chipperfield, 1994a). The 15 February data sets are representative of the systematic differences in ClO and temperature between 1992 and 1993 and, hence, also demonstrate interannual variability characteristic of the Northern Hemisphere vortex (see Section 3.4.2).

Observed changes in ClO are also consistent with changes within the reactive nitrogen reservoir. Activation of a large fraction of available chlorine to ClO sets an upper limit on NO_x (= NO + NO_2) that can be present in the NO_y reservoir (see Equation (3-2)) to form $ClONO_2$. From *in situ* observations near the vortex edge, nitric oxide (NO) is suppressed wherever ClO is enhanced (Toohey *et al.*, 1993; Kawa *et al.*, 1992a). The same reactions that activate chlorine (see Table 3-1) reduce NO and NO_x through the formation of HNO_3, a longer-lived species. In addition, NO_x is reduced indirectly through denitrification, the irreversible removal of NO_y (see Section 3.3.2.5). Column measurements of nitrogen dioxide (NO_2) and HNO_3 are generally consistent with expected changes in NO_y partitioning (Solomon and Keys, 1992; Keys *et al.*, 1993; Wahner *et al.*, 1990a; Koike *et al.*, 1994).

Activation of chlorine is also indicated by increases in OClO, formed in the reaction ClO + BrO (Solomon *et al.*, 1989; Tung *et al.*, 1986; Sanders *et al.*, 1993). OClO has been observed in both vortices, with the largest column abundances found in the Antarctic vortex

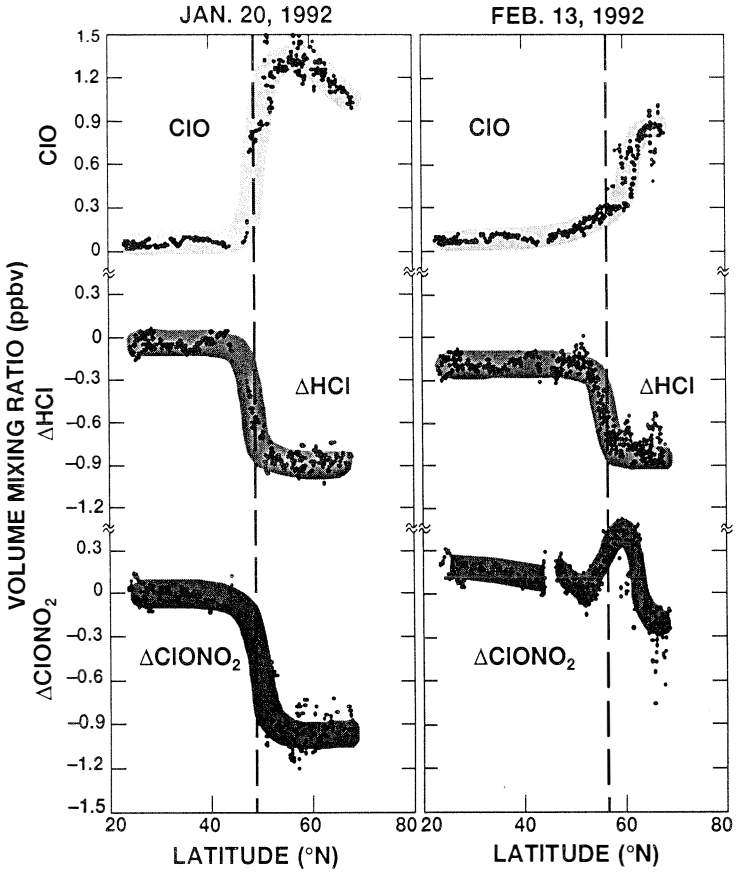

Figure 3-13. Aircraft data from 20 January and 13 February in the 1992 Arctic winter. Values for the changes in HCl and $ClONO_2$ are noted as ΔHCl and $\Delta ClONO_2$, respectively, where negative values indicate depletion. Values of ΔHCl are determined using the observed correlation with N_2O as a reference. Values for $\Delta ClONO_2$ are derived in three steps. First, total inorganic chlorine is estimated along the flight track from the correlation of total organic chlorine with N_2O (see Figure 3-6) (Kawa *et al.*, 1992a). Second, $ClONO_2$ is assumed to be the balance in the inorganic chlorine reservoir after account is made for measured HCl, ClO, and calculated Cl_2O_2. Third, changes in $ClONO_2$ from that calculated using the reference value of HCl are designated as $\Delta ClONO_2$. The dotted vertical line indicates the vortex edge determined from the maximum zonal wind measured on board the aircraft (Webster *et al.*, 1993a).

(Schiller *et al.*, 1990; Sanders *et al.*, 1993; Brandtjen *et al.*, 1994). The abundances are broadly consistent with expectations from model simulations. In the Arctic and Antarctic vortex regions following the eruption of Mt. Pinatubo, increases in OClO were observed before PSC temperatures were noted in the lower stratosphere (Solomon *et al.*, 1993; Perner *et al.*, 1994). Such measurements are a sensitive indicator of changes in active chlorine, especially for the low Sun conditions characteristic of high-latitude winter. The activation, attributed to enhancements in the rate of Reaction (3-5) on volcanic sulfate aerosols, implies additional ozone destruction at high latitudes during periods of enhanced aerosol.

3.3.2.3 Changes in Reservoir Chlorine

The selective conversion of the inactive chlorine reservoirs HCl and $ClONO_2$ in surface reactions occurring in the polar vortices is a fundamental aspect of the ozone depletion process depicted in Figure 3-1. In previous assessments, polar observations of these reservoir species were limited to remote soundings from the ground and aircraft *in situ* measurements. However, the

general feature of the winter conversion of the reservoirs and their subsequent formation in spring can be found in these observations. New observations include simultaneous *in situ* measurements of HCl and ClO in the Arctic region (see Figure 3-13) (Webster *et al.*, 1993a, b). In addition, $ClONO_2$ is deduced as the residual in the Cl_y reservoir after account is made for HCl, ClO, and estimated Cl_2O_2 (see Figure 3-6). Near-complete removal of HCl was observed in some air masses at 20 km in the vortex. Changes at the vortex edge show losses in the reservoir species that correlate with increased ClO. Losses in the reservoir species are comparable and equate well with the sum of observed ClO and calculated Cl_2O_2, indicating stoichiometric conversion of HCl and $ClONO_2$ in Reaction (3-3). Before PSC processing, *in situ* HCl values are somewhat less than those of estimated $ClONO_2$ at mid- to high northern latitudes, conflicting with standard photochemical models which find HCl to be in excess. At lower latitudes away from PSC processing, the sum of the inorganic and organic chlorine species is constant throughout the lower and upper stratosphere, indicating that chlorine is conserved in the conversion of chlorine to inorganic forms (Zander *et al.*, 1992).

In remote ground-based measurements, the column abundance of HCl over northern Sweden was observed throughout midwinter 1991/92 (Bell *et al.*, 1994). The anticorrelation with column ClO clearly shows the conversion of HCl to active forms (see Figure 3-14). Earlier column measurements from aircraft showed the complete conversion of HCl and $ClONO_2$ deep inside the northern vortex in January and early February 1989 (Toon *et al.*, 1992). The measurements are consistent with complete removal of HCl up to 27 km. Profile measurements of $ClONO_2$ show that the midwinter depletion extends throughout a broad vertical region in the Arctic stratosphere (see Figure 3-15) (von Clarmann *et al.*, 1993).

The UARS remote measurements of HCl and $ClONO_2$ significantly extend the spatial and temporal scale of previous observations. Inside the edge of the Antarctic vortex in late September, significant depletion of HCl is found around a latitude circle near the vortex edge (see Figure 3-16) when HCl values are compared with those of the long-lived tracer species CH_4 and HF. These data sets confirm the large-scale depletion of HCl in low-temperature regions in the Antarctic vortex. Sat-

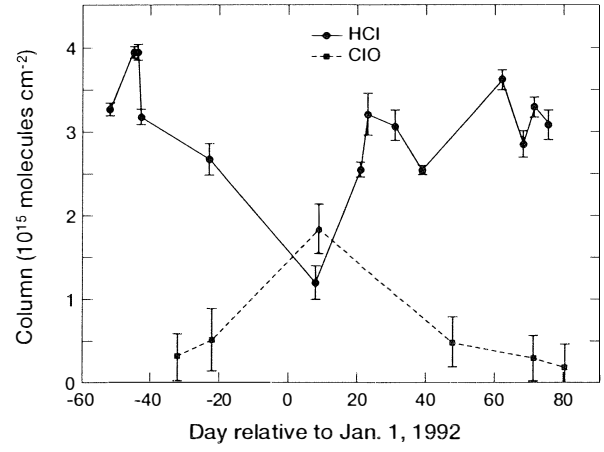

Figure 3-14. HCl and ClO column abundances over Åre, Sweden (63.4°N) during the EASOE campaign in 1992. The HCl column is measured by ground-based, infrared solar absorption spectroscopy. The ClO column is the amount above 100 mb (~16 km) at the same location as measured by the UARS MLS satellite instrument (Bell *et al.*, 1994).

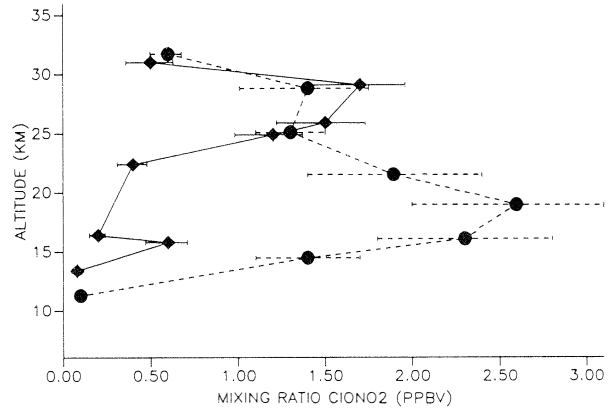

Figure 3-15. Retrieved Michelson Interferometric Passive Atmosphere Sounder-B (MIPAS-B) $ClONO_2$ profiles from balloon flights near Kiruna, Sweden (68°N) during the EASOE campaign in 1992. The peak of the 13 January mixing ratio profile (solid curve) is at a higher altitude than the peak of the 14/15 March profile (dashed curve). Similar values are obtained above 25 km, but large differences between the profiles appear in the lower stratosphere (von Clarmann *et al.*, 1993).

ellite measurements also show low abundances of $ClONO_2$ and HNO_3 inside the Antarctic vortex as early as mid-June (early winter), suggesting substantial PSC processing (see Figure 3-17) (Santee *et al.*, 1994; Roche *et al.*, 1993b, 1994). In addition, a region of high $ClONO_2$ surrounding the vortex is noted in late winter. $ClONO_2$ values will be enhanced in areas where processing is limited or infrequent, and where sunlight is available to produce NO_2 in the photolysis of HNO_3 and, thereby, reform $ClONO_2$ in advance of HCl (see Figures 3-1 and 3-17 and Section 3.4). This region, termed the "collar" region as first noted in remote soundings from aircraft (Toon *et al.*, 1989a), is also identifiable in estimates of $ClONO_2$ based on *in situ* observations near the vortex edge (see Figure 3-13). In late winter, the "collar" region extends into the sunlit vortex, as noted in Arctic soundings which show recovery of the vertical profile of $ClONO_2$ (see Figure 3-15). Although the early UARS observations are made in years of high volcanic aerosol loading, these observations and estimates of $ClONO_2$ add confidence to the role reservoir species play in the activation of chlorine.

3.3.2.4 Active Bromine

Although the bromine source gases in the stratosphere are less than one percent the size of chlorine source gases, active bromine in the form of BrO plays an important role in photochemical ozone destruction. *In situ* and remote observations establish the abundance of BrO in the range of 4 to 10 parts per trillion by volume (pptv), corresponding to approximately half of total available bromine (Toohey *et al.*, 1990; Wahner *et al.*, 1990b; Carroll *et al.*, 1989). Observations of high levels of OClO also confirm the presence of BrO since OClO is formed in the reaction ClO + BrO (see Section 3.3.2.2) (Salawitch *et al.*, 1988). Since gas phase photochemistry rapidly couples BrO with the inactive reservoirs ($BrONO_2$, HBr), BrO is readily available to participate in catalytic reaction cycles as described in detail in Chapter 10. Calculations based on observed abundances estimate that, depending on temperature, between 25 and 50 percent of ozone loss in the polar vortices is due to the ClO + BrO catalytic cycle (see Section 3.4.1) (Salawitch *et al.*, 1993). The fractional contribution to total ozone loss is estimated to be greater in the Arctic, where higher temperatures reduce the effectiveness of the ClO + ClO cycle.

3.3.2.5 Denitrification and Dehydration

PSC particles formed at low temperatures inside the polar vortices become large enough to sediment appreciable distances in the lower stratosphere over time periods much shorter than the winter season. As a result, up to 90 percent of available reactive nitrogen has been observed to be irreversibly removed from air parcels sampled *in situ* in both polar vortices (Fahey *et al.*, 1990a, b; Schlager and Arnold, 1990; Kondo *et al.*, 1992, 1994a; Arnold *et al.*, 1992). This irreversible removal defines denitrification. Removal of reactive nitrogen in the form of HNO_3 helps sustain active chlorine in an air parcel (see Section 3.4.3). Denitrification is quantified by using the NO_y/N_2O correlation observed at high latitudes in the absence of PSCs (see Section 3.2). *In situ* measurements indicate that the temporal and spatial extent of denitrification is substantially greater in the Antarctic, consistent with observed lower temperatures (see Figure 3-3). In the Arctic, at altitudes below particle formation, the evaporation of sedimenting aerosols enhances NO_y values (Hübler *et al.*, 1990). Another example of this redistribution is provided by the comparison of HNO_3 profile measurements and estimates of the unperturbed NO_y reservoir from the N_2O tracer correlation (Murcray *et al.*, 1994; Bauer *et al.*, 1994).

Satellite observations of HNO_3 at high latitudes now confirm the temporal and spatial scale of HNO_3 removal and the contrast between the two polar regions (Santee *et al.*, 1994; Roche *et al.*, 1994). In the Southern Hemisphere (see Figure 3-17), removal or sequestering of HNO_3 in aerosol particles is observed in late fall. Sequestering occurs when HNO_3 is reversibly incorporated into particles that do not undergo sedimentation. By midwinter, HNO_3 values less than 0.5 ppbv fill a large fraction of the vortex where ClO values are above 1 ppbv in the sunlit portion (see Figure 3-11a). Values of HNO_3 comparable to those expected from tracer correlations with NO_y (about 10 ppbv) surround the vortex at lower latitudes. By late winter, after PSC temperatures cease to occur, low HNO_3 values persist in the vortex, indicating denitrification. In the Northern Hemisphere (see Figure 3-17), higher average temperatures than in the Antarctic (see Figure 3-3) generally limit the removal or sequestering of HNO_3. An example is the local minimum in HNO_3 near Iceland in observations on 22 February 1993 (see Figure 3-17). Thus, sequestering and removal of HNO_3 is a predominant feature of the Antarctic vortex

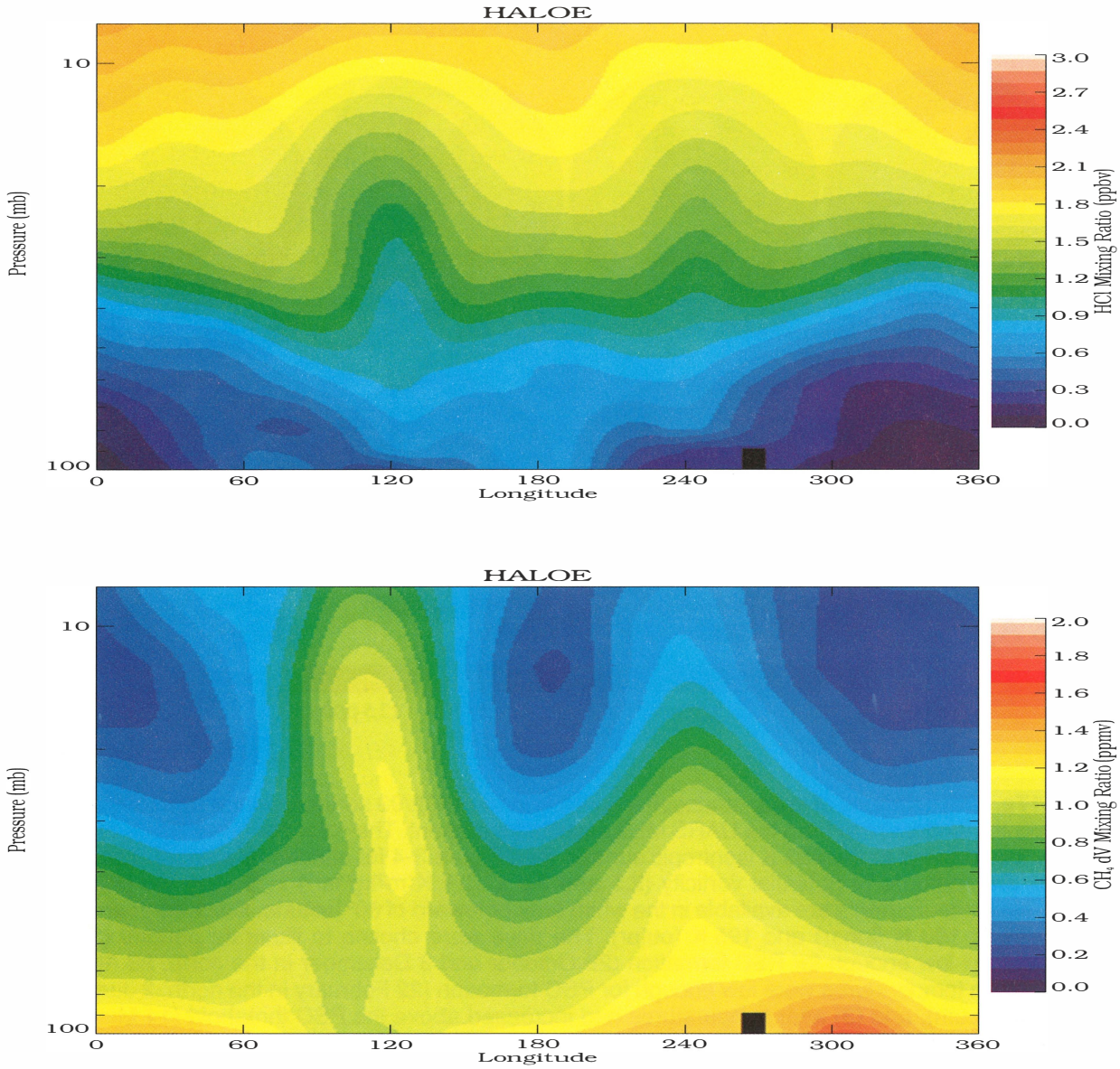

Figure 3-16. UARS HALOE satellite observations of HCl (top) and CH_4 (bottom) on 27 September 1992 in the Southern Hemisphere at 66°S latitude. The data are from sunrise scans analyzed with the version-16 algorithm. The pressure range corresponds to altitudes between 16 and 30 km. At low and high longitude values, the spatial gradients and low absolute values of HCl relative to CH_4 indicate depletion of HCl (adapted from Russell *et al.*, 1993b).

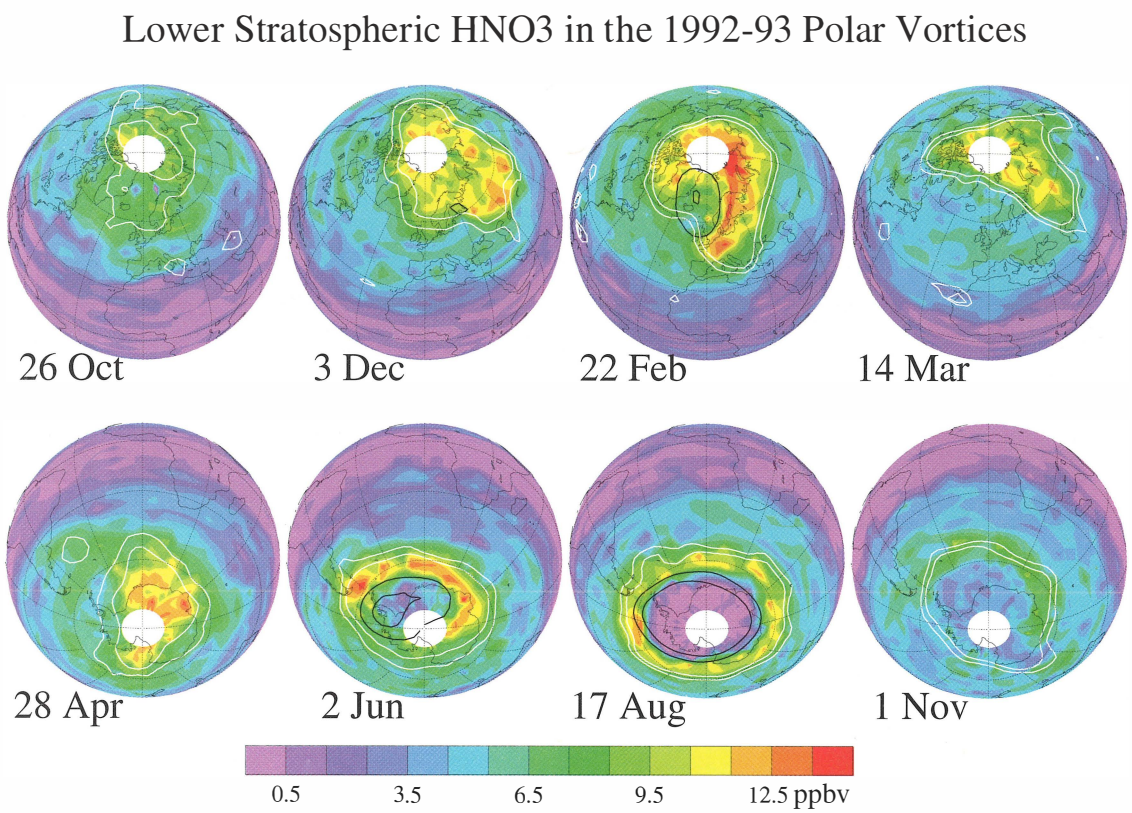

Figure 3-17a. Observations of lower stratospheric HNO_3 in the 1992/93 northern winter (top row) and 1992 southern winter (bottom row) from the UARS MLS satellite instrument. The color bar gives HNO_3 abundances in ppbv interpolated to the 465 K isentropic surface (see Figure 3-4 for altitude reference). The irregular white lines are contours of potential vorticity (2.5 and 3.0 x 10^{-5} K $m^2kg^{-1}s^{-1}$) indicating the polar vortex boundary. No measurements are available in the white area poleward of 80° latitude. Black contours indicate temperatures of 190 K (inner) and 195 K (outer). The days were chosen to illustrate periods (1) before temperatures fell low enough for PSC formation (26 October and 3 December in the north, 28 April in the south), (2) when temperatures were low enough for PSC formation (22 February in the north, 2 June and 17 August in the south), and (3) after temperatures had increased above the PSC threshold (14 March in the north, 1 November in the south) (Santee *et al.*, 1994).

for much of the winter, whereas removal in the Arctic is much less intense and more localized.

The irreversible removal of water, or dehydration, accompanies denitrification in the Antarctic but not in the Arctic (Fahey *et al.*, 1990b). Dehydration requires the sedimentation of Type II PSCs in order to effect the removal of 50 percent of available water as observed in the Antarctic region. Water vapor profiles in the winter vortices show interhemispheric differences, with lower values in the Antarctic. The differences reflect the more frequent occurrence of low temperatures in the Antarctic that facilitate Type II PSC formation (Kelly *et al.*, 1989; 1990). Balloon and satellite observations of H_2O and CH_4 in the Southern Hemisphere confirm extensive dehydration in the vortex and its near environment (Hofmann and Oltmans, 1992; Tuck *et al.*, 1993; Rind *et al.*, 1993). Because H_2O and molecular hydrogen (H_2) are produced in the oxidation of CH_4 in the stratosphere and mesosphere, changes in the quantity [$2CH_4 + H_2O$] are a more sensitive indicator of dehydration than changes in H_2O alone (see Figure 3-18 and Section 3.5.2). The large spatial and temporal scales of dehydration observed over the Antarctic are not observed anywhere else in the atmosphere (Tuck *et al.*, 1993). The combined re-

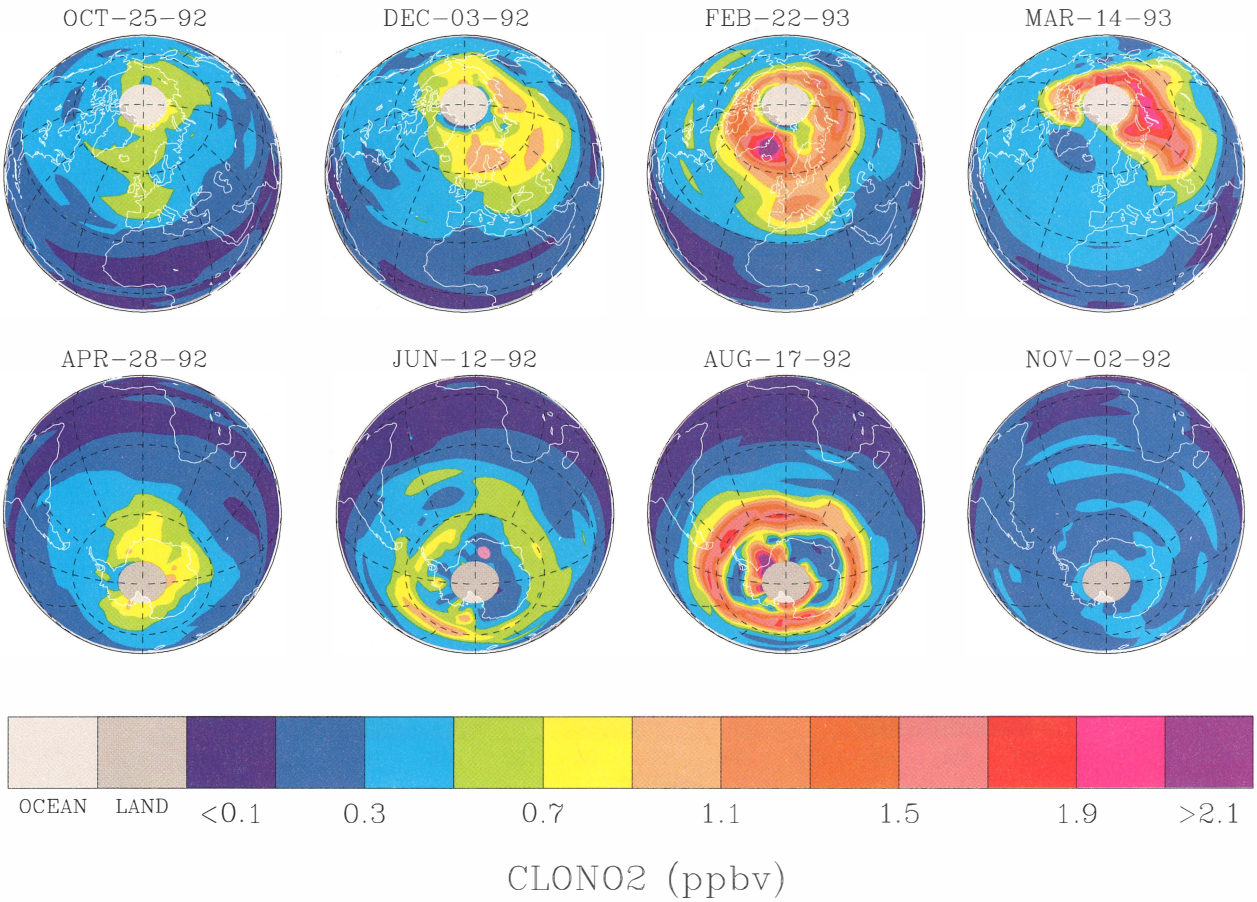

Figure 3-17b. Observations of lower stratospheric $ClONO_2$ in the 1992/93 northern winter (top row) and in the 1993 southern winter (bottom row) from the UARS Cryogenic Limb Array Etalon Spectrometer (CLAES) satellite instrument. The color bar gives $ClONO_2$ abundances in ppbv interpolated to the 465 K isentropic surface (see Figure 3-4 for altitude reference). The instrument does not see poleward of 80° latitude. The days were chosen to illustrate periods (1) before temperatures fell low enough for PSC formation (25 October and 3 December in the north, 28 April in the south), (2) when temperatures were low enough for PSC formation (22 February in the north, 12 June and 17 August in the south), and (3) after temperatures had increased above the PSC threshold (14 March in the north, 2 November in the south) (adapted from Roche *et al.*, 1994).

moval of H_2O and HNO_3 reduces the available condensable material for the formation of PSCs and, hence, lowers the minimum formation temperature. This feature is most notable in the Antarctic between the early and late winter periods (see Figure 3-10) (Poole and Pitts, 1994).

Despite extensive observational evidence for dehydration and denitrification, all of the underlying microphysical mechanisms and atmospheric conditions that control particle formation and sedimentation have not been completely confirmed in observational or laboratory studies. The overall process is complicated by the potential roles of air parcel cooling rates and barriers to nucleation of aerosol particles (Toon *et al.*, 1989b; Wofsy *et al.*, 1990a, b). The sedimentation process is generally better understood (Müller and Peter, 1992). The combined *in situ* data from both vortices show that intense denitrification (about 90-percent removal) oc-

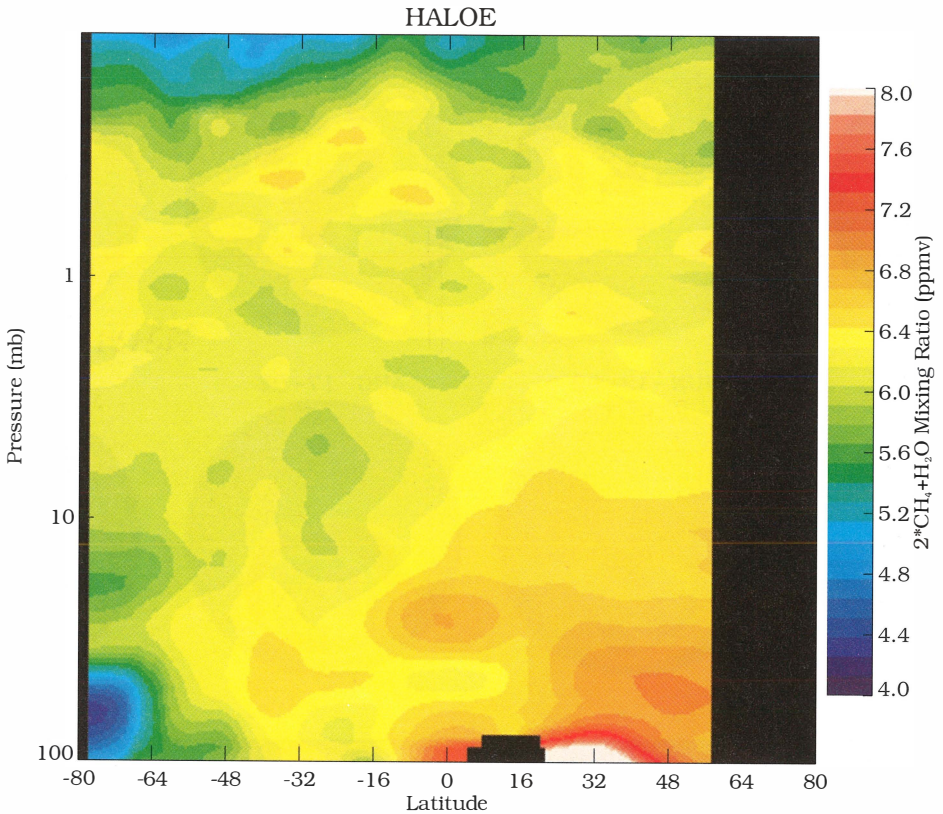

Figure 3-18. Latitude-altitude cross section of UARS HALOE satellite data for the period 21 September to 15 October 1992 for values of [$2CH_4 + H_2O$]. The data are from sunset scans analyzed with the version-17 algorithm. The progression of viewing latitude with date is shown above the panel, and the pressure range corresponds approximately to the 16 to 65 km altitude range. Latitude is expressed in degrees, with negative latitude values corresponding to the Southern Hemisphere (adapted from Tuck *et al.*, 1993).

curs with and without intense dehydration (about 50-percent removal). However, intense dehydration has not been observed without intense denitrification (Fahey *et al.*, 1990b). Observations do not preclude independent processes for intense denitrification and dehydration, as discussed in theoretical studies (Toon *et al.*, 1990b; Salawitch *et al.*, 1989; Wofsy *et al.*, 1990a, b). Water vapor plays a role in denitrification due to its presence in condensed hydrates of HNO_3 (see Figure 3-8). However, since gas phase abundances of water vapor exceed those of HNO_3 by large factors, changes in water vapor are negligible as denitrification occurs. In addition, the analysis of the export of denitrified and dehydrated air from the Antarctic vortex reveals a quantitative inconsistency that may be explained by independent removal processes (Tuck *et al.*, 1994).

3.3.3 Role of Mt. Pinatubo Aerosol

Volcanic eruptions are potentially important sources of sulfur dioxide (SO_2), HCl, and H_2O for the lower stratosphere (GRL, 1992). The eruption of Mt. Pinatubo in the Philippines in June 1991 is a recent large event that affected stratospheric measurements during this assessment period. The injection of SO_2 into the lower stratosphere in the tropics exceeded that of the El Chichón eruption in 1982 by three times (McCormick and Veiga, 1992). The SO_2 cloud rapidly forms H_2SO_4, which augments the formation and growth of sulfate aerosol particles in the stratosphere (Wilson *et al.*, 1993; Borrmann *et al.*, 1993). Figure 3-19 shows the evolution of aerosol extinction from near-background conditions before the 1991 eruption to one year later. Surface area

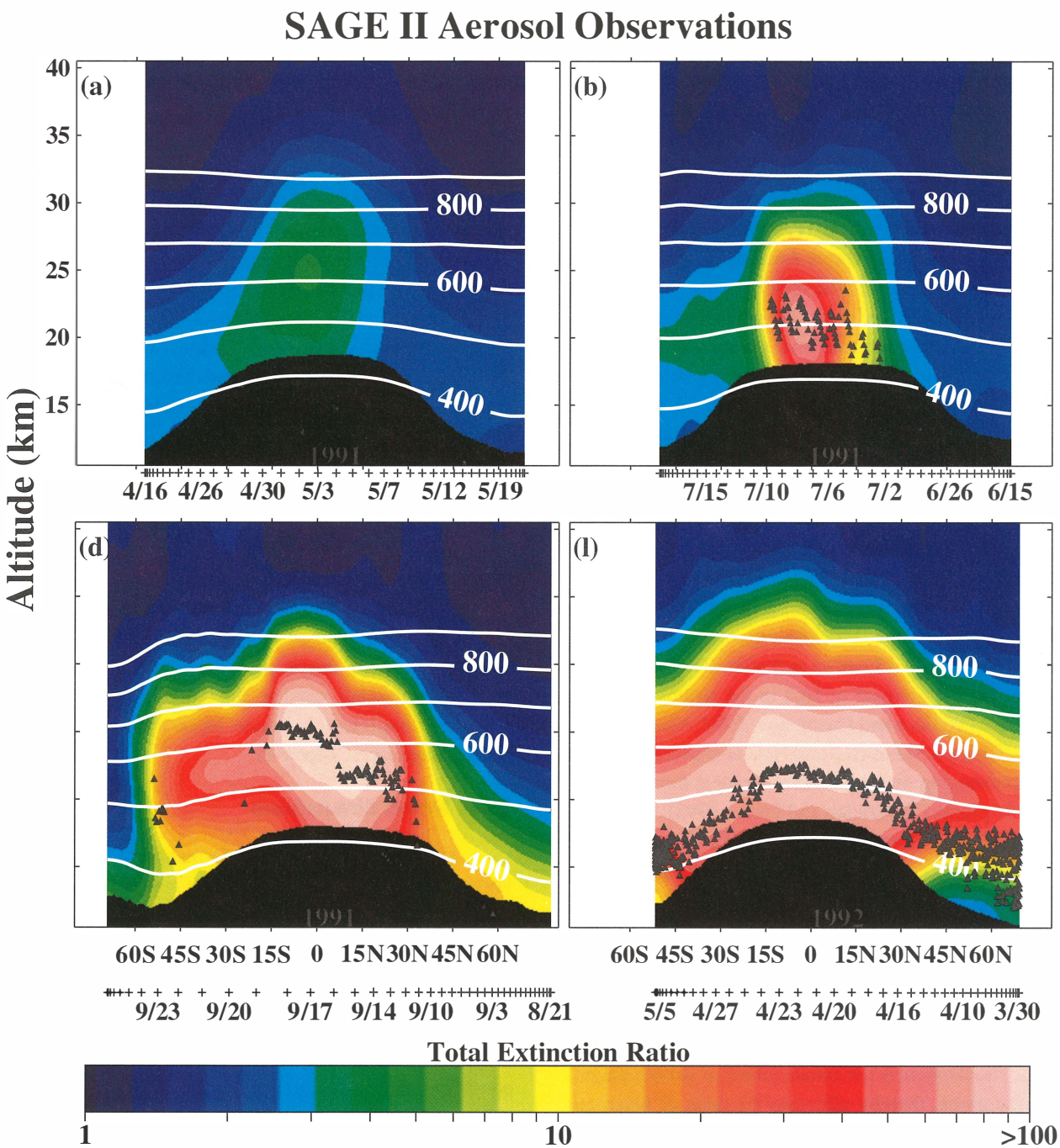

Figure 3-19. Latitude-altitude cross sections of the Stratospheric Aerosol and Gas Experiment II (SAGE II) 1-µm extinction ratio measurements that show the effect of the eruption of Mt. Pinatubo in June 1991 on aerosol abundance in the lower atmosphere. The specific dates of observation are indicated with crosses below each panel for the periods: (a) 15 April to 25 May 1991 (pre-eruption); (b) 14 June to 26 July 1991 (early austral winter); (d) 20 August to 30 September 1991 (late austral winter); and (l) 29 March to 9 May 1992 (full dispersal). No data were used 2 km below the tropopause (blacked out). Small triangles indicate truncation altitude for the SAGE II data. Lidar data were used below this altitude. Isentropes (constant potential temperature in K) appear as white contour lines (adapted from Trepte *et al.*, 1993).

values are increased by factors up to 100 over much of both hemispheres within the year. Since the residual circulation in the stratosphere is upward in the tropics and poleward and downward at higher latitudes, volcanic aerosol is transported to the polar regions, where it is incorporated into the polar vortices. Mt. Pinatubo aerosol did not appear in the Antarctic vortex during the austral winter of 1991 (see Figure 3-19d) but was present at the South Pole following vortex breakup (Cacciani *et al.*, 1993) and was present in the vortex during the following austral winter (Deshler *et al.*, 1994). In the 1991/92 boreal winter, some enhanced levels were observed in the vortex (Wilson *et al.*, 1993). The decay of volcanic aerosol in the lower stratosphere occurs with a time constant that varies with latitude and particle size, but generally averages about one year for an integral parameter such as particle surface area.

Although the emission of HCl from volcanoes can exceed the annual anthropogenic emissions of chlorine to the atmosphere, emitted HCl is largely removed in the troposphere before appreciable amounts can enter the stratosphere. For the Mt. Pinatubo eruption, column measurements of HCl before and after the eruption confirmed that the increase of HCl in the stratosphere was negligible (Wallace and Livingston, 1992; Mankin *et al.*, 1992). The removal of HCl and H_2O is expected to result from scavenging on liquid water droplets formed in the volcanic plume (Tabazadeh and Turco, 1993). These and other dissolution processes reduce HCl abundances by several orders of magnitude, thereby limiting the availability of HCl for transport to the stratosphere. In contrast, only 0.5 to 1.5 percent of SO_2 in the plume is removed by dissolution, thereby facilitating the transport of SO_2 to the stratosphere, where it is oxidized to form H_2SO_4.

The principal consequence of volcanic eruptions for the stratosphere is the enhancement of sulfate aerosol over the globe, thereby affecting the rates of heterogeneous reactions that convert reactive chlorine and nitrogen species (see Table 3-1). In midlatitudes, volcanic aerosol drives the conversion of dinitrogen pentoxide (N_2O_5) to HNO_3 (see Reaction (3-6)) to saturation (Prather, 1992; Fahey *et al.*, 1993; Koike *et al.*, 1994). Volcanic aerosol in the Antarctic is associated with an increased frequency of PSCs and a reduction in large particle formation within the cloud (Deshler *et al.*, 1994). Aerosol surface area densities found in the vortex following the eruption of Mt. Pinatubo are comparable to those in a Type I PSC formed in the absence of volcanic influence. Thus, increased rates of chlorine activation above Type I PSC temperatures are expected in 1992 and 1993 (see Figure 3-8). However, Type II PSC surface areas are still predominant at lower temperatures. In the center of the ozone depletion region (14-18 km), chlorine is fully activated in both vortices in most years and the presence of volcanic aerosol here will not increase the intensity of chlorine activation. However, in the 10 to 14 km region and the region above 18 km where chlorine is usually not fully activated, additional surface area provided by volcanic aerosol can result in increased chemical processing. Furthermore, because the sulfate aerosol is active at temperatures above the PSC formation threshold, the spatial and temporal extent of chlorine activation will be increased, especially in the vortex edge region. Chlorine activation there has been observed to be greater than that in non-volcanic periods and is associated with enhanced ozone loss (Solomon *et al.*, 1993; Hofmann *et al.*, 1992; Hofmann and Oltmans, 1993). Since the scale of this near-vortex region can be comparable to or larger than the vortex interior, enhanced processing outside the vortex edge may be especially important in ozone balance throughout the hemispheres (see Chapter 4).

3.3.4 Model Simulations

Model simulations of the formation of PSCs in the vortex require detailed knowledge of both the thermodynamics inherent in Figure 3-8 and of the nucleation and growth features of the various aerosol particles. Several studies have met with success in simulating the general features of a PSC (Peter *et al.*, 1992; Drdla and Turco, 1991; Toon *et al.*, 1989b, 1990b). However, significant uncertainties remain in the prediction of PSC formation conditions and other characteristics (Dye *et al.*, 1992; Kawa *et al.*, 1992b). Specifically, the threshold temperature for the appearance of Type I aerosols is well below the saturation temperature in Arctic observations. Various explanations are possible, but remain unconfirmed at present. In addition, details of the PSC sedimentation process causing denitrification and dehydration are uncertain. Specifically, uncertainty in the coupling of denitrification and dehydration affects model simulations of PSC activity as well as ozone depletion.

As a result of these uncertainties, model simulations adopt a simplified parameterization of PSC formation and sedimentation processes. These studies confirm the effectiveness of the heterogeneous reactions listed in Table 3-1 for the conversion of inactive to active chlorine (Brasseur and Granier, 1992; Cariolle *et al.*, 1990; Eckman *et al.*, 1993; Lutman *et al.*, 1994a; Chipperfield *et al.*, 1994b, c; Newman *et al.*, 1993; Lefèvre *et al.*, 1994). PSCs formed in localized low-temperature regions in the strong zonal flow of the vortex can fully activate the vortex in the lower stratosphere in a matter of days. Thus, predicting intense activation of chlorine in the vortex seems not to require detailed knowledge of PSC events. Using a 3-D transport and chemistry model, a comparison of modeled and satellite observations of ClO in Arctic winter shows excellent agreement (see Figure 3-11b). In a similar study, the comparison reveals differences in the dynamic structures that force PSC activity at high latitudes (Douglass *et al.*, 1993). In addition, *in situ* and satellite observations of vortex ClO over a wide range of values can be simulated with trajectory models that account for exposure to PSCs as well as the recovery of inactive chlorine in sunlight following a PSC event (Lutman *et al.*, 1994a, b; Schoeberl *et al.*, 1993a, b; Toohey *et al.*, 1993).

Other model simulations are used to evaluate ground-based measurements of OClO in Antarctica that were made when volcanic aerosol was present (Solomon *et al.*, 1993; Hanson *et al.*, 1994). In matching the observed activation of chlorine, the simulations demonstrate the importance of regions that have temperatures close to, but above those required for PSC formation and modest solar illumination. In these regions, chlorine activation on sulfate aerosols (see Table 3-1) effectively competes with the photolysis of HNO_3 which drives the recovery of the inactive $ClONO_2$ reservoir. The activation of chlorine has the potential to enhance ozone depletion in these regions, especially when volcanic aerosols are present.

3.4 DESTRUCTION OF OZONE

3.4.1 Ozone Loss: Observations and Calculations

Significant ozone loss in polar regions requires the activation of chlorine and exposure to sunlight (see Figure 3-1). This association has been substantiated in previous assessments using active chlorine observations over limited regions of the vortex and limited time periods (Anderson *et al.*, 1991; Brune *et al.*, 1991). Photochemical loss of ozone is attributed to catalytic reaction cycles involving enhanced ClO, namely

$$\mathrm{ClO + ClO + M \rightarrow (ClO)_2 + M} \qquad (3\text{-}8)$$
$$\mathrm{(ClO)_2 + h\nu \rightarrow ClOO + Cl} \qquad (3\text{-}8a)$$
$$\mathrm{ClOO \rightarrow Cl + O_2}$$
$$\mathrm{2(Cl + O_3 \rightarrow ClO + O_2)}$$
$$\mathrm{Net:\ 2O_3 \rightarrow 3O_2}$$

$$\mathrm{ClO + BrO \rightarrow Cl + Br + O_2} \qquad (3\text{-}9)$$
$$\mathrm{\rightarrow Br + OClO} \qquad (3\text{-}9a)$$
$$\mathrm{\rightarrow BrCl + O_2}$$
$$\mathrm{BrCl + h\nu \rightarrow Br + Cl}$$
$$\mathrm{Br + O_3 \rightarrow BrO + O_2}$$
$$\mathrm{Cl + O_3 \rightarrow ClO + O_2}$$
$$\mathrm{Net:\ 2O_3 \rightarrow 3O_2}$$

$$\mathrm{ClO + O \rightarrow Cl + O_2} \qquad (3\text{-}10)$$
$$\mathrm{Cl + O_3 \rightarrow ClO + O_2}$$
$$\mathrm{Net:\ O + O_3 \rightarrow 2O_2}$$

where reaction steps (3-8a) and (3-9a) do not result in ozone destruction and where the cycles are listed in order of importance for ozone destruction inside the vortex (Salawitch *et al.*, 1993; Lutman *et al.*, 1994b; Molina and Molina, 1987; McElroy *et al.*, 1986; Solomon *et al.*, 1986; Tung *et al.*, 1986). The rates of the homogeneous photochemical reactions involved in chlorine catalytic cycles follow from a wide variety of laboratory investigations and are generally well understood (JPL, 1992). However, studies continue to improve the precision of earlier results. For example, the temperature dependence of HNO_3 and $ClONO_2$ photolysis cross sections have been remeasured. Those of $ClONO_2$ were found to be in good agreement with previous recommendations for temperatures characteristic of the lower stratosphere, whereas those of HNO_3 were reduced somewhat at stratospheric temperatures (Burkholder *et al.*, 1994a, b).

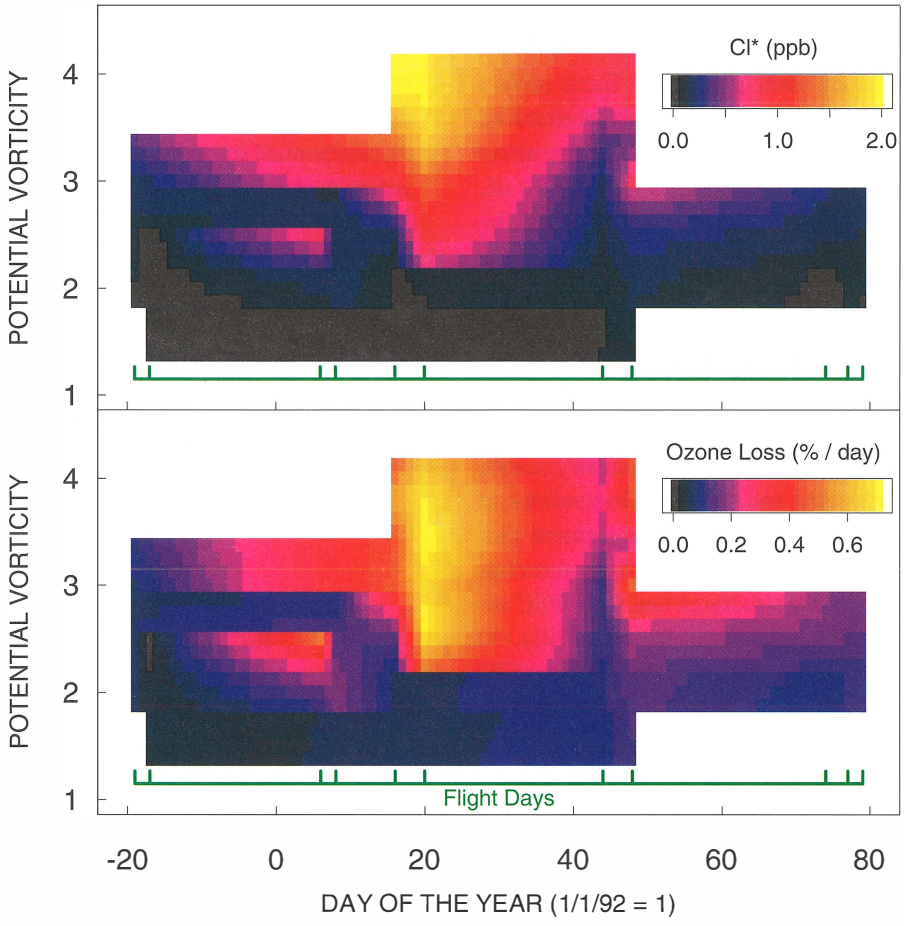

Figure 3-20. Calculation of Cl* (= ClO + $2Cl_2O_2$) (top) and the 24-hour mean loss rate for ozone on the 470 K potential temperature surface (bottom) from a full diurnal photochemical model calculation. Both are plotted as a function of potential vorticity (PV), in units of (10^{-5} K $m^2kg^{-1}s^{-1}$), and day of the year for the Arctic vortex in 1991/92 (day 1 = 1 January 1992). The approximate mean latitudes of parcels with PV of 2 and 4 are 40° and 65°N, respectively, for this period (Salawitch *et al.*, 1993).

A cycle involving $ClONO_2$ has also been recognized to contribute to ozone depletion. After PSCs are no longer present and the recovery period begins (see Section 3.4.3), active chlorine forms elevated amounts of $ClONO_2$. The production of Cl from $ClONO_2$ photolysis initiates a catalytic cycle similar to Reaction (3-8) (Toumi *et al.*, 1993; Minton *et al.*, 1992). In full models of ozone destruction, $ClONO_2$ photolysis and associated reactions are typically included, but the associated ozone loss is often not distinguished from the primary catalytic loss cycles represented in Reactions (3-8, 3-9, and 3-10).

Quantitative evaluation of ozone destruction rates, constrained by observed ClO, provides reasonable agreement with the measured decay of ozone over the Antarctic where ozone loss is rapid and the vortex is assumed to be isolated over the measurement period (see Chapter 1) (Anderson *et al.*, 1989; Solomon, 1990; Anderson *et al.*, 1991). Loss rates of about one percent per day are found there when chlorine is fully activated in sunlight. Recent model calculations for the Arctic show a detailed relationship between active chlorine abundance and ozone loss rates in the lower stratosphere in early 1992 (see Figure 3-20) (Salawitch *et al.*, 1993). The model represents vortex photochemistry more comprehensively than in previous studies because of the use of extensive *in situ* and satellite observations of reactive

and trace species, meteorological analyses, and recent laboratory results for gas phase and heterogeneous reactions. After parameterization, ozone loss rates are estimated using a full-diurnal photochemical calculation. The maximum loss rates are similar to the Antarctic, but the rates are sustained for a shorter period, resulting in smaller total losses. For a given chlorine level, loss rates on an isentropic surface are greater at lower latitude (or lower PV) values where solar illumination is greater. Cumulative losses of 15 to 20 percent in the Arctic implied by Figure 3-20 are corroborated by estimates made using *in situ* observations of ozone (Browell *et al.*, 1993) and changes in the relationship between ozone and the long-lived tracer N_2O (Proffitt *et al.*, 1993) (see Section 3.2). Corroboration is also provided by model simulations that utilize the extensive ozonesonde data available in the 1991/92 northern winter. The data are analyzed by using estimates of descent of polar air over winter months and by using trajectories to identify air parcels sampled twice in sonde measurements separated in time and space (Lucic *et al.*, 1994; von der Gathen *et al.*, 1994). These recent results increase confidence in earlier estimates of ozone loss in the Arctic vortex (Schoeberl *et al.*, 1990; McKenna *et al.*, 1990; Salawitch *et al.*, 1990).

With extensive observations of ClO and ozone, the UARS satellite substantially increases the evidence that ozone loss occurs in both polar regions and that reactions involving ClO are the cause of this depletion (Waters *et al.*, 1993a; Manney *et al.*, 1994b). Total column amounts of ClO correlate well with regions depleted in column ozone in two consecutive years in the Antarctic (see Figure 3-21). In addition, this correlation has been observed in mid-August in the Antarctic (Waters *et al.*, 1993b), in agreement with the interpretation of *in situ* observations (Proffitt *et al.*, 1989a). In the Arctic, variability in column ozone abundances tends to obscure the smaller Arctic losses. However, averages of ClO and ozone in the Arctic show a negative correlation during peak ClO values, with ozone loss rates in reasonable agreement with calculations. Satellite N_2O observations or PV analyses are used to account for ozone changes resulting from the transport of ozone. These results suggest that conclusions and interpretation derived from the highly localized *in situ* and ground-based data sets have relevance on the vortex scale.

A new perspective of ozone loss comes from satellite observations of late-winter changes in ozone averaged around PV contours (see Figure 3-22) (Manney *et al.*, 1993, 1994b). This approach can detect significant changes in the 3-D distribution of ozone without *a priori* assumptions about the specific role of photochemistry or transport of ozone. With PV generally increasing poleward, poleward transport of ozone-rich air at upper levels and ozone loss at lower levels are both evident in the Antarctic vortex region in each year. In contrast, ozone increases are expected to extend to the lowest potential temperatures in these regions without localized, *in situ* photochemical loss. In the Arctic, ozone increases are found in both 1992 and 1993, but significant ozone loss in the February-to-March time period is found only in 1993 in the lower stratosphere. The loss is consistent with enhanced ClO values in 1993 that resulted from more extensive low temperatures (see Figures 3-11 and 3-12).

3.4.2 Variability

Perhaps the greatest difficulty in increasing the accuracy of predictions of ozone loss in polar regions is the interannual and intra-annual variability of the conditions that determine loss rates. Large variability in meteorological and photochemical parameters featured in Figure 3-1 increases the difficulty of the interpretation of limited data sets and reduces their value for predicting future changes in ozone. Variability largely follows from the fluid mechanical features of the vortex and its environment, and the stochastic nature of the forces that act to change the vortex and its environment. Of greatest concern are changes in the spatial and temporal extent of low temperatures and the duration of the vortex into the spring season (Austin *et al.*, 1992; Austin and Butchart, 1994; Salawitch *et al.*, 1993). Lower temperatures promote activation of chlorine, and a long-lived vortex promotes the photochemical destruction of ozone by active chlorine. The northern winters of 1991/92 and 1992/93 present a striking example of interannual variability in ClO and ozone (see Figures 3-12 and 3-22) (Larsen *et al.*, 1994). In general, variability in the Arctic vortex is greater than in the Antarctic, particularly for minimum temperatures (see Figure 3-3). Because the formation of PSCs requires temperatures below a certain threshold, fluctuations of a few degrees will substantially change

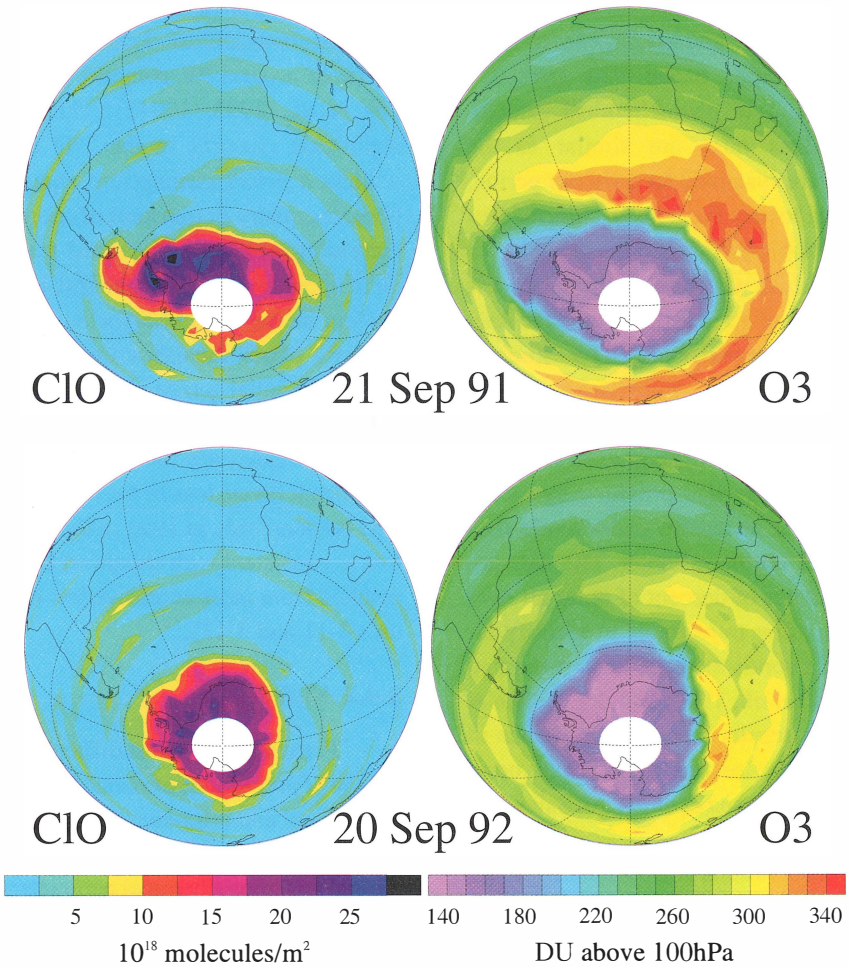

Figure 3-21. Observations of column abundances of ClO (10^{18} molecules m^{-2}) and ozone (Dobson units) above 100 hPa (about 16 km) in the Antarctic in September 1991 and 1992 from the UARS MLS satellite instrument (Waters *et al.*, 1993a).

the extent of processing inside the vortex and the extent of denitrification as sunlight returns to the vortex in spring. Ozone destruction rates in the late vortex strongly depend on the extent of denitrification (see Figure 3-23) (Brune *et al.*, 1991; Salawitch *et al.*, 1993). Reduced values of reactive nitrogen slow the formation of the $ClONO_2$ reservoir and thereby maintain active chlorine levels as sunlight returns to high latitudes.

The variability in both polar regions follows from wave activity near the vortex and the interaction of waves with tropospheric weather systems. These wave perturbations can change the chemical evolution of the vortex through the associated temperature changes (Farman *et al.*, 1994; Gobbi and Adriani, 1993; Rood *et al.*, 1992) or the transport into and out of the vortex, especially for the weaker Arctic vortex (Dahlberg and Bowman, 1994; Manney *et al.*, 1994c). Regions cooled to PSC temperatures can process a large fraction of vortex air in a relatively short period of time, contributing significantly to the total amount of vortex processing (MacKenzie *et al.*, 1994; Newman *et al.*, 1993; Lefèvre *et al.*, 1994). When these low-temperature regions are near the vortex edge, the resultant processing may influence midlatitude ozone destruction (see Chapter 4). Wave activity also distorts the vortex from a symmetric polar flow, thereby transporting processed air into sunlight at lower latitudes. Because ozone loss rates increase substantially in sunlight when chlorine is acti-

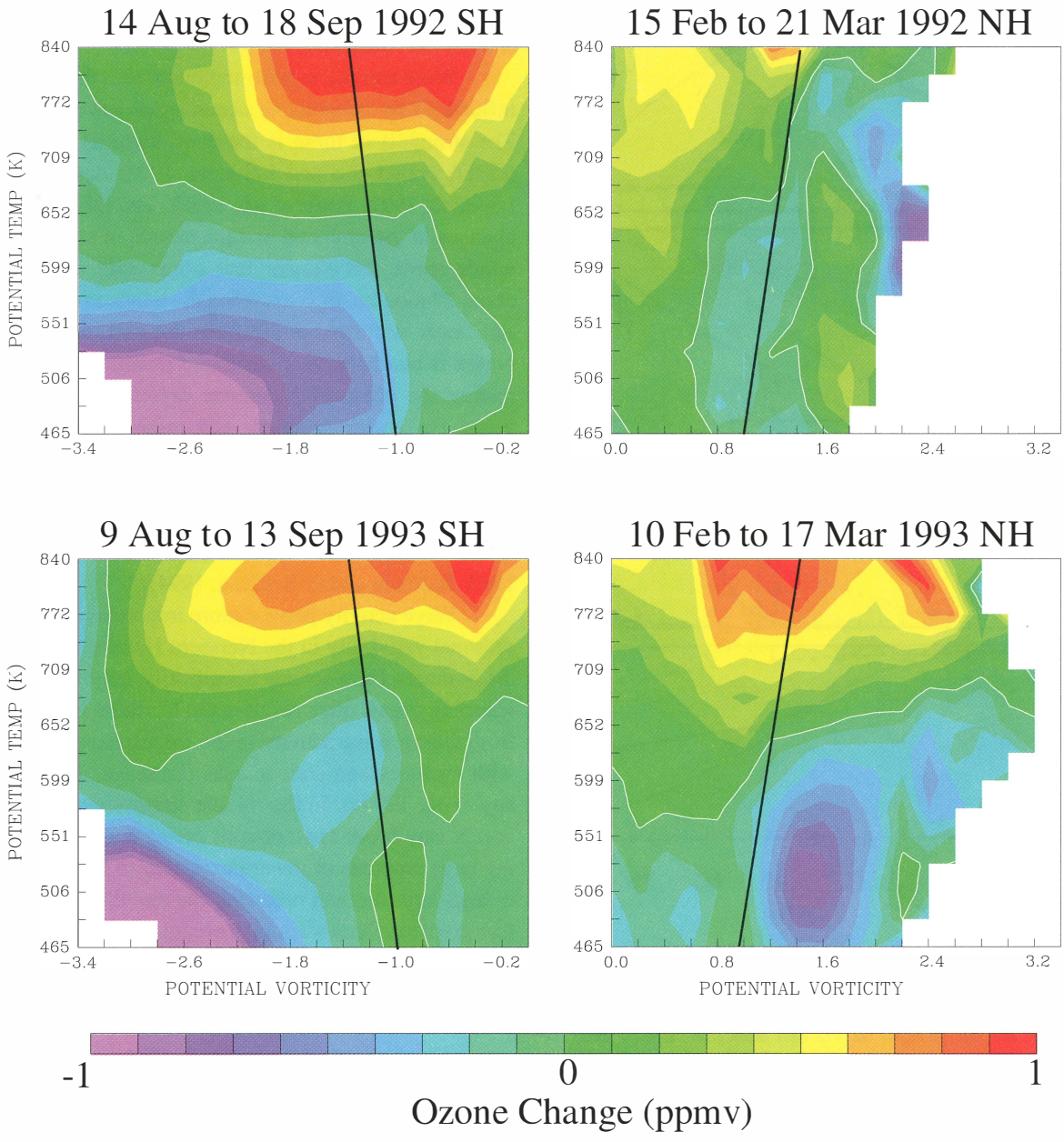

Figure 3-22. Observations of late winter ozone changes for 1992 (top) and 1993 (bottom) in the Arctic (right) and Antarctic (left) from the UARS MLS instrument. The horizontal coordinate is scaled PV. PV is a surrogate for latitude, with values increasing with increasing latitude. The vertical coordinate is potential temperature, a surrogate for altitude, covering the range of approximately 15 to 30 km (see Figure 3-4). These coordinates help separate chemical and diabatic effects from adiabatic and transport effects occurring at constant potential temperature. Measurements shown here are the difference in ozone averaged around contours of PV between the two dates indicated in each panel. The black line gives the approximate edge of the vortex, with the interior to the right in the Northern Hemisphere (NH) and to the left in the Southern Hemisphere (SH). During the periods shown here, the vortex edge extended as far equatorward as 40° latitude in the Northern Hemisphere and 50° latitude in the Southern Hemisphere (see Figures 3-11 and 3-17). The zero-change contour is indicated in white (Manney *et al.*, 1994b).

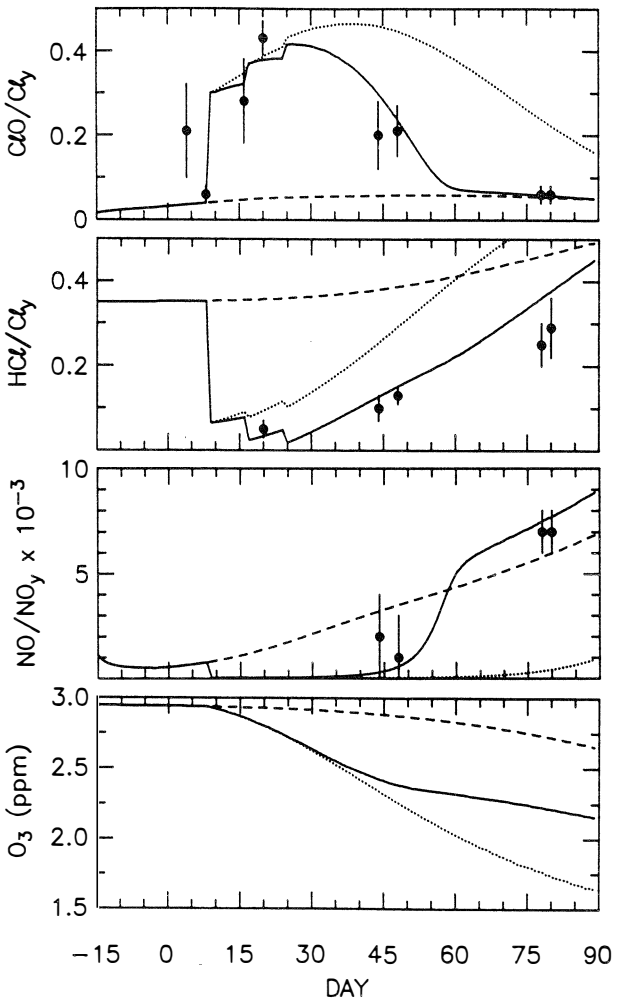

Figure 3-23. Calculated seasonal evolution (day 1 = 1 January 1992) of ClO, HCl, NO, and ozone at noon for an air parcel at 18 km altitude, 65°N latitude, processed periodically by PSCs. Case A: No denitrification (solid line). Case B: 90-percent denitrification following the first PSC event (dotted line). Case C: No PSC processing (dashed line). Reduction in ozone during March in the absence of PSC processing occurs because of reactions involving NO_x. Data points represent mean and standard deviation of aircraft observations during AASE II for the 470 K potential temperature surface and potential vorticity values greater than 2.8 x 10^{-5} K $m^2kg^{-1}s^{-1}$. Data used for ClO and NO are restricted to daytime observations (solar zenith angle < 86°). Concentrations of ClO, HCl, and NO have been normalized to their respective reservoirs to remove the influence of small-scale atmospheric gradients (Salawitch *et al.*, 1993).

vated, total ozone loss may increase significantly (Brune *et al.*, 1991; Solomon, 1990).

Wave activity in polar regions is also thought to be influenced by phenomena occurring at lower latitudes. The strongest of these is the quasi-biennial oscillation (QBO) (van Loon and Labitzke, 1993; Angell, 1993; Labitzke, 1992; Poole *et al.*, 1989). The QBO refers to changes in the direction and magnitude of stratospheric winds above the equator that occur with a period of about 27 months. In years when the winds in the equatorial lower stratosphere are from the east, the northern vortex is comparatively weak and warm, thereby minimizing the potential for ozone depletion. In westerly years, the vortex is colder and more intense in both hemispheres. El Niño/Southern Oscillation (ENSO) effects, referring to changes in sea surface temperature and associated shifts in atmospheric mass in the South Pacific Ocean, represent a much weaker influence (Angell, 1993; Baldwin and O'Sullivan, 1994).

Wave activity plays a more important role in subseasonal variability in the Northern Hemisphere than in the Southern Hemisphere. Specifically, major midwinter warming events often result in the Northern Hemisphere from strong wave activity in the troposphere associated with cyclones and anticyclones (Labitzke, 1992; Manney *et al.*, 1994a). In the middle stratosphere, the polar vortex may break apart or split during a warming, causing large amounts of lower latitude air to be transported to high latitudes and reversing the meridional temperature gradient. Such warmings eventually mark the end of PSC temperatures throughout the vortex and change the effectiveness of ozone catalytic loss cycles. Wave activity also creates variability in column ozone by changing tropopause heights and temperatures in localized regions (Farman *et al.*, 1994; Petzoldt *et al.*, 1994). Ozone column amounts are reduced by convergence of ozone-poor air below and divergence of ozone-rich air above, and by rapid advection of low-latitude air in the case of persistent ridge formation in the upper troposphere/lower stratosphere (Orsolini *et al.*, 1994). These changes do much to obscure ozone changes due to photochemical loss.

Volcanic eruptions are also a source of variability in the stratosphere. In addition to chemical effects (see Section 3.3.3), increases in stratospheric aerosol that follow an eruption have direct and indirect effects on temperature and circulation in both the stratosphere and

troposphere (Rind *et al.*, 1992). The direct effect in the lower stratosphere is a warming in the tropics (Kinne *et al.*, 1992; Labitzke and McCormick, 1992) and a cooling in polar regions. These and other changes may influence the vortex and the formation of PSCs.

As a final consideration, trends in source gas emissions in the troposphere may eventually affect polar ozone loss and its variability. Of greatest interest are changes in H_2O, CH_4, carbon dioxide (CO_2), N_2O, and halogen-containing species (see Chapter 2), which all participate in establishing the meteorological and photochemical context of the depletion process. Increases in CO_2 are expected to decrease temperatures in the lower stratosphere, thereby increasing the frequency and extent of PSCs (Austin and Butchart, 1994; Austin *et al.*, 1992). With additional cooling caused by the subsequent destruction of ozone, total ozone loss in the Arctic could become comparable to that in the Antarctic. More directly, a doubling of inorganic chlorine species in the stratosphere would likely result in Arctic ozone losses that are comparable to those in the Antarctic (Salawitch *et al.*, 1993). PSC frequency would also increase in response to growth in atmospheric CH_4 and to an increase in the amount of H_2O entering the stratosphere in the tropics. A more direct source is the emission of H_2O and NO_y species from aircraft operating in the upper troposphere and lower stratosphere (Peter *et al.*, 1991).

3.4.3 Photochemical Recovery

After the cessation of PSC formation inside the vortex, the conversion rate of inactive reservoir chlorine to active chlorine is reduced to pre-winter values (see Figure 3-1). Accordingly, ClO values fall from their midwinter peak values throughout the vortex (see Figures 3-20 and 3-23) (Waters *et al.*, 1993a, b; Toohey *et al.*, 1993; Salawitch *et al.*, 1993). In this recovery period, changes caused by PSCs are reversed as photochemistry restores reservoir chlorine to pre-winter values. In the Northern Hemisphere, air usually experiences PSC temperatures on only a few occasions and for only a small fraction of time throughout midwinter (Newman *et al.*, 1993). Thus, recovery is ongoing throughout the winter, in contrast to the Southern Hemisphere. Recovery proceeds with reactions involving active chlorine and reactive nitrogen species:

$$ClO + NO_2 + M \rightarrow ClONO_2 + M \qquad (3\text{-}11)$$

$$ClO + NO \rightarrow Cl + NO_2 \qquad (3\text{-}12)$$

$$Cl + CH_4 \rightarrow HCl + CH_3 \qquad (3\text{-}13)$$

$$HNO_3 + h\nu \rightarrow NO_2 + OH \qquad (3\text{-}14)$$

where $h\nu$ is solar radiation and OH is the hydroxyl radical. Reaction (3-14) is key to maintaining the partitioning within the NO_y reservoir in Equation (3-2). Reaction (3-11) is predominant in the early recovery phase because of the availability of NO_2 from Reaction (3-14). NO_2 increases dramatically with the return of sunlight to the poles when HNO_3 is available (Keys *et al.*, 1993; Solomon and Keys, 1992). Changes in reservoir chlorine have been confirmed with *in situ* measurements of HCl and remote soundings of $ClONO_2$ near the vortex edge and inside the vortex in the Arctic when denitrification is low (see Figures 3-13, 3-14, 3-15, 3-16, and 3-17) (Lutman *et al.*, 1994b; Roche *et al.*, 1993b, 1994). Specifically, the enhancement of $ClONO_2$ estimates in the early recovery phase is evident in aircraft measurements in the Arctic in February 1992 (see Figure 3-13). As recovery progresses, more reservoir chlorine shifts from $ClONO_2$ to HCl, until values present in late fall are restored (Liu *et al.*, 1992). When denitrification is significant entering the recovery phase, $ClONO_2$ may not be formed as readily as indicated in Figure 3-1. Instead, Reaction (3-13) dominates, restoring HCl rapidly and causing HCl to exceed $ClONO_2$ temporarily. As reactive nitrogen is mixed back into the air parcel, more $ClONO_2$ is formed and $ClONO_2$ and HCl return to unperturbed values.

Ozone loss during the recovery phase depends strongly on the extent of denitrification. With extensive denitrification, the abundance of NO_2 produced by Reaction (3-14) is limited, thereby enhancing ozone loss rates (see Figure 3-23) (Salawitch *et al.*, 1993; Kondo *et al.*, 1994b; Brune *et al.*, 1991). Full recovery must then wait until breakup of the vortex facilitates mixing with lower latitude air that has not been denitrified. The enhancement of $ClONO_2$ values during recovery and elevated temperatures mean that catalytic cycles other than ClO + ClO contribute to ozone loss during this period (Toumi *et al.*, 1993).

Ultimately, the importance of the recovery phase for ozone depletion depends on details of vortex breakup. Planetary wave activity in the spring breaks apart the

vortex weakened by the reduction in radiative forcing. In the Antarctic, variability is lower, but significant interannual differences still occur in the lifetime of the vortex (see Figure 3-3). As the area covered by PSC temperatures lessens, the distortion of the vortex in a wave event can typically lead to a rapid breakup of the vortex (Krueger *et al.*, 1992). In any year, an early breakup phase minimizes ozone depletion. However, in the breakup process, the vortex may distort to reach lower latitudes, significantly increasing local ozone loss rates (Solomon, 1990; Brune *et al.*, 1991). After breakup, the transport of lower latitude air to the poles displaces air parcels depleted in ozone. At the same time, processed air that is low in ozone, contains active chlorine, or is potentially denitrified and dehydrated is transported to lower latitudes (Atkinson *et al.*, 1989; Harwood *et al.*, 1993). As ozone loss continues in these air parcels, midlatitude ozone may be significantly impacted (see Chapter 4).

3.5 VORTEX ISOLATION AND EXPORT TO MIDLATITUDES

Understanding the isolation of the winter polar vortex is a key factor in understanding the budgets of ozone and other trace constituents at high latitudes. If a large flow exists through the region of processed air inside the vortex (see Figure 3-2), then photochemical loss rates of ozone must be substantially larger than in an isolated vortex to cause observed ozone depletion (Anderson *et al.*, 1991). In addition, export of processed air to lower latitudes and lower altitudes may enhance ozone depletion in those regions (see Chapter 4) (Brune *et al.*, 1991). However, even if highly isolated during winter, processed air in the vortex has the potential to influence lower latitudes following vortex breakup in late winter/early spring. Significant progress has occurred in this assessment period in the modeling and interpretation of data related to the transport of air in and near the vortex. Trace constituent observations, radiative balance arguments, and various fluid mechanical models of the vortex have all provided valuable insights into vortex motion. In addition, the identification of a vortex edge region and a range of definitions for the vortex boundary have become important concepts. A large body of those results supports a substantial isolation in winter of an inner vortex region that is surrounded by an edge region in which stronger mixing to midlatitudes occurs.

3.5.1 Vortex Boundaries

The motion of mass into the winter polar vortex is poleward and downward from the upper stratosphere and mesosphere (see Figure 3-2) (Schoeberl and Hartmann, 1991; Schoeberl *et al.*, 1992). Flow out of the vortex in the lower stratosphere must cross through the outer boundary or edge region or through a lower boundary or bottom of the vortex. Since pressure increases with depth into the vortex from above, the velocities associated with such mass flow decrease accordingly. The edge region is denoted by the location of strong horizontal gradients in parameters associated with the vortex. These gradients provide definitions for a boundary of the vortex. Choices include the maximum in the speed of the polar wind jet, the maximum latitude gradient in PV, a large change in one or more trace constituents with latitude, and a kinematic barrier as identified in transport model simulations. Because of the convergence of the meridians at high latitudes, the vortex edge region represents most of the mass of the vortex and, hence, is crucial for the evaluation of outflow and its influence at midlatitudes.

The maximum wind speed in the circumpolar flow of the polar jet provides the most accessible definition of the boundary (see Figure 3-2). PV gradients, though obtained from highly derived quantities, are more directly related to dynamical barriers within the flow (Schoeberl *et al.*, 1992). PV combines the absolute vorticity of an air parcel with static stability expressed as the vertical gradient of potential temperature (Hoskins *et al.*, 1985). In isentropic and frictionless flow, PV is conserved, making it a useful diagnostic for air motion over limited periods. Large meridional gradients of PV (generally increasing poleward) form in the polar regions as a result of diabatic cooling and Rossby wave breaking in the winter season. The polar jet is a response to the temperature gradient formed by the cooling at high latitudes in winter. A boundary defined with a change in a trace constituent is often associated with processing of polar air by PSCs formed at the low vortex temperatures (Proffitt *et al.*, 1989b, c). As discussed above, processing results in chlorine activation, dehydration, denitrification, and, ultimately, ozone loss on the scale of the vortex. Finally,

a kinematic barrier to large-scale isentropic flow is revealed in the Lagrangian evolution of air masses on isentropic surfaces (Pierce and Fairlie, 1993). The approach uses assimilated wind fields to move material lines initialized on closed streamlines encircling the Antarctic vortex. In some instances, a particular material line is found which shows no irreversible deformation for periods of days to weeks. This "separating material line" defines a kinematic boundary to large-scale isentropic transport in the polar region. Material poleward of this separating material line remains highly isolated from the surrounding circulation.

These boundary definitions are interrelated since each is derived from or caused by features of the wind and temperature fields in the winter season. The kinematic barrier, the maximum PV gradient, and the jet maximum are generally located within a few degrees of latitude of each other within the polar jet core. However, transient distortions of the vortex caused in the lower stratosphere by tropospheric weather systems cause an interweaving and distortion of these boundaries within the edge region. While circumnavigating the vortex in the jet, an air parcel may cross the PV or jet maximum boundary while remaining inside the kinematic barrier and/or outside the chemical boundary. Thus, an evaluation of the vortex export of air that resides near a boundary will, in general, be dependent on the chosen boundary.

In the quantification of outflow, the choice of a vortex edge is complicated by the fact that much of the air "outside" of the vortex remains close to the edge and varies with the large-scale fluctuations of the vortex (Figure 15 in Rood *et al.*, 1992; Manney *et al.*, 1994c; Waugh *et al.*, 1994). For changes in midlatitude ozone, the important factors are the extent to which air undergoes horizontal transport away from the center of the vortex or away from the edge region to lower latitudes and the extent to which this air has undergone processing and, perhaps, loss of ozone. A substantial amount of processing can occur within the vortex edge region, particularly in the Antarctic vortex (Tao and Tuck, 1994). As a result, transport within the edge region, perhaps across a particular boundary, is of considerably less importance. In the evaluation of ozone loss photochemistry within the vortex, the total loss of processed air from the center of the vortex and edge region is the quantity of interest.

At the lower boundary of the vortex region, a transition is noted below which there is a much weaker barrier to transport out of the vortex region to lower latitudes (Tuck, 1989; Loewenstein *et al.*, 1989; Manney *et al.*, 1994c). The transition is clearly noted in the vertical distribution of long-lived stratospheric tracers. At these low altitudes (< 15 km), the polar jet is considerably weaker, consequently weakening the identification of vortex boundaries as defined above. Transport through the bottom of the vortex is driven by diabatic descent throughout the vortex lifetime as air cools, approaching radiative equilibrium over the Antarctic (Rosenfield *et al.*, 1994; Proffitt *et al.*, 1989b, 1990, 1993). The rate of cooling varies with time during the winter season, with the largest cooling rates occurring early when air is farthest from radiative equilibrium. Without strong barriers to horizontal transport, air that is transported through the lower vortex boundary is readily transported and mixed to lower latitudes. Processed air that leaves the vortex through the lower boundary rather than through the edge region has relatively less influence on midlatitude ozone because of the higher altitude of the ozone layer in midlatitudes.

3.5.2 Constituent Observations

Constituent observations from aircraft and satellites have been used as a diagnostic for vortex outflow in the winter from both vortices. In the Antarctic, the intense dehydration that occurs inside the vortex is of particular importance (see Section 3.3.2.5). Significant export of this dehydrated air to midlatitudes is considered to be a source of low values of $[2CH_4 + H_2O]$ above 400 K (about 15 km) outside the Antarctic vortex in September and October (Tuck, 1989; Kelly *et al.*, 1989; Tuck *et al.*, 1993). The value of CH_4 is included in the sum in order to account for H_2O produced in CH_4 oxidation in the stratosphere. Values of $[2CH_4 + H_2O]$ in the range 6.4 to 6.7 ppmv are characteristic of air that has passed through the tropical tropopause. The dehydration signal, defined as values below this range, extended to the subtropical jet in the early interpretation of satellite data sets, suggesting significant outflow in the 15 to 20 km altitude range from the vortex (Tuck *et al.*, 1993). Using the relative mass of the vortex in the Southern Hemisphere, a residence time of 30 days (e-folding time) is required to lower $[2CH_4 + H_2O]$ to the reported values

at midlatitudes. This corresponds to replacing the air in the vortex in approximately 90 days. Subsequent revisions of the satellite H_2O data set (version 17) significantly reduce the vertical and horizontal extent of the dehydration signature at midlatitudes (see Figure 3-18) (Russell, private communication, 1994), increasing the vortex replacement time to about 120 days. With a replacement time in this range, processed air inside the dehydrated Antarctic vortex can be characterized as largely isolated from influencing midlatitudes.

Further study of satellite observations of H_2O and CH_4 confirms the isolated character of the inner vortex (Pierce *et al.*, 1994). The distribution of these species over the winter reveals sustained diabatic descent accompanied by dehydration in the middle of the vortex. A gradient in dehydration is established between the center of the vortex and the jet core region where both normal and dehydrated air are found. Trajectory calculations that follow air parcels sampled by satellite for 25 days in early spring show no evidence for large-scale transport of significantly dehydrated jet core air into midlatitudes on either the 425 K (16 km) or 700 K (28 km) potential temperature surfaces. However, some irreversible transport from the edge region to lower latitudes does take place. In addition, the observations also show descent in the jet core region bringing down air with higher values of $[2CH_4 + H_2O]$.

In the Arctic, the absence of intense and widespread dehydration within the vortex makes the use of H_2O and CH_4 observations to detect vortex outflow more difficult. However, using PV as a substitute tracer in meteorological analyses, significant outflow of processed air from the vortex edge region was deduced for the vortex near 18 km (475 K) (Tuck *et al.*, 1992). This result is not inconsistent with an isolated center of the vortex because the outflow is from the vortex edge region. Analysis of aircraft observations shows that the residual motion in regions of high active chlorine inside the vortex is poleward and downward (Proffitt *et al.*, 1989c, 1990, 1993). The descent rates imply significant flow through the vortex lower boundary and large diabatic cooling rates. The Arctic region has also been used as a reference state to show the existence of denitrification and dehydration outside the Antarctic vortex (Tuck *et al.*, 1994). However, a quantitative inconsistency remains between the amount of denitrification and dehydration observed outside and inside the vortex, suggesting that the understanding of the respective removal processes or vortex export processes remains incomplete (see Section 3.3.2.5).

Apart from the effort to evaluate vortex outflow with the signature of dehydration, the basic observation of a large hemispheric asymmetry in water vapor in the lower stratosphere remains (Kelly *et al.*, 1990). After account is made for CH_4 oxidation in mid- to late-winter observations, water vapor in the Northern Hemisphere is larger by about 1.5 ppmv. The export of dehydrated air from the Antarctic is one explanation of the difference. Other explanations include the role of the tropics in removing water upon entry of air into the stratosphere (Tuck, 1989; Tuck *et al.*, 1993; Kelly *et al.*, 1989).

3.5.3 Radiative Cooling

To provide continuity for a substantial material flux outward through the Antarctic vortex, either a strong vertical transport between the middle and lower stratosphere or compensating inward horizontal transport is required. To exchange the mass of the vortex between 16 to 24 km with a 30-day time scale requires a vertical velocity of -0.1 cm s^{-1} at 16 km, which is equivalent to a potential temperature change near 1.3 K per day. However, both N_2O trends (Hartmann *et al.*, 1989; Loewenstein *et al.*, 1989; Schoeberl *et al.*, 1992) and radiative calculations (Shine, 1989; Rosenfield *et al.*, 1987; Schoeberl *et al.*, 1992; Manney *et al.*, 1994c; Strahan *et al.*, 1994) give much smaller values for this velocity, near -0.02 cm s^{-1} (0.2 K per day). Hence, a substantial body of interpretation supports a small net flux through the Antarctic vortex on sub-seasonal time scales.

Using more recent satellite observations of CH_4 and HF, rapid and deep descent into the Antarctic vortex has been observed (Russell *et al.*, 1993b; Schoeberl *et al.*, 1994; Fischer *et al.*, 1993). The descent rate is consistent with expected cooling rates in the upper stratosphere (Rosenfield *et al.*, 1994). Lower in the stratosphere, the descent rate slows, with an upper limit of 0.07 cm s^{-1}, corresponding to a replacement time of vortex air of about 120 days (Schoeberl *et al.*, 1994). This is consistent with the estimates made from the appearance of dehydrated air at midlatitudes in the satellite observations as noted above (see Section 3.5.2)

Consistent with the enhanced wave activity, the vertical flux between the middle and lower stratosphere in the Arctic is much larger than that found in the Antarctic; mean vertical velocities in the Arctic lower stratosphere are near -0.06 cm s^{-1}, or 0.6 K per day (Schoeberl *et al.*, 1992; Strahan *et al.*, 1994; Bauer *et al.*, 1994; Manney *et al.*, 1994c). Interannual variability in the wave disturbances in the Arctic also creates variability in the vortex transport. In isentropic trajectory studies examining 14 years of meteorological data, interannual differences were found in the predominance of inward and outward transport across the vortex boundary (Dahlberg and Bowman, 1994). Thus, quantification and prediction of interannual variability are fundamentally more difficult in the Arctic than in the Antarctic, impacting prediction of ozone changes both in the vortex and at midlatitudes.

3.5.4 Trajectory Models

In trajectory models, transport is examined by calculating the dispersion of an ensemble of notional air parcels over a typical one-month period, where the initial position of each parcel is specified. Studies are based on National Meteorological Center (NMC)-derived winds (Bowman, 1993) or on United Kingdom Meteorological Office-analyzed or modeled wind fields (Chen *et al.*, 1994; Manney *et al.*, 1994c; Pierce *et al.*, 1994; Pierce and Fairlie, 1993). Approaches include following individual parcels or ensembles of parcels forming material lines around vortex streamlines. In each case, large-scale horizontal transport through the vortex edge region in the Antarctic is small near 20 km (450 K isentropic level) (see Figure 3-24). In the figure, parcels that are initiated inside the vortex, as defined by column ozone values, remain in the vortex after 30 days. Similarly, the evolution of material lines in the vortex region reveals a kinematic barrier to large-scale isentropic flow out of the vortex (Pierce and Fairlie, 1993). However, substantial mixing and transport does occur across the lower vortex boundary (16 to 20 km, or 375 to 425 K). This transport is consistent with transport deduced from constituent observations (Tuck, 1989; Proffitt *et al.*, 1989b, 1990, 1993). However, omission of diabatic effects and inertial gravity waves in such isentropic trajectory studies may significantly underestimate transport and mixing processes at the vortex boundary (Pierce *et al.*, 1994).

In the Arctic vortex, large episodic disruptions occur as a result of planetary and synoptic wave disturbances. These events, which are less frequent in the Antarctic, are associated with transport of vortex air to midlatitudes in the lower stratosphere in the form of narrow tongues, or filaments, that are pulled from the edge of the vortex (Juckes and McIntyre, 1987; Norton, 1993; Pierce and Fairlie, 1993; Waugh *et al.*, 1994; Manney *et al.*, 1994c). These features are simulated in contour advection modeling in which high spatial resolution is maintained in the advection of material contours. The result is that approximately 5 to 10 percent of the vortex area is typically transported outward, with up to 20 percent during exceptionally large events (Waugh *et al.*, 1994). As an example, the total export from the vortex in January 1992 represents only nine percent of the area between 30°N and the vortex edge. There is also evidence that low-latitude air is entrained into the vortex during large disruptions, although the volume of air involved is probably small (Plumb *et al.*, 1994). At the rate of one to two planetary-scale events per month, the e-folding time for vortex exchange to midlatitudes by this mechanism is on the order of three to six months in the lower stratosphere, depending on the intensity and number of such events.

3.5.5 Three-Dimensional Models

In addition to trajectory models, three-dimensional (3-D) chemistry transport models (CTMs), 3-D mechanistic models, and 3-D general circulation models (GCMs) driven by winds from meteorological data assimilation systems support relatively limited flow through the vortex in winter. Three-dimensional models improve the evaluation of vortex outflow because they include both the horizontal transport through the vortex edge and the vertical transport connecting the lower stratosphere with the upper stratosphere and the mesosphere. For example, satellite data clearly show the descent of mesospheric air deep into the stratosphere sometime during the winter (see Figure 3-5) (Russell *et al.*, 1993b). Furthermore, since outflow will likely result from zonally asymmetric mechanisms driving transport at the vortex edge, both planetary-scale events and synoptic-scale events in the lower stratosphere can be considered in 3-D models.

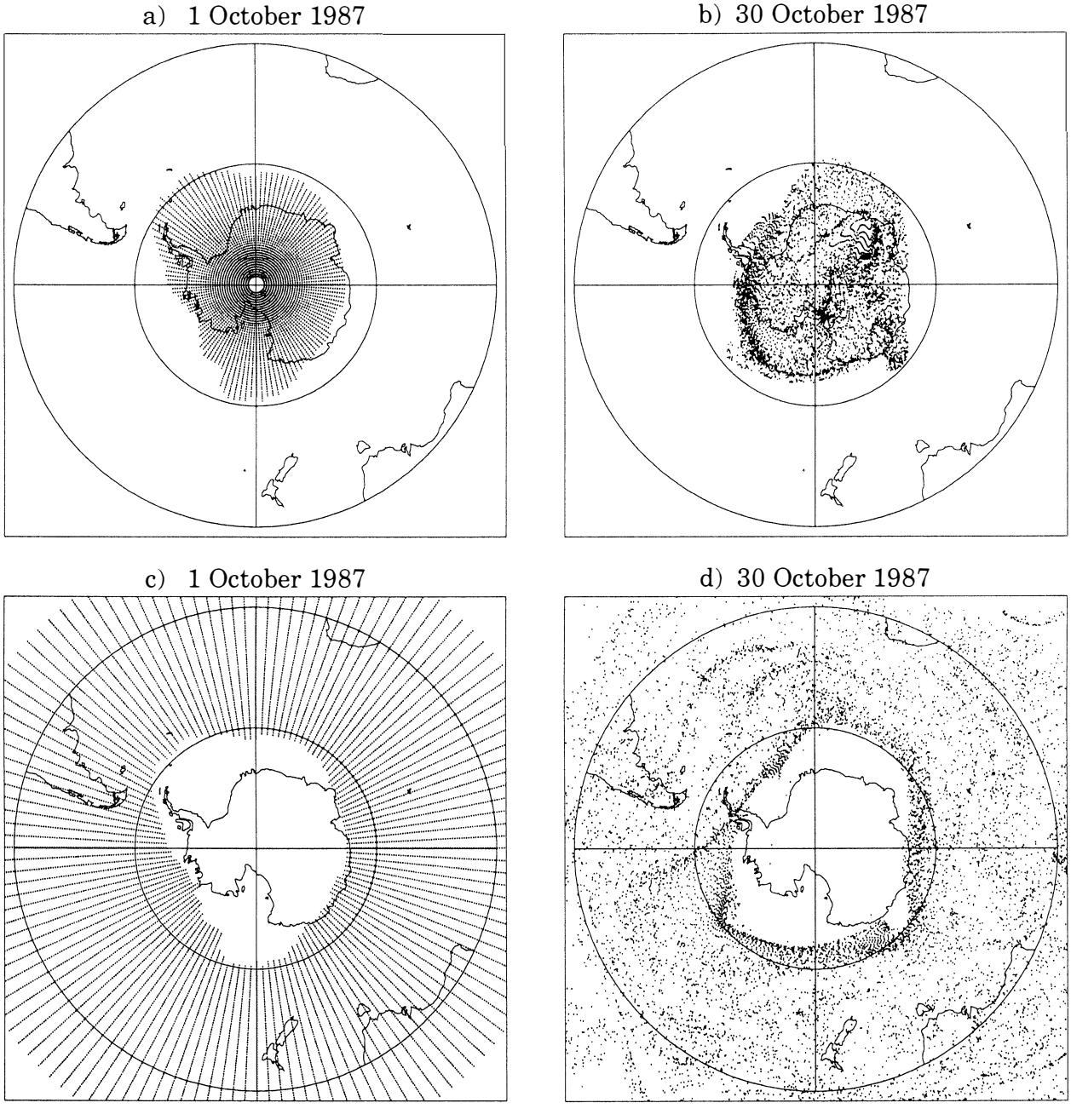

Figure 3-24. Evolution of air parcels on the 450 K (19 to 20 km) surface in the lower stratosphere over the period 1-30 October 1987 in the Antarctic. Initial locations for approximately 16,000 parcels on 1 October are indicated in (a) and (c) for interior and exterior vortex parcels, respectively. Final locations on 30 October are shown in (b) and (d) for the same groups, respectively. In each panel, the vertical line is the Greenwich meridian and the large and small circles correspond to 30° and 60° latitude, respectively. The 250 Dobson unit (DU) contour from the TOMS satellite observations of total ozone is used to separate the two parcel groups. Parcel motion is determined by trajectory calculations using winds derived from National Meteorological Center-analyzed height fields (Bowman, 1993).

In results from 3-D CTMs using winds from data assimilation systems, relatively little flow is found from within the vortex to midlatitudes (Rood *et al.*, 1992). These models incorporate diabatic and mixing effects that have not been considered in all trajectory and contour surgery models. In evaluations using aircraft, balloon, and satellite measurements, these models have been shown to represent synoptic- and planetary-scale variability on seasonal time scales. These models can simulate satellite ozone observations (*e.g.*, Limb Infrared Monitor of the Stratosphere [LIMS] and Total Ozone Mapping Spectrometer [TOMS]) for the entire winter season equally well in vortical and non-vortical air, suggesting that the transport mechanisms are at least qualitatively correct. These CTMs also show material peeling off the edge of the vortex into subpolar latitudes. This transport is wave-driven, with the planetary scales dominating the synoptic scales at altitudes above 20 mb. The results of Rood *et al.* (1992) in the Northern Hemisphere found that typically five percent of the air poleward of the subtropical jet stream and outside of the vortex had been processed by PSCs. During extreme events, this fraction could increase to 20 percent, in broad agreement with others (Plumb *et al.*, 1994; Tuck *et al.*, 1992).

A significant uncertainty in 3-D CTMs is whether or not the spatial resolution is adequate to simulate vortex processes. For instance, in Douglass *et al.* (1991), the general characteristics of aircraft ClO measurements were well simulated, but the detailed structure close to the vortex edge was not matched. Waugh *et al.* (1994) have shown that winds from the relatively coarse NMC analyses indeed contain enough information that, through differential advection, detailed structure can be meaningfully simulated. Therefore, in 3-D models and contour advection, the problem becomes one of choosing the appropriate mixing scale. The ability of carefully formulated 3-D models to perform seasonal integrations while maintaining realistic contrast between the vortex and midlatitudes suggests that they are reasonably mixed. Hence, the results suggest that it is not necessary to simulate the details of the fine structure, but it is necessary to simulate a self-consistent advective cascade with subscale mixing. Furthermore, transport studies driven by winds from assimilation analyses are likely to be of sufficient quality that transport across the vortex edge can be properly evaluated. High resolution may still be required for a quantitative evaluation of ozone depletion that occurs as processed air originating in the vortex is transported and mixed with lower latitude air.

Plumb *et al.* (1994) have also identified a discrete event of air being transported on horizontal surfaces into the lower vortex. Dahlberg and Bowman (1994) have performed a systematic evaluation of Arctic winters and find only limited transport into the vortex, with most of the activity remaining on the edge. Occasional inward transport is associated with planetary-scale blocking patterns and concomitant synoptic-scale lows that are associated with meteorological conditions in the troposphere. These studies all suggest only limited horizontal transport of extravortex air into the vortex throughout the winter.

Mechanistic 3-D models are a good tool for studying descent. They are forced from observations at some lower boundary (*e.g.,* 100 mb), with the stratosphere allowed to evolve self-consistently in balance with this forcing (*e.g.,* Fisher *et al.*, 1993). Because of the proximity of the forcing to the lower boundary, this approach has limited utility in the lower stratosphere. However, mechanistic models do provide an effective way to address the cold-pole problem (Mahlman and Umscheid, 1987) and other biases present in GCMs. Specifically, forcing from observations raises the polar temperature closer to observations, affording a more accurate representation of diabatic descent. Recent studies (*e.g.,* Jackman *et al.*, 1993; Nielsen *et al.*, 1994) show that mechanistic models can reproduce the descent of mesospheric ozone depletion and NO_2 enhancement that occurs during solar proton events (SPEs). This wintertime descent occurs across all stratospheric and mesospheric altitudes and requires consistent representation of mean-meridional flow in the mesosphere. The models do, in fact, represent the cross-equatorial transport of long-lived tracers observed in the mesosphere by satellite. Mechanistic models show unmixed descent consistent with satellite observations (Russell *et al.*, 1993b; Fisher *et al.*, 1993). Satellite data also indicate descent with little or no large-scale mixing across the vortex edge in the mid-stratosphere (Lahoz *et al.*, 1993). During midwinter, very little of the mesospheric air leaves the vortex in the lower stratosphere. This is consistent with the Stratospheric Aerosol and Gas Experiment (SAGE) NO_2 enhancements observed during an SPE. Mixing of mesospheric air that has

undergone descent occurs dramatically during vortex breakdown in the winter-to-spring seasonal transition, as has been observed in satellite data (Harwood *et al.*, 1993; Lahoz *et al.*, 1993). However, this is one-time mixing of air that was contained in the vortex, and does not provide a continual flow of air through the vortex. The mechanistic models establish that, given a realistic temperature distribution, radiative models calculate descent rates that are fundamentally in agreement with observed constituent behavior in the mid- to upper stratosphere. In the lower stratosphere, some uncertainty remains in modeling the relative effects of dynamical mixing and diabatic descent. However, Schoeberl *et al.* (1994) and Strahan *et al.* (1994) have shown that the aircraft N_2O data are in agreement with calculated radiative descent. The uncertainty that remains in the 3-D models will not substantially alter the arguments presented here.

GCMs provide an internally consistent, deterministic simulation of the atmosphere, although they cannot be used to simulate specific events for more than a few days, inhibiting direct day-to-day comparisons with constituent observations. Traditionally, GCMs underestimate polar temperatures (cold-pole), apparently due to a lack of dynamic activity (Mahlman and Umscheid, 1987). This leaves the model atmosphere too close to radiative equilibrium and, subsequently, leads to weak estimates of wintertime descent. The current generation of GCMs that extend up to the mesosphere (Strahan and Mahlman, 1994a, b; Boville, 1991; Cariolle *et al.*, 1992) has now been integrated for several seasonal cycles. In the Northern Hemisphere, the models can produce a disturbed flow in winter with the development of stratospheric warmings associated with the amplification of planetary waves. The model vortex is about 20 K warmer in the Northern Hemisphere than in the Southern Hemisphere, reasonably consistent with atmospheric observations. Comparisons with N_2O data show that the fall-to-winter descent can be simulated with considerable accuracy, and that the wintertime descent is maintained at a level comparable to observations (Strahan *et al.*, 1994). Transport of vortex edge air is simulated with mixing in the midlatitudes. Deep vortical air remains relatively isolated.

N_2O distributions from a GCM have also been compared with aircraft measurements (Strahan and Mahlman, 1994a, b). These studies show that, within the resolution constraints of the model, the processes that produce shredding from the vortex edge are consistent with observations. In addition, the mesoscale component of the variance, which is linked to planetary wave breaking processes, is also consistent in the Northern Hemisphere. A separate study of the N_2O aircraft observations supports only a limited outward flow near the vortex edge (Bacmeister *et al.*, 1992). These observations, when combined with theory and modeling results, provide a very powerful statement about transport through the vortex and model fidelity.

GCM simulations of the troposphere and stratosphere in the Antarctic are not as good as those in the Arctic, because the cold-pole problem is still significant and synoptic-scale activity is poorly represented in the southern ocean. In data assimilation approaches, the observations in the Southern Hemisphere are not sufficient to define many of the important waves. With less wave activity, the model atmosphere is closer to radiative equilibrium, resulting in less wintertime polar-night descent and a more isolated vortex. The observations of the Antarctic vortex strongly indicate that it is closer to radiative equilibrium than the Arctic vortex. The Antarctic temperatures are lower, the vortex is larger, and there is significantly less wave activity perturbing the flow, further suggesting that the Antarctic vortex is more isolated than the Arctic vortex.

These 3-D model approaches provide a consistent picture of dynamical processes of the polar vortex. The mechanisms in the 3-D global models are consistent with the barotropic models (*e.g.*, Juckes and McIntyre, 1987) and the contour advection models (*e.g.*, Waugh *et al.*, 1994) that have been used to isolate transport mechanisms. Most of the transport into and out of the vortex occurs along the edges, and deep vortical air is largely isolated throughout the winter. The material that is shred out of the vortex is spread broadly in midlatitudes, but satellite observations and model studies (Rood *et al.*, 1992, 1993) suggest that the midlatitudes are not homogeneously mixed. There is one-time mixing of the deep vortex air during the winter-to-spring transition, with processed air reaching mid- to low latitudes. There is continual circulation of midlatitude air towards the poles at high altitudes, followed by descent as the air enters polar night and cools. This circulation is largely on the edge of the vortex and should not see the full impact of polar processing. There can be substantial local mixing at low altitudes associated with dissipating synoptic

scales. Given the local nature of this transport, it does not require compensation by transport from above. In summary, given the seasonal lifetime of the vortex, the mixing times inferred from observations and models, the confinement of mixing to the edges, and the mixing in the winter-to-spring transition, it seems unlikely that the total volume of air that experiences polar chemical processing can exceed two times the volume of the midwinter vortex.

REFERENCES

Abbatt, J. P. D., and M. J. Molina, Heterogeneous interactions of $ClONO_2$ and HCl on nitric acid trihydrate at 202 K, *J. Phys. Chem., 96,* 7674-7679, 1992a.

Abbatt, J. P. D., and M. J. Molina, The heterogeneous reaction $HOCl + HCl \rightarrow Cl_2 + H_2O$ on ice and nitric acid trihydrate: Reaction probabilities and stratospheric implications, *Geophys. Res. Lett., 19,* 461-464, 1992b.

Adriani, A., T. Deshler, G. P. Gobbi, and G. Di Donfrancesco, Polar stratospheric clouds and volcanic aerosol during 1992 spring over McMurdo Station, Antarctica: Lidar and particle counter comparisons, *J. Geophys. Res.,* in press, 1994.

Anderson, J. G., W. H. Brune, S. A. Lloyd, D. W. Toohey, S. P. Sander, W. L. Starr, M. Loewenstein, and J. R. Podolske, Kinetics of O_3 destruction by ClO and BrO within the Antarctic vortex: An analysis based on *in situ* ER-2 data, *J. Geophys. Res., 94,* 11480-11520, 1989.

Anderson, J. G., D. W. Toohey, and W. H. Brune, Free radicals within the Antarctic vortex: The role of CFCs in Antarctic ozone loss, *Science, 251,* 39-46, 1991.

Anderson, J. G., and O. B. Toon, Airborne Arctic Stratospheric Expedition II: An overview, *Geophys. Res. Lett., 20,* 2499-2502, 1993.

Angell, J., Reexamination of the relation between depth of the Antarctic ozone hole, and equatorial QBO and SST, 1962-1992, *Geophys. Res. Lett., 20,* 1559-1562, 1993.

Arnold, F., K. Petzoldt, and E. Reimer, On the formation and sedimentation of stratospheric nitric acid aerosols—Implications for polar ozone destruction, *Geophys. Res. Lett., 19,* 677-680, 1992.

Atkinson, R. J., W. A. Matthews, P. A. Newman, and R. A. Plumb, Evidence of the mid-latitude impact of Antarctic ozone depletion, *Nature, 340,* 290-294, 1989.

Austin, J. N., N. Butchart, and K. P. Shine, Possibility of an Arctic ozone hole in a doubled-CO_2 climate, *Nature, 360,* 221-225, 1992.

Austin, J. N., and N. Butchart, The influence of climate change and the timing of stratospheric warmings on Arctic ozone depletion, *J. Geophys. Res., 99,* 1127-1145, 1994.

Bacmeister, J. T., M. R. Schoeberl, M. Loewenstein, J. R. Podolske, S. E. Strahan, and K. R. Chan, An estimate of the relative magnitude of small-scale tracer fluxes, *Geophys. Res. Lett., 19,* 1101-1104, 1992.

Baldwin, M. P., and D. O'Sullivan, Stratospheric effects of ENSO-related tropospheric circulation anomalies, *J. Climate*, in press, 1994.

Barath, F. T., M. C. Chavez, R. E. Cofield, D. A. Flower, M. A. Frerking, M. B. Gram, W. M. Harris, J. R. Holden, R. F. Jarnot, W. G. Kloezeman, G. J. Klose, G. K. Lau, M. S. Loo, B. J. Maddison, R. J. Mattauch, R. P. McKinney, G. E. Peckham, H. M. Pickett, G. Siebes, F. S. Soltis, R. A. Suttie, J. A. Tarsala, J. W. Waters, and W. J. Wilson, The Upper Atmosphere Research Satellite Microwave Limb Sounder Experiment, *J. Geophys. Res., 98,* 10751-10762, 1993.

Bauer, R., A. Engel, H. Franken, E. Klein, G. Kulessa, C. Schiller, U. Schmidt, R. Borchers, and J. Lee, Monitoring the vertical structure of the Arctic polar vortex over northern Scandinavia during EASOE: Regular N_2O profile observations, *Geophys. Res. Lett., 21,* 1211-1214, 1994.

Bell, W., N. A. Martin, T. D. Gardiner, N. R. Swann, P. T. Woods, P. F. Fogal, and J. W. Waters, Column measurements of stratospheric trace species over Åre, Sweden in the winter of 1991-92, *Geophys. Res. Lett., 21,* 1347-1350, 1994.

Borrmann, S., J. E. Dye, D. Baumgardner, J. C. Wilson, H. H. Jonsson, C. A. Brock, M. Loewenstein, J. R. Podolske, G. V. Ferry, and K. S. Barr, *In-situ* measurements of changes in stratospheric aerosol and the N_2O-aerosol relationship inside and outside of the polar vortex, *Geophys. Res. Lett., 20,* 2559-2562, 1993.

Boville, B., Sensitivity of simulated climate to model resolution, *J. Climate, 4,* 469-485, 1991.

Bowman, K. P., Large-scale isentropic mixing properties of the Antarctic polar vortex from analyzed winds, *J. Geophys. Res., 98,* 23013-23027, 1993.

Brandtjen, R., T. Klüpfel, D. Perner, and B. M. Knudsen, Airborne measurements during the European Arctic Stratospheric Ozone Experiment: Observation of OClO, *Geophys. Res. Lett., 21,* 1363-1366, 1994.

Brasseur, G. P., and C. Granier, Mount Pinatubo aerosols, chlorofluorocarbons, and ozone depletion, *Science, 257,* 1239-1242, 1992.

Browell, E. V., C. F. Butler, S. Ismail, P. A. Robinette, A. F. Carter, N. S. Higdon, O. B. Toon, M. R. Schoeberl, and A. F. Tuck, Airborne lidar observations in the wintertime Arctic stratosphere: Polar stratospheric clouds, *Geophys. Res. Lett., 17,* 385-388, 1990.

Browell, E. V., C. F. Butler, M. A. Fenn, W. B. Grant, S. Ismail, M. R. Schoeberl, O. B. Toon, M. Loewenstein, and J. R. Podolske, Ozone and aerosol changes during the 1991-1992 Airborne Arctic Stratospheric Expedition, *Science, 261,* 1155-1158, 1993.

Brune, W. H., J. G. Anderson, D. W. Toohey, D. W. Fahey, S. R. Kawa, R. L. Jones, D. S. McKenna, and L. R. Poole, The potential for ozone depletion in the Arctic polar stratosphere, *Science, 252,* 1260-1266, 1991.

Burkholder, J. B., R. K. Talukdar, A. R. Ravishankara, and S. Solomon, Temperature dependence of the HNO_3 UV absorption cross sections, *J. Geophys. Res., 98,* 22937-22948, 1994a.

Burkholder, J. B., R. K. Talukdar, and A. R. Ravishankara, Temperature dependence of the $ClONO_2$ UV absorption spectrum, *Geophys. Res. Lett., 21,* 585-588, 1994b.

Cacciani, M., P. Di Girolamo, A. di Sarra, G. Fiocco, and D. Fuà, Volcanic aerosol layers observed by lidar at South Pole, September 1991-June 1992, *Geophys. Res. Lett., 20,* 807-810, 1993.

Cariolle, D., A. Lasserre-Bigorry, and J. F. Boyer, A general circulation model simulation of the springtime Antarctic ozone decrease and its impact on mid-latitudes, *J. Geophys. Res., 95,* 1883-1898, 1990.

Cariolle, D., M. Amodei, and P. Simon, Dynamics and the ozone distribution in the winter stratosphere: Modelling the inter-hemispheric differences, *J. Atmos. Terr. Phys., 54,* 627-640, 1992.

Carroll, M. A., R. W. Sanders, S. Solomon, and A. L. Schmeltekopf, Visible and near-ultraviolet spectroscopy at McMurdo Station, Antarctica 6. Observations of BrO, *J. Geophys. Res., 94,* 16633-16638, 1989.

Carslaw, K., B. P. Luo, S. L. Clegg, Th. Peter, P. Brimblecombe, and P. J. Crutzen, Stratospheric aerosol growth and HNO_3 gas phase depletion from coupled HNO_3 and water uptake by liquid particles, *Geophys. Res. Lett.,* in press, 1994.

Chen, P., J. R. Holton, A. O'Neill, and R. Swinbank, Quasi-horizontal transport and mixing in the Antarctic stratosphere, *J. Geophys. Res., 99,* 16851-16866, 1994.

Chipperfield, M. P., A 3-D model comparison of PSC processing during the Arctic winters of 1991/92 and 1992/93, *Annales Geophysicae, 12,* 342-354, 1994a.

Chipperfield, M. P., D. Cariolle, and P. Simon, A 3D transport model study of chlorine activation during EASOE, *Geophys. Res. Lett., 21,* 1467-1470, 1994b.

Chipperfield, M. P., D. Cariolle, and P. Simon, A three-dimensional transport model study of PSC processing during EASOE, *Geophys. Res. Lett., 21,* 1463-1466, 1994c.

Chu, L. T., M.-T. Leu, and L. F. Keyser, Heterogeneous reactions of $HOCl + HCl \rightarrow Cl_2 + H_2O$ and $ClONO_2 + HCl \rightarrow Cl_2 + HNO_3$ on ice surfaces at polar stratospheric conditions, *J. Phys. Chem.,* in press, 1994.

Cox, R. A., A. R. MacKenzie, R. H. Müller, Th. Peter, and P. J. Crutzen, Activation of stratospheric chlorine by reactions in liquid sulfuric acid, *Geophys. Res. Lett., 21,* 1439-1442, 1994.

Crewell, S., K. Künzi, H. Nett, T. Wehr, and P. Hartogh, Aircraft measurements of ClO and HCl during EASOE 1991/92, *Geophys. Res. Lett., 21,* 1267-1270, 1994.

Dahlberg, S. P., and K. P. Bowman, Climatology of large-scale isentropic mixing in the Arctic winter stratosphere from analyzed winds, *J. Geophys. Res., 99,* 20585-20599, 1994.

Danielsen, E. F., and H. Houben, Dynamics of the Antarctic stratosphere and implications for the ozone hole, *Anthropogene Beeinflussung der Ozonschicht,* 191-242, DECHEMA, Frankfurt-am-Main, 1988.

Deshler, T., B. J. Johnson, and W. R. Rozier, Changes in the character of polar stratospheric clouds over Antarctica in 1992 due to the Pinatubo volcanic aerosol, *Geophys. Res. Lett., 21,* 273-276, 1994.

deZafra, R. L., M. Jaramillo, A. Parrish, P. Solomon, R. Connor, and J. Barrett, High concentrations of chlorine monoxide at low altitudes in the Antarctic spring stratosphere: Diurnal variation, *Nature, 328,* 408-411, 1987.

Douglass, A. R., R. B. Rood, J. A. Kaye, R. S. Stolarski, D. J. Allen, and E. M. Larson, The influence of polar heterogeneous processes on reactive chlorine at middle latitudes: Three-dimensional model implications, *Geophys. Res. Lett., 18,* 25-28, 1991.

Douglass, A. R., R. B. Rood, J. W. Waters, L. Froidevaux, W. Read, L. S. Elson, M. Geller, Y. Chi, M. C. Cerniglia, and S. Steenrod, A 3D simulation of the early winter distribution of reactive chlorine in the north polar vortex, *Geophys. Res. Lett., 20,* 1271-1274, 1993.

Drdla, K., and R. P. Turco, Denitrification through PSC formation: A 1-D model incorporating temperature oscillations, *J. Atmos. Chem., 12,* 319, 1991.

Dritschel, D. G., and B. Legras, Modeling oceanic and atmospheric vortices, *Phys. Today,* 44-51, March 1993.

Dye, J. E., D. Baumgardner, B. W. Gandrud, S. R. Kawa, K. K. Kelly, M. Loewenstein, G. V. Ferry, K. R. Chan, and B. L. Gary, Particle size distributions in Arctic polar stratospheric clouds, growth and freezing of sulfuric acid droplets, and implications for cloud formation, *J. Geophys. Res., 97,* 8015-8034, 1992.

Eckman, R. S., R. E. Turner, W. T. Blackshear, T. D. A. Fairlie, and W. L. Grose, Some aspects of the interaction between chemical and dynamic processes relating to the Antarctic ozone hole, *Adv. Space Res., 13,* 311-319, 1993.

Fahey, D. W., S. Solomon, S. R. Kawa, M. Loewenstein, J. R. Podolske, S. E. Strahan, and K. R. Chan, A diagnostic for denitrification in the winter polar stratospheres, *Nature, 345,* 698-702, 1990a.

Fahey, D. W., K. K. Kelly, S. R. Kawa, A. F. Tuck, M. Loewenstein, K. R. Chan, and L. E. Heidt, Observations of denitrification and dehydration in the winter polar stratospheres, *Nature, 344,* 321-324, 1990b.

Fahey, D. W., S. R. Kawa, E. L. Woodbridge, P. Tin, J. C. Wilson, H. H. Jonsson, J. E. Dye, D. Baumgardner, S. Borrmann, D. W. Toohey, L. M. Avallone, M. H. Proffitt, J. J. Margitan, M. Loewenstein, J. R. Podolske, R. J. Salawitch, S. C. Wofsy, M. K. W. Ko, D. E. Anderson, M. R. Schoeberl, and K. R. Chan, *In situ* measurements constraining the role of sulfate aerosols in mid-latitude ozone depletion, *Nature, 363,* 509-514, 1993.

Farman, J. C., A. O'Neill, and R. Swinbank, The dynamics of the Arctic polar vortex during the EASOE campaign, *Geophys. Res. Lett., 21,* 1195-1198, 1994.

Fisher, M. A., A. O'Neill, and R. Sutton, Rapid descent of mesospheric air into the stratospheric polar vortex, *Geophys. Res. Lett., 20,* 1267-1270, 1993.

Fried, A., B. E. Henry, J. G. Calvert, and M. Mozurkewich, The reaction probability of N_2O_5 with sulfuric acid aerosols at stratospheric temperatures and compositions, *J. Geophys. Res., 99,* 3517-3532, 1994.

Garcia, R. R., F. Stordal, S. Solomon, and J. T. Kiehl, A new numerical model of the middle atmosphere 1. Dynamics and transport of tropospheric source gases, *J. Geophys. Res., 97,* 12967-12991, 1992.

Gerber, L., and N. Kämpfer, Millimeter-wave measurements of chlorine monoxide at the Jungfraujoch Alpine Station, *Geophys. Res. Lett., 21,* 1279-1282, 1994.

Gobbi, G. P., and A. Adriani, Mechanisms of formation of stratospheric clouds observed during the Antarctic late winter of 1992, *Geophys. Res. Lett., 20,* 1427-1430, 1993.

GRL, Special Section, The stratospheric and climatic effects of the 1991 Mt. Pinatubo eruption: An initial assessment, *Geophys. Res. Lett., 19,* 149-218, 1992.

Hanson, D. R., and A. R. Ravishankara, The reaction probabilities of $ClONO_2$ and N_2O_5 on 40 to 75 percent sulfuric acid solutions, *J. Geophys. Res., 96,* 17307-17314, 1991.

Kelly, K. K., A. F. Tuck, D. M. Murphy, M. H. Proffitt, D. W. Fahey, R. L. Jones, D. S. McKenna, M. Loewenstein, J. R. Podolske, S. E. Strahan, G. V. Ferry, K. R. Chan, J. F. Vedder, G. L. Gregory, W. D. Hypes, M. P. McCormick, E. V. Browell, and L. E. Heidt, Dehydration in the lower Antarctic stratosphere during late winter and early spring, 1987, *J. Geophys. Res., 94,* 11317-11357, 1989.

Kelly, K. K., A. F. Tuck, L. E. Heidt, M. Loewenstein, J. R. Podolske, S. E. Strahan, and J. F. Vedder, A comparison of ER-2 measurements of stratospheric water vapor between the 1987 Antarctic and 1989 Arctic Airborne Missions, *Geophys. Res. Lett., 17,* 465-468, 1990.

Kent, G. S., L. R. Poole, M. P. McCormick, S. F. Schaffner, W. H. Hunt, and M. T. Osborn, Optical backscatter characteristics of Arctic polar stratospheric clouds, *Geophys. Res. Lett., 17,* 377-380, 1990.

Keys, J. G., P. V. Johnston, R. D. Blatherwick, and F. J. Murcray, Evidence for heterogeneous reactions in the Antarctic autumn stratosphere, *Nature, 361,* 49-51, 1993.

Kinne, S., O. B. Toon, and M. J. Prather, Buffering of stratospheric circulation by changing amounts of tropical ozone: A Pinatubo case study, *Geophys. Res. Lett., 19,* 1927-1930, 1992.

Koike, M., N. B. Jones, W. A. Matthews, P. V. Johnston, R. L. McKenzie, D. Kinnison, and J. Rodriguez, Impact of Pinatubo aerosols on the partitioning between NO_2 and HNO_3, *Geophys. Res. Lett., 21,* 597-600, 1994.

Kolb, C. E., D. R. Worsnop, M. S. Zahniser, P. Davidovits, L. F. Keyser, M.-T. Leu, M. J. Molina, D. R. Hanson, A. R. Ravishankara, L. R. Williams, and M. R. Tolbert, Laboratory studies of atmospheric heterogeneous chemistry, in *Current Problems in Atmospheric Chemistry*, edited by J. R. Barker, in press, 1994.

Kondo, Y., P. Aimedieu, M. Koike, Y. Iwasaka, P. A. Newman, U. Schmidt, W. A. Matthews, M. Hayashi, and W. R. Sheldon, Reactive nitrogen, ozone, and nitrate aerosols observed in the Arctic stratosphere in January 1990, *J. Geophys. Res., 97,* 13025-13038, 1992.

Kondo, Y., U. Schmidt, T. Sugita, P. Aimedieu, M. Koike, H. Ziereis, and Y. Iwasaka, Total reactive nitrogen, N_2O, and ozone in the winter Arctic stratosphere, *Geophys. Res. Lett., 21,* 1247-1250, 1994a.

Kondo, Y., W. A. Matthews, S. Solomon, M. Koike, M. Hayashi, K. Yamazaki, H. Nakajima, and K. Tsukui, Ground based measurements of column amounts of NO_2 over Syowa Station, Antarctica, *J. Geophys. Res., 99,* 14535-14548, 1994b.

Krueger, A., M. R. Schoeberl, P. A. Newman, and R. S. Stolarski, The 1991 Antarctic ozone hole: TOMS observations, *Geophys. Res. Lett., 19,* 1215-1218, 1992.

Labitzke, K., On the variability of the stratosphere in the Arctic regions in winter, *Ber. Bunsenges. Phys. Chem., 96,* 496-501, 1992.

Labitzke, K., and M. P. McCormick, Stratospheric temperature increases due to Pinatubo aerosols, *Geophys. Res. Lett., 19,* 207-210, 1992.

Lahoz, W. A., E. S. Carr, L. Froidevaux, R. S. Harwood, J. B. Kumer, J. L. Mergenthaler, G. E. Peckham, W. G. Read, P. D. Ricaud, A. E. Roche, and J. W. Waters, Northern Hemisphere mid-stratosphere vortex processes diagnosed from H_2O, N_2O, and potential vorticity, *Geophys. Res. Lett., 20,* 2671-2674, 1993.

Larsen, N., B. Knudsen, I. S. Mikkelsen, T. S. Jørgensen, and P. Eriksen, Ozone depletion in the Arctic stratosphere in early 1993, *Geophys. Res. Lett., 21,* 1611-1614, 1994.

Lefèvre, F., G. P. Brasseur, I. Folkins, A. K. Smith, and P. Simon, The chemistry of the 1991-92 stratospheric winter: Three-dimensional model simulations, *J. Geophys. Res., 99,* 8183-8195, 1994.

Liu, X., R. D. Blatherwick, F. J. Murcray, J. G. Keys, and S. Solomon, Measurements and model calculations of HCl column amounts and related parameters over McMurdo during the Austral spring in 1989, *J. Geophys. Res., 97,* 20795-20804, 1992.

Loewenstein, M., J. R. Podolske, K. R. Chan, and S. E. Strahan, Nitrous oxide as a dynamical tracer in the 1987 Airborne Antarctic Ozone Experiment, *J. Geophys. Res., 94,* 11589-11598, 1989.

Loewenstein, M., J. R. Podolske, D. W. Fahey, E. L. Woodbridge, P. Tin, A. Weaver, P. A. Newman, S. E. Strahan, S. R. Kawa, M. R. Schoeberl, and L. R. Lait, New observations of the NO_y/N_2O correlation in the lower stratosphere, *Geophys. Res. Lett., 20,* 2531-2534, 1993.

Lucic, D., N. R. P. Harris, J. A. Pyle, and R. L. Jones, Diagnosing ozone loss in the Northern Hemisphere for the 1991/92 winter, *J. Geophys. Res.,* in press, 1994.

Luo, B. P., Th. Peter, and P. J. Crutzen, Freezing of stratospheric aerosol droplets, *Geophys. Res. Lett., 21,* 1447-1450, 1994a.

Luo, B. P., Th. Peter, and P. J. Crutzen, HCl solubility and liquid diffusion in aqueous sulfuric acid under stratospheric conditions, *Geophys. Res. Lett., 21,* 49-52, 1994b.

Lutman, E. R., J. A. Pyle, R. L. Jones, D. J. Lary, A. R. MacKenzie, I. Kilbane-Dawe, N. Larsen, and B. M. Knudsen, Trajectory model studies of ClO_x activation during the 1991/92 Northern Hemispheric winter, *Geophys. Res. Lett., 21,* 1419-1422, 1994a.

Lutman, E. R., R. Toumi, R. L. Jones, D. J. Lary, and J. A. Pyle, Box model studies of ClO_x deactivation and ozone loss during the 1991/92 Northern Hemispheric winter, *Geophys. Res. Lett., 21,* 1415-1418, 1994b.

MacKenzie, A. R., B. M. Knudsen, R. L. Jones, and E. R. Lutman, The spatial and temporal extent of chlorine activation by polar stratospheric clouds in the Northern Hemisphere winters of 1988/89 and 1991/92, *Geophys. Res., Lett., 21,* 1423-1426, 1994.

Mahlman, J. D., H. Levy II, and W. J. Moxim, Three-dimensional tracer structure and behavior as simulated in two ozone precursor experiments, *J. Atmos. Sci., 37,* 655-685, 1980.

Mahlman, J. D., and L. Umscheid, Comprehensive modeling of the middle atmosphere: The influence of horizontal resolution, in *Transport Processes in the Middle Atmosphere*, edited by G. Visconti and R. Garcia, D. Reidel, Hingham, Massachusetts, 251-266, 1987.

Mankin, M. G., M. T. Coffey, and A. Goldman, Airborne observations of SO_2, HCl, and O_3 in the stratospheric plume of the Pinatubo volcano in July 1991, *Geophys. Res. Lett., 19,* 179-182, 1992.

Manney, G. L., and R. W. Zurek, Interhemispheric comparison of the development of the stratospheric polar vortex during fall: A 3-dimensional perspective for 1991-1992, *Geophys. Res. Lett., 20,* 1275-1278, 1993.

Manney, G. L., L. Froidevaux, J. W. Waters, L. S. Elson, E. F. Fishbein, R. W. Zurek, R. S. Harwood, and W. A. Lahoz, The evolution of ozone observed by UARS MLS in the 1992 late winter southern polar vortex, *Geophys. Res. Lett., 20,* 1279-1282, 1993.

Manney, G. L., R. W. Zurek, A. O'Neill, R. Swinbank, J. B. Kumer, J. L. Mergenthaler, and A. E. Roche, Stratospheric warmings during February and March 1993, *Geophys. Res. Lett., 21,* 813-816, 1994a.

Manney, G. L., L. Froidevaux, J. W. Waters, R. W. Zurek, W. G. Read, L. S. Elson, J. B. Kumer, J. L. Mergenthaler, A. E. Roche, A. O'Neill, R. S. Harwood, I. MacKenzie, and R. Swinbank, Chemical depletion of lower stratospheric ozone in the 1992-1993 northern winter vortex, *Nature, 370,* 429-434, 1994b.

Manney, G. L., R. W. Zurek, A. O'Neill, and R. Swinbank, On the motion of air through the stratospheric polar vortex, *J. Atmos. Sci., 51,* 2973-2994, 1994c.

McCormick, M. P., and R. E. Veiga, SAGE II measurements of early Pinatubo aerosols, *Geophys. Res. Lett., 19,* 155-158, 1992.

McElroy, M. B., R. J. Salawitch, S. C. Wofsy, and J. A. Logan, Reduction of Antarctic ozone due to synergistic interactions of chlorine and bromine, *Nature, 321,* 759-762, 1986.

McKenna, D. S., R. L. Jones, L. R. Poole, S. Solomon, D. W. Fahey, K. K. Kelly, M. H. Proffitt, W. H. Brune, M. Loewenstein, and K. R. Chan, Calculations of ozone destruction during the 1988/89 Arctic winter, *Geophys. Res. Lett., 17,* 553-556, 1990.

Middlebrook, A. M., B. G. Koehler, L. S. McNeill, and M. A. Tolbert, Formation of model polar stratospheric cloud films, *Geophys. Res. Lett., 24,* 2417-2420, 1992.

Middlebrook, A. M., L. T. Iraci, L. S. McNeill, B. G. Koehler, O. W. Saastad, and M. A. Tolbert, FTIR studies of thin H_2SO_4/H_2O films: Formation, water uptake, and solid-liquid phase changes, *J. Geophys. Res.*, in press, 1994.

Minton, T. K., C. M. Nelson, T. A. Moore, and M. Okamura, Direct observation of ClO from chlorine nitrate photolysis, *Nature, 328,* 1342-1345, 1992.

Molina, L. T., and M. J. Molina, Production of Cl_2O_2 from the self-reaction of the ClO radical, *J. Phys. Chem., 91,* 433-436, 1987.

Molina, M. J., R. Zhang, P. J. Wooldridge, J. R. McMahon, J. E. Kim., H. Y. Chang, and K. Beyer, Physical chemistry of the $H_2SO_4/HNO_3/H_2O$ system: Implications for the formation of polar stratospheric clouds and heterogeneous chemistry, *Science, 261,* 1418-1423, 1993.

Müller, R., and T. Peter, The numerical modeling of the sedimentation of polar stratospheric cloud particles, *Ber. Bunsenges. Phys. Chem., 96,* 353-361, 1992.

Murcray, F. J., J. R. Starkey, W. J. Williams, W. A. Matthews, U. Schmidt, P. Aimedieu, and C. Camy-Peyret, HNO_3 profiles obtained during the EASOE campaign, *Geophys. Res. Lett., 21,* 1223-1226, 1994.

Nagatani, R. M., A. J. Miller, M. E. Gelman, and P. A. Newman, A comparison of Arctic lower stratospheric winter temperatures for 1988-89 with temperatures since 1964, *Geophys. Res. Lett., 17,* 333-336, 1990.

Newman, P. A., L. R. Lait, M. R. Schoeberl, E. R. Nash, K. K. Kelly, D. W. Fahey, R. M. Nagatani, D. W. Toohey, L. M. Avallone, and J. G. Anderson, Stratospheric meteorological conditions in the Arctic polar vortex, 1991 to 1992, *Science, 261,* 1143-1146, 1993.

Nielsen, J. E., R. B. Rood, A. R. Douglass, M. C. Cerniglia, D. J. Allen, and J. E. Rosenfield, Tracer evolution in winds generated by a global spectral mechanistic model, *J. Geophys. Res., 99,* 5399-5420, 1994.

Norton, W. A., Breaking Rossby waves in a model stratosphere diagnosed by a vortex following system and contour advection technique, *J. Atmos. Sci., 51,* 654-673, 1993.

Ohtake, T., Freezing points of H_2SO_4 aqueous solutions and formation of stratospheric ice clouds, *Tellus, 45B,* 138-144, 1993.

Orsolini, Y. D., D. Cariolle, and M. Déqué, A GCM study of the late January 1992 'mini-hole' event observed during EASOE, *Geophys Res. Lett., 21,* 1459-1462, 1994.

Osborn, M. T., M. C. Pitts, K. A. Powell, and M. P. McCormick, SAM II aerosol measurements during the 1989 AASE, *Geophys. Res. Lett., 17,* 397-400, 1990.

Perliski, L. M., S. Solomon, and J. London, On the interpretation of the seasonal variations of stratospheric ozone, *Planet. Space Sci., 37,* 1527-1538, 1989.

Perner, D., A. Roth, and T. Klüpfel, Groundbased measurements of stratospheric OClO, NO_2, and O_3 at Søndre Strømfjord in winter 1991/92, *Geophys. Res. Lett., 21,* 1367-1370, 1994.

Peter, Th., C. Brühl, and P. J. Crutzen, Increase in the PSC-formation probability caused by high-flying aircraft, *Geophys. Res. Lett., 18,* 1465-1468, 1991.

Peter, Th., R. Müller, K. Drdla, K. Petzoldt, and E. Reimer, A micro-physical box model for EASOE: Preliminary results for the January/February 1990 PSC event over Kiruna, *Ber. Bunsenges. Phys. Chem., 96,* 362-367, 1992.

Petzoldt, K., B. Naujokat, and K. Neugebohren, Correlation between stratospheric temperature, total ozone, and tropospheric weather systems, *Geophys. Res. Lett., 21,* 1203-1206, 1994.

Pierce, R. B., and T. D. A. Fairlie, Chaotic advection in the stratosphere: Implications for the dispersal of chemically perturbed air from the polar vortex, *J. Geophys. Res., 98,* 18589-18595, 1993.

Pierce, R. B., W. L. Grose, J. M. Russell III, and A. F. Tuck, Spring dehydration in the Antarctic vortex observed by HALOE, *J. Atmos. Sci., 51,* 2931-2941, 1994.

Plumb, R. A., and M. K. W. Ko, Interrelationships between mixing ratios of long-lived stratospheric constituents, *J. Geophys. Res., 97,* 10145-10156, 1992.

Plumb, R. A., D. W. Waugh, R. J. Atkinson, P. A. Newman, L. R. Lait, M. R. Schoeberl, E. V. Browell, A. J. Simmons, and M. Loewenstein, Intrusions into the lower stratospheric Arctic vortex during the winter of 1991/92, *J. Geophys. Res., 99,* 1089-1105, 1994.

Podolske, J. R., M. Loewenstein, A. Weaver, S. E. Strahan, and K. R. Chan, Northern Hemisphere nitrous oxide morphology during the 1989 AASE and the 1991-92 AASE II campaigns, *Geophys. Res. Lett., 20,* 2535-2538, 1993.

Poole, L. R., S. Solomon, M. P. McCormick, and M. C. Pitts, The interannual variability of polar stratospheric clouds and related parameters in Antarctica during September and October, *Geophys. Res. Lett., 16,* 1157-1160, 1989.

Poole, L. R., and M. C. Pitts, Polar stratospheric cloud climatology based on Stratospheric Aerosol Measurement II observations from 1978 to 1989, *J. Geophys. Res., 99,* 13083-13089, 1994.

Prather, M. J., Catastrophic loss of ozone in dense volcanic clouds, *J. Geophys. Res., 97,* 10187-10191, 1992.

Proffitt, M. H., D. W. Fahey, K. K. Kelly, and A. F. Tuck, High-latitude ozone loss outside the Antarctic ozone hole, *Nature, 342,* 233-237, 1989a.

Proffitt, M. H., K. K. Kelly, J. A. Powell, B. L. Gary, M. Loewenstein, J. R. Podolske, S. E. Strahan, and K. R. Chan, Evidence for diabatic cooling and poleward transport within and around the 1987 Antarctic ozone hole, *J. Geophys. Res., 94,* 16797-16813, 1989b.

Proffitt, M. H., J. A. Powell, A. F. Tuck, D. W. Fahey, K. K. Kelly, A. J. Krueger, M. R. Schoeberl, B. L. Gary, J. J. Margitan, K. R. Chan, M. Loewenstein, and J. R. Podolske, A chemical definition of the boundary of the Antarctic ozone hole, *J. Geophys. Res., 94,* 11437-11448, 1989c.

Proffitt, M. H., J. J. Margitan, K. K. Kelly, M. Loewenstein, J. R. Podolske, and K. R. Chan, Ozone loss in the Arctic polar vortex inferred from high-altitude aircraft measurements, *Nature, 347,* 31-36, 1990.

Proffitt, M. H., S. Solomon, and M. Loewenstein, Comparison of 2-D model simulations of ozone and nitrous oxide at high latitudes with stratospheric measurements, *J. Geophys. Res., 97,* 939-944, 1992.

Proffitt, M. H., K. Aikin, J. J. Margitan, M. Loewenstein, J. R. Podolske, S. E. Strahan, and A. Weaver, Ozone loss inside the northern polar vortex during the 1991-1992 winter, *Science, 261,* 1150-1154, 1993.

Pyle, J. A., N. R. P. Harris, J. C. Farman, F. Arnold, G. Braathen, R. A. Cox, P. Faucon, R. L. Jones, G. Mégie, A. O'Neill, U. Platt, J.-P. Pommereau, U. Schmidt, and F. Stordal, An overview of the EASOE campaign, *Geophys. Res. Lett., 21,* 1191-1194, 1994.

Reber, C. A., The Upper Atmosphere Research Satellite, *EOS Transactions, 71,* 1867-1878, 1990.

Reber, C. A., C. E. Trevathan, R. J. McNeal, and M. R. Luther, The Upper Atmosphere Research Satellite (UARS) mission, *J. Geophys. Res., 98,* 10643-10647, 1993.

Reihs, C. M., D. M. Golden, and M. A. Tolbert, Nitric acid uptake by sulfuric acid solutions under stratospheric conditions: Determination of Henry's law solubility, *J. Geophys. Res., 95,* 16545-16550, 1990.

Rind, D., N. K. Balachandran, and R. Suozzo, Climate change and the middle atmosphere. Part II: The impact of volcanic aerosols, *J. Climate, 5,* 189-208, 1992.

Rind, D., E.-W. Chiou, W. Chu, S. Oltmans, J. Lerner, J. Larsen, M. P. McCormick, and L. McMaster, Overview of the Stratospheric Aerosol and Gas Experiment II water vapor observations: Method, validation, and data characteristics, *J. Geophys. Res., 98,* 4835-4856, 1993.

Roche, A. E., J. B. Kumer, J. L. Mergenthaler, G. A. Ely, W. G. Uplinger, J. F. Potter, T. C. James, and L. W. Sterritt, The Cryogenic Limb Array Etalon Spectrometer (CLAES) on UARS: Experiment description and performance, *J. Geophys. Res., 98,* 10763-10775, 1993a.

Roche, A. E., J. B. Kumer, and J. L. Mergenthaler, CLAES observations of $ClONO_2$ and HNO_3 in the Antarctic stratosphere, between June 15 and September 17, 1992, *Geophys. Res. Lett., 20,* 1223-1226, 1993b.

Roche, A. E., J. B. Kumer, J. L. Mergenthaler, R. W. Nightingale, W. G. Uplinger, G. A. Ely, J. F. Potter, D. J. Wuebbles, P. S. Connell, and D. E. Kinnison, Observations of lower stratospheric $ClONO_2$, HNO_3, and aerosol by the UARS CLAES experiment between January 1992 and April 1993, *J. Atmos. Sci., 51,* 2877-2902, 1994.

Rood, R. B., J. E. Nelson, R. S. Stolarski, A. R. Douglass, J. A. Kaye, and D. J. Allen, Episodic total ozone minima and associated effects on heterogeneous chemistry and lower stratospheric transport, *J. Geophys. Res., 97,* 7979-7996, 1992.

Rood, R. B., A. R. Douglass, J. A. Kaye, and D. B. Considine, Characteristics of wintertime and autumn nitric acid chemistry as defined by Limb Infrared Monitor of the Stratosphere (LIMS) data, *J. Geophys. Res., 98,* 18533-18545, 1993.

Rosenfield, J. E., M. R. Schoeberl, and M. A. Geller, A computation of the stratospheric diabatic circulation using an accurate radiative transfer model, *J. Atmos. Sci., 44,* 859-876, 1987.

Rosenfield, J. E., P. A. Newman, and M. R. Schoeberl, Computations of diabatic descent in the stratospheric polar vortex, *J. Geophys. Res., 99,* 16677-16689, 1994.

Russell, J. M., III, L. L. Gordley, J. H. Park, S. R. Drayson, W. D. Hesketh, R. J. Cicerone, A. F. Tuck, J. E. Frederick, J. E. Harries, and P. J. Crutzen, The Halogen Occultation Experiment, *J. Geophys. Res., 98,* 10777-10797, 1993a.

Russell, J. M., III, A. F. Tuck, L. L. Gordley, J. H. Park, S. R. Drayson, J. E. Harries, R. J. Cicerone, and P. J. Crutzen, HALOE Antarctic observations in the spring of 1991, *Geophys. Res. Lett., 20,* 719-722, 1993b.

Salawitch, R. J., S. C. Wofsy, M. B. McElroy, Chemistry of OClO in the Antarctic stratosphere: Implications for bromine, *Planet. Space Sci., 36,* 213-224, 1988.

Salawitch, R. J., G. P. Gobbi, S. C. Wofsy, and M. B. McElroy, Denitrification in the Antarctic stratosphere, *Nature, 339,* 525-527, 1989.

Salawitch, R. J., M. B. McElroy, J. H. Yatteau, S. C. Wofsy, M. R. Schoeberl, L. R. Lait, P. A. Newman, K. R. Chan, M. Loewenstein, J. R. Podolske, S. E. Strahan, and M. H. Proffitt, Loss of ozone in the Arctic vortex for the winter of 1989, *Geophys. Res. Lett., 17,* 561-564, 1990.

Salawitch, R. J., S. C. Wofsy, E. Gottlieb, L. R. Lait, P. A. Newman, M. R. Schoeberl, M. Loewenstein, J. R. Podolske, S. E. Strahan, M. H. Proffitt, C. R. Webster, R. D. May, D. W. Fahey, D. Baumgardner, J. E. Dye, J. C. Wilson, K. K. Kelly, J. W. Elkins, K. R. Chan, and J. G. Anderson, Chemical loss of ozone in the Arctic polar vortex in the winter of 1991-1992, *Science, 261,* 1146-1149, 1993.

Sanders, R. W., S. Solomon, J. P. Smith, L. Perliski, H. L. Miller, G. H. Mount, J. G. Keys, and A. L. Schmeltekopf, Visible and near-ultraviolet spectroscopy at McMurdo Station, Antarctica 9. Observations of OClO from April to October 1991, *J. Geophys. Res., 98,* 7219-7228, 1993.

Santee, M. L., W. G. Read, J. W. Waters, L. Froidevaux, G. L. Manney, D. A. Flower, R. F. Jarnot, R. S. Harwood, and G. E. Peckham, Interhemispheric differences in polar stratospheric HNO_3, H_2O, ClO, and O_3 from UARS MLS, submitted to *Science,* 1994.

Schauffler, S. M., L. E. Heidt, W. H. Pollock, T. M. Gilpin, J. F. Vedder, S. Solomon, R. A. Lueb, and E. L. Atlas, Measurements of halogenated organic compounds near the tropical tropopause, *Geophys. Res. Lett., 20,* 2567-2570, 1993.

Schiller, C., A. Wahner, U. Platt, H.-P. Dorn, J. Callies, and D. H. Ehhalt, Near UV atmospheric absorption measurements of column abundances during Airborne Arctic Stratospheric Expedition, January-February 1989: 2. OClO observations, *Geophys. Res. Lett., 17,* 501-504, 1990.

Schlager, H., and F. Arnold, Measurements of stratospheric gaseous nitric acid in the winter Arctic vortex using a novel rocket-borne mass spectrometric method, *Geophys. Res. Lett., 17,* 433-436, 1990.

Schmidt, U., R. Bauer, A. Khedim, E. Klein, G. Kulessa, and C. Schiller, Profile observations of long-lived trace gases in the Arctic vortex, *Geophys. Res. Lett., 18,* 767-770, 1991.

Schmidt, U., R. Bauer, A. Engel, R. Borchers, and J. Lee, The variation of available chlorine, Cl_y, in the Arctic polar vortex during EASOE, *Geophys. Res. Lett., 21,* 1215-1218, 1994.

Schoeberl, M. R., M. H. Proffitt, K. K. Kelly, L. R. Lait, P. A. Newman, J. E. Rosenfield, M. Loewenstein, J. R. Podolske, S. E. Strahan, and K. R. Chan, Stratospheric constituent trends from ER-2 profile data, *Geophys. Res. Lett., 17,* 469-472, 1990.

Schoeberl, M. R., and D. L. Hartmann, The dynamics of the stratospheric polar vortex and its relation to springtime ozone depletions, *Science, 251,* 46-52, 1991.

Schoeberl, M. R., L. R. Lait, P. A. Newman, and J. E. Rosenfield, The structure of the polar vortex, *J. Geophys. Res., 97,* 7859-7882, 1992.

Schoeberl, M. R., A. R. Douglass, R. S. Stolarski, P. A. Newman, L. R. Lait, D. W. Toohey, L. M. Avallone, J. G. Anderson, W. H. Brune, D. W. Fahey, and K. K. Kelly, The evolution of ClO and NO along air parcel trajectories, *Geophys. Res. Lett., 20,* 2511-2514, 1993a.

Schoeberl, M. R., R. S. Stolarski, A. R. Douglass, P. A. Newman, L. R. Lait, J. W. Waters, L. Froidevaux, and W. G. Read, MLS ClO observations and Arctic polar vortex temperatures, *Geophys. Res. Lett., 20,* 2861-2864, 1993b.

Schoeberl, M. R., M. Luo, and J. E. Rosenfield, An analysis of the Antarctic HALOE trace gas observations, *J. Geophys. Res.,* in press, 1994.

Shine, K. P., Sources and sinks of zonal momentum in the middle atmosphere diagnosed using the diabatic circulation, *Quart. J. Roy. Meteorol. Soc., 115,* 265-292, 1989.

Solomon, S., Progress towards a quantitative understanding of Antarctic ozone depletion, *Nature, 347,* 347-354, 1990.

Solomon, S., R. R. Garcia, F. S. Rowland, and D. J. Wuebbles, On the depletion of Antarctic ozone, *Nature, 321,* 755-758, 1986.

Solomon, S., R. W. Sanders, M. A. Carroll, and A. L. Schmeltekopf, Visible and near-ultraviolet spectroscopy at McMurdo Station, Antarctica 5. Observations of the diurnal variations of BrO and OClO, *J. Geophys. Res., 94,* 11393-11403, 1989.

Solomon, S., and J. G. Keys, Seasonal variations in Antarctic NO_x chemistry, *J. Geophys. Res., 97,* 7971-7978, 1992.

Solomon, S., R. W. Sanders, R. R. Garcia, and J. G. Keys, Increased chlorine dioxide over Antarctica caused by volcanic aerosols from Mount Pinatubo, *Nature, 363,* 245-248, 1993.

Strahan, S. E., and J. D. Mahlman, Evaluation of the SKYHI general circulation model using aircraft N_2O measurements: 1. Polar winter stratospheric meteorology and tracer morphology, *J. Geophys. Res., 99,* 10305-10318, 1994a.

Strahan, S. E., and J. D. Mahlman, Evaluation of the SKYHI general circulation model using aircraft N_2O measurements: 2. Tracer variability and diabatic meridional circulation, *J. Geophys. Res., 99,* 10319-10332, 1994b.

Strahan, S. E., J. E. Rosenfield, M. Loewenstein, J. R. Podolske, and A. Weaver, Evolution of the 1991-1992 Arctic vortex and comparison with the GFDL SKYHI general circulation model, *J. Geophys. Res., 99,* 20713-20723, 1994.

Tabazadeh, A., and R. P. Turco, Stratospheric chlorine injection by volcanic eruptions: HCl scavenging and implications for ozone, *Science, 260,* 1082-1086, 1993.

Tabazadeh, A., R. P. Turco, and M. Z. Jacobson, A model for studying the composition and chemical effects of stratospheric aerosols, *J. Geophys. Res., 99,* 12897-12914, 1994.

Tao, X., and A. F. Tuck, On the distribution of cold air near the vortex edge in the lower stratosphere, *J. Geophys. Res., 99,* 3431-3450, 1994.

Taylor, F. W., C. D. Rodgers, J. G. Whitney, S. T. Werrett, J. J. Barnett, G. D. Peskett, P. Venters, J. Ballard, C. W. P. Palmer, R. J. Knight, P. Morris, T. Nightingale, and A. Dudhia, Remote sensing of atmospheric structure and composition by pressure modulator radiometry from space: The ISAMS experiment on UARS, *J. Geophys. Res., 98,* 10799-10814, 1993.

Toohey, D. W., J. G. Anderson, W. H. Brune, and K. R. Chan, *In situ* measurements of BrO in the Arctic stratosphere, *Geophys. Res. Lett., 17,* 513-516, 1990.

Toohey, D. W., L. M. Avallone, L. R. Lait, P. A. Newman, M. R. Schoeberl, D. W. Fahey, E. L. Woodbridge, and J. G. Anderson, The seasonal evolution of reactive chlorine in the Northern Hemisphere stratosphere, *Science, 261,* 1134-1136, 1993.

Toon, G. C., C. B. Farmer, L. L. Lowes, P. W. Schaper, J.-F. Blavier, and R. H. Norton, Infrared aircraft measurements of stratospheric composition over Antarctica during September 1987, *J. Geophys. Res., 94,* 16571-16596, 1989a.

Toon, G. C., C. B. Farmer, P. W. Schaper, L. L. Lowes, and R. H. Norton, Composition measurements of the 1989 Arctic winter stratosphere by airborne infrared solar absorption spectroscopy, *J. Geophys. Res., 97,* 7939-7962, 1992.

Toon, O. B., R. P. Turco, J. Jordan, J. Goodman, and G. Ferry, Physical processes in polar stratospheric ice clouds, *J. Geophys. Res., 94,* 11359-11380, 1989b.

Toon, O. B., E. V. Browell, S. Kinne, and J. Jordan, An analysis of lidar observations of polar stratospheric clouds, *Geophys. Res., Lett., 17,* 393-396, 1990a.

Toon, O. B., R. P. Turco, and P. Hamill, Denitrification mechanisms in the polar stratospheres, *Geophys. Res., Lett., 17,* 445-448, 1990b.

Toumi, R., R. L. Jones, and J. A. Pyle, Stratospheric ozone depletion by $ClONO_2$ photolysis, *Nature, 365,* 37-39, 1993.

Trepte, C. R., R. E. Veiga, and M. P. McCormick, The poleward dispersal of Mount Pinatubo volcanic aerosol, *J. Geophys. Res., 98,* 18563-18573, 1993.

Tuck, A. F., Synoptic and chemical evolution of the Antarctic vortex in late winter and early spring, 1987, *J. Geophys. Res., 94,* 11687-11737, 1989.

Tuck, A. F., T. Davies, S. J. Hovde, M. Noguer-Alba, D. W. Fahey, S. R. Kawa, K. K. Kelly, D. M. Murphy, M. H. Proffitt, J. J. Margitan, M. Loewenstein, J. R. Podolske, S. E. Strahan, and K. R. Chan, Polar stratospheric cloud processed air and potential vorticity in the Northern Hemisphere lower stratosphere at mid-latitudes during winter, *J. Geophys. Res., 97,* 7883-7904, 1992.

Tuck, A. F., J. M. Russell III, and J. E. Harries, Stratospheric dryness: Antiphased desiccation over Micronesia and Antarctica, *Geophys. Res. Lett., 20,* 1227-1230, 1993.

Tuck, A. F., D. W. Fahey, M. Loewenstein, J. R. Podolske, K. K. Kelly, S. J. Hovde, D. M. Murphy, and J. W. Elkins, Spread of denitrification from 1987 Antarctic and 1988-1989 Arctic stratospheric vortices, *J. Geophys. Res., 99,* 20573-20583, 1994.

Tung, K. K., M. K. W. Ko, J. M. Rodriguez, and N.-D. Sze, Are Antarctic ozone variations a manifestation of dynamics or chemistry?, *Nature, 322,* 811-814, 1986.

Van Doren, J. M., L. R. Watson, P. Davidovits, D. R. Worsnop, M. S. Zahniser, and C. E. Kolb, Uptake of N_2O_5 and HNO_3 by aqueous sulfuric acid droplets, *J. Phys. Chem., 95,* 1684-1689, 1991.

van Loon, H., and K. Labitzke, Interannual variations in the stratosphere of the Northern Hemisphere: A description of some probable influences, in *Interactions between Global Climate Subsystems, The Legacy of Hann, Geophysical Monograph, 75,* IUGG Volume 15, 111-122, 1993.

von Clarmann, T., H. Fischer, F. Friedl-Valoon, A. Linden, H. Oelhaf, C. Piesch, M. Seefeldner, and W. Völker, Retrieval of stratospheric O_3, HNO_3, and $ClONO_2$ profiles from 1992 MIPAS-B limb emission spectra: Method, results, and error analysis, *J. Geophys. Res., 98,* 20495-20506, 1993.

von der Gathen, P., M. Rex, N. R. P. Harris, D. Lucic, B. Knudsen, R. Fabian, H. Fast, I. B. Mikkelsen, M. Rummukainen, J. Staehelin, and C. Varotsos, Chemical depletion of ozone observed during the 1991/1992 winter, submitted to *J. Geophys. Res.*, 1994.

Wahner, A., J. Callies, H.-P. Dorn, U. Platt, and C. Schiller, Near UV atmospheric absorption measurements of column abundances during Airborne Arctic Stratospheric Expedition, January-February 1989: 1. Technique and NO_2 observations, *Geophys. Res. Lett., 17,* 497-500, 1990a.

Wahner, A., J. Callies, H.-P. Dorn, U. Platt, and C. Schiller, Near UV atmospheric absorption measurements of column abundances during Airborne Arctic Stratospheric Expedition, January-February 1989: 3. BrO observations, *Geophys. Res. Lett., 17,* 517-520, 1990b.

Wallace, L., and W. Livingston, The effect of the Pinatubo cloud on hydrogen chloride and hydrogen fluoride, *Geophys. Res. Lett., 19,* 1209, 1992.

Waters, J. W., L. Froidevaux, W. G. Read, G. L. Manney, L. S. Elson, D. A. Flower, R. F. Jarnot, and R. S. Harwood, Stratospheric ClO and ozone from the Microwave Limb Sounder on the Upper Atmosphere Research Satellite, *Nature, 362,* 597-602, 1993a.

Waters, J. W., L. Froidevaux, G. L. Manney, W. G. Read, and L. S. Elson, MLS observations of lower stratospheric ClO and O_3 in the 1992 Southern Hemisphere winter, *Geophys. Res. Lett., 20,* 1219-1222, 1993b.

Waugh, D. W., R. A. Plumb, R. J. Atkinson, M. R. Schoeberl, L. R. Lait, P. A. Newman, M. Loewenstein, D. W. Toohey, L. M. Avallone, C. R. Webster, and R. D. May, Transport of material out of the stratospheric Arctic vortex by Rossby wave breaking, *J. Geophys. Res., 99,* 1071-1088, 1994.

Weaver, A., M. Loewenstein, J. R. Podolske, S. E. Strahan, M. H. Proffitt, K. Aikin, J. J. Margitan, H. H. Jonsson, C. A. Brock, J. C. Wilson, and O. B. Toon, Effects of Pinatubo aerosol on stratospheric ozone at mid-latitudes, *Geophys. Res. Lett., 20,* 2515-2518, 1993.

Webster, C. R., R. D. May, D. W. Toohey, L. M. Avallone, J. G. Anderson, P. A. Newman, L. R. Lait, M. R. Schoeberl, J. W. Elkins, and K. R. Chan, Chlorine chemistry on polar stratospheric cloud particles in the Arctic winter, *Science, 261,* 1130-1134, 1993a.

Webster, C. R., R. D. May, D. W. Toohey, L. M. Avallone, J. G. Anderson, and S. Solomon, In situ measurements of the ClO/HCl ratio: Heterogeneous processing on sulfate aerosols and polar stratospheric clouds, *Geophys. Res. Lett., 20,* 2523-2526, 1993b.

Wilson, J. C., H. H. Jonsson, C. A. Brock, D. W. Toohey, L. M. Avallone, D. Baumgardner, J. E. Dye, L. R. Poole, D. C. Woods, R. J. DeCoursey, M. Osborn, M. C. Pitts, K. K. Kelly, K. R. Chan, G. V. Ferry, M. Loewenstein, J. R. Podolske, and A. Weaver, In situ observations of aerosol and chlorine monoxide after the 1991 eruption of Mount Pinatubo: Effects of reactions on sulfate aerosol, *Science, 261,* 1140-1143, 1993.

WMO, *Scientific Assessment of Ozone Depletion: 1991,* Global Ozone Research and Monitoring Project—Report No. 25, World Meteorological Organization, Geneva, 1992.

Wofsy, S. C., G. P. Gobbi, R. J. Salawitch, and M. B. McElroy, Nucleation and growth of $HNO_3 \cdot 3H_2O$ particles in the polar stratosphere, *J. Atmos. Sci., 47,* 2004-2012, 1990a.

Wofsy, S. C., R. J. Salawitch, J. H. Yatteau, M. B. McElroy, B. W. Gandrud, J. E. Dye, and D. Baumgardner, Condensation of HNO_3 on falling ice particles: Mechanism for denitrification of the polar stratosphere, *Geophys. Res. Lett., 17,* 449-452, 1990b.

Woodbridge, E. L., J. W. Elkins, D. W. Fahey, L. E. Heidt, S. Solomon, T. J. Baring, T. J. Gilpin, W. H. Pollock, S. M. Schauffler, E. L. Atlas, M. Loewenstein, J. R. Podolske, C. R. Webster, R. D. May, R. J. Salawitch, S. C. Wofsy, J. M. Gilligan, and S. A. Montzka, Estimates of total organic and inorganic chlorine in the lower stratosphere from in situ measurements during AASE II, *J. Geophys. Res.*, in press, 1994.

Worsnop, D. R., L. E. Fox, M. S. Zahniser, and S. C. Wofsy, Vapor pressures of solid hydrates of nitric acid: Implications for polar stratospheric clouds, *Science, 259,* 71-74, 1993.

Zander, R., M. R. Gunson, C. B. Farmer, C. P. Rinsland, F. W. Irion, and E. Mahieu, The 1985 chlorine and fluorine inventories in the stratosphere based on ATMOS observations at 30 north latitude, *J. Atm. Chem., 15,* 171-186, 1992.

Zhang, R., P. J. Wooldridge, J. P. D. Abbatt, and M. J. Molina, Physical chemistry of the H_2SO_4/H_2O binary system at low temperatures: Stratospheric implications, *J. Phys. Chem., 97,* 7351-7358, 1993a.

Zhang, R., P. J. Wooldridge, and M. J. Molina, Vapor pressure measurements for the $H_2SO_4/HNO_3/H_2O$ and $H_2SO_4/HCl/H_2O$ systems: Incorporation of stratospheric acids into background sulfate aerosols, *J. Phys. Chem., 97,* 8541-8548, 1993b.

Zhang, R., J. T. Jayne, and M. J. Molina, Heterogeneous interactions of $ClONO_2$ and HCl with sulfuric acid tetrahydrate: Implications for the stratosphere, *J. Phys. Chem.*, in press, 1994.